Astro/Phys 224 Spring 2014

Origin and Evolution of the Universe

Week 8

Galaxy Evolution

Joel Primack

University of California, Santa Cruz

From last Thursday's lecture

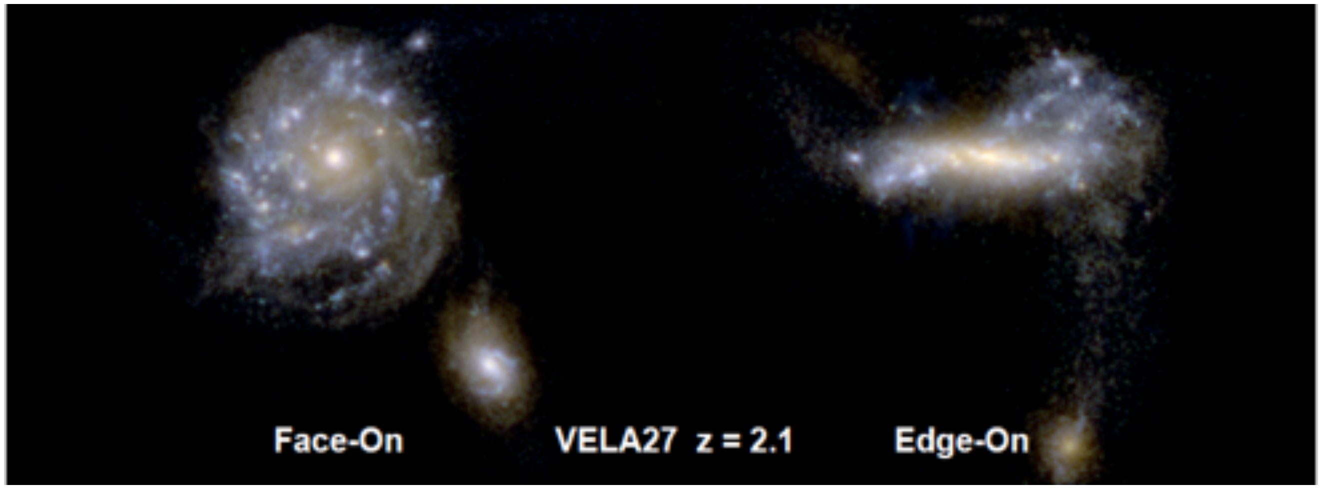

Face-On **Edge-On**

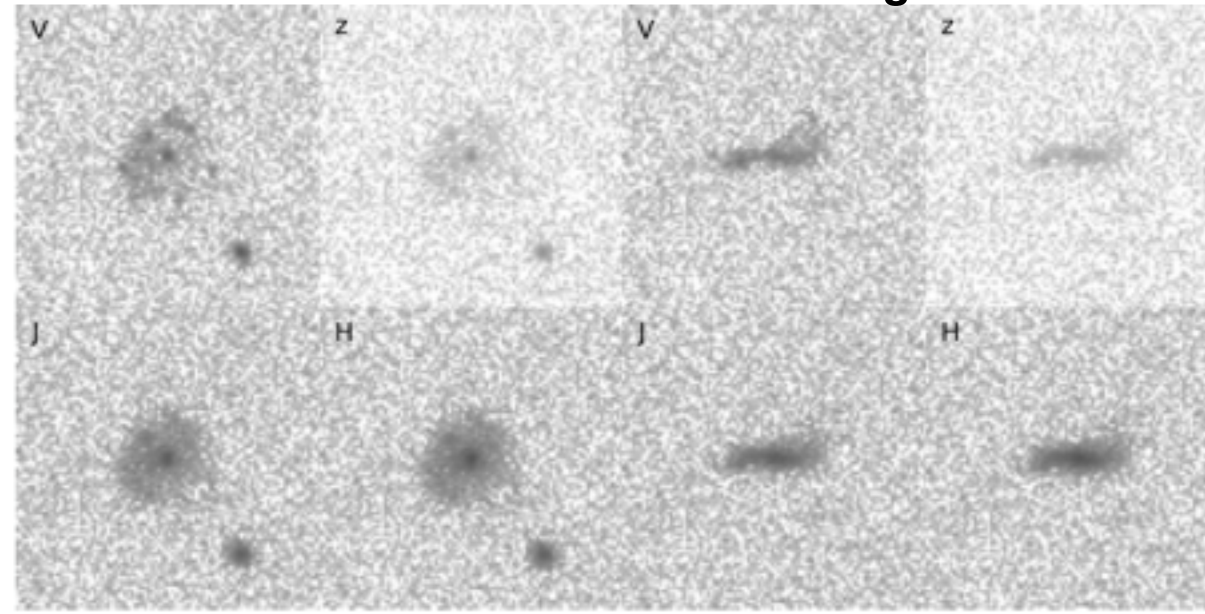

From June 2014 *Sky & Telescope* article

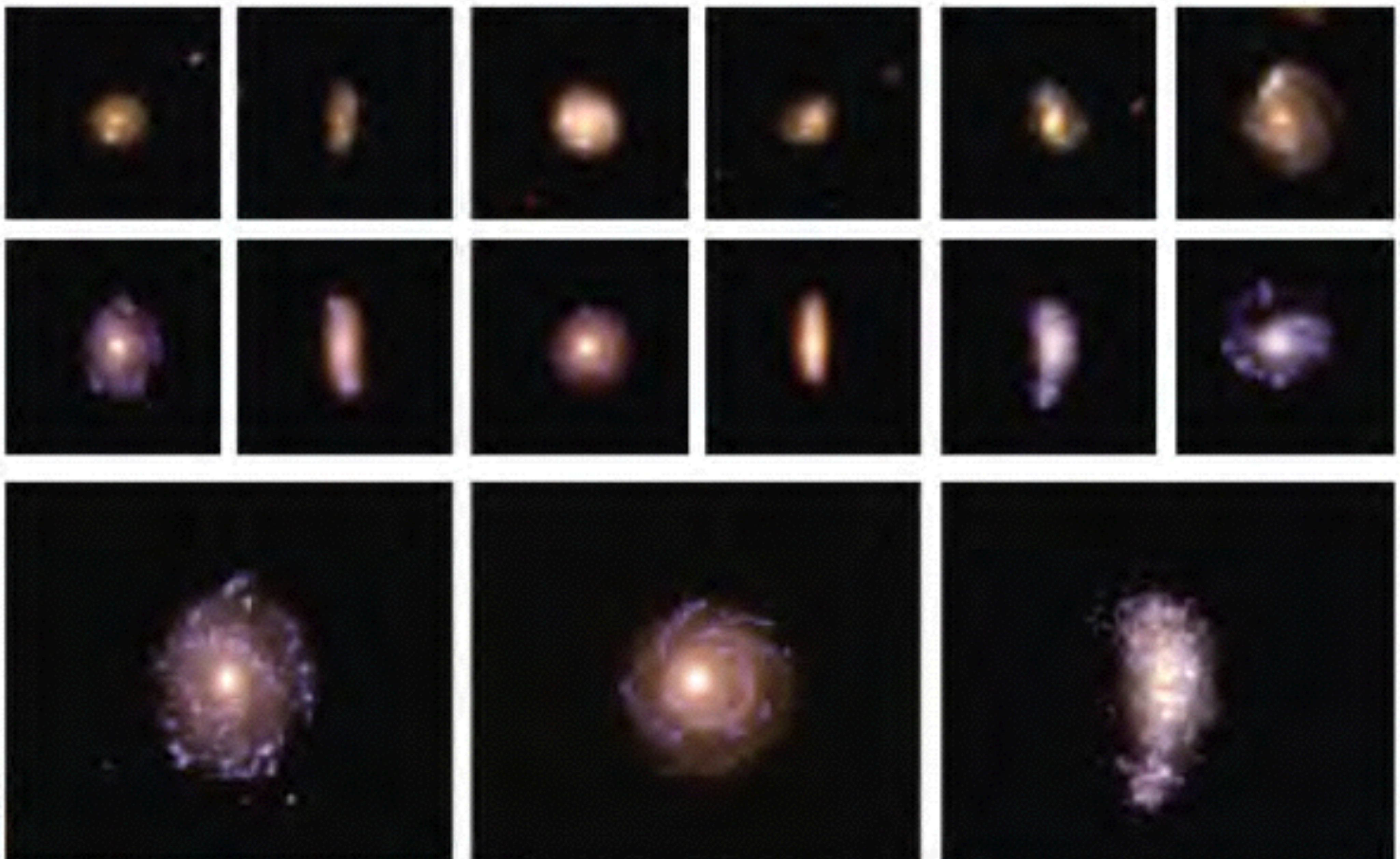

CLUMPY GALAXIES

Top row: Six galaxies from CANDELS are seen when the universe was 4 to 6 billion years old. *Middle row:* These computer simulation frames show three disk galaxies as if imaged by CANDELS when viewed roughly face-on (*left of pair*) and edge-on (*right*). *Bottom row:* This is how these galaxies would appear if we could see them closer up from one angle. All three are about 4 billion years old and have large clumps of rapidly forming stars ignited by instabilities in their disks.

AGORA Assembling Galaxies of Resolved Anatomy

A High-resolution Galaxy Simulations Comparison Initiative To Tackle Longstanding Challenges in Galaxy Formation

High-res Galaxy Simulations

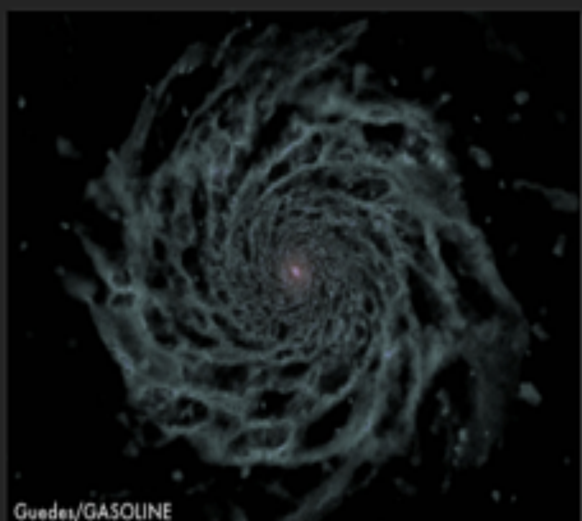

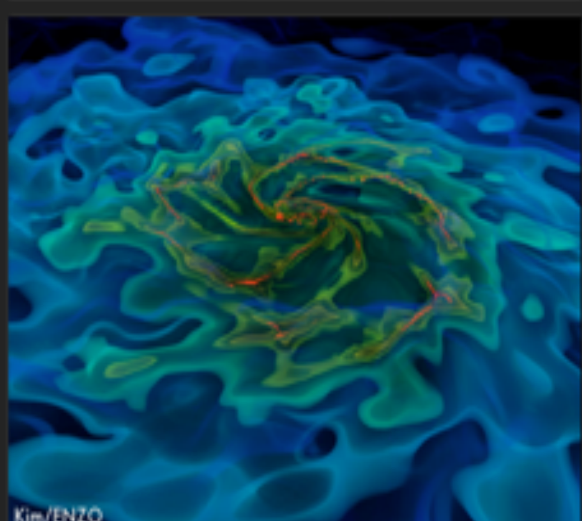

AGORA Comparison Infrastructure

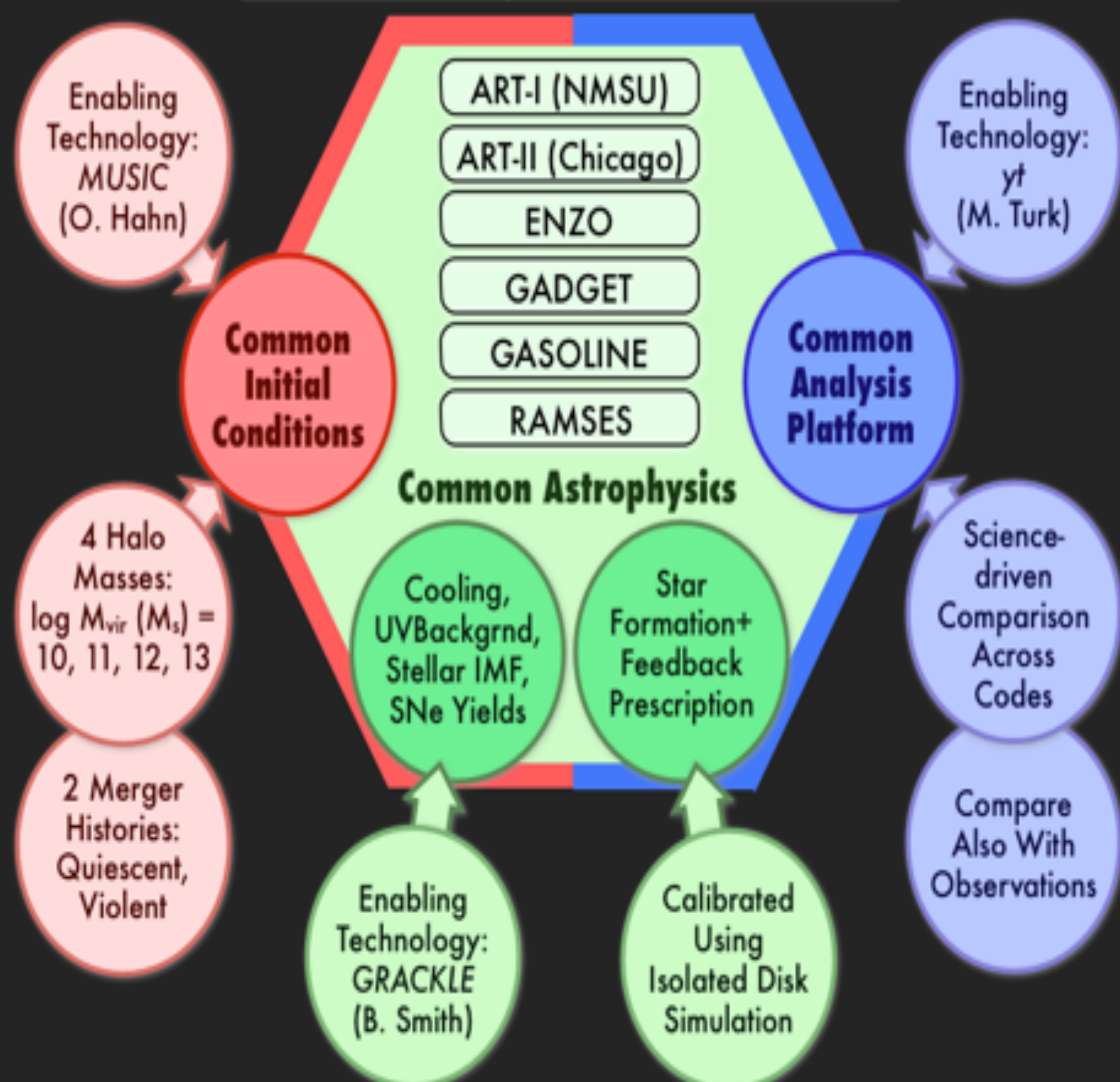

AGORA Goal & Team

- GOAL: A multi-platform study to raise the realism and predictive power of high-resolution (<100 pc) galaxy simulations collectively
- TEAM: 4 task working groups and 9+ science working groups, 94 participants from 47 institutions as of 2nd Workshop, Aug. 2013
- DATA SHARE: Simulation data will be radpily available to public

- AGORA First light: Flagship paper by Ji-hoon Kim et al. (arXiv:1308.2669; www.AGORAsimulations.org)
- Project funded in part by:

University of California
High-Performance
AstroComputing Center
(UC-HiPACC)
Joel Primack, Director

University of California
Santa Cruz
Next Telescope Science
Institute (NEXSI)
Piero Madau, Director

Assembling Galaxies of Resolved Anatomy

AGORA High-Resolution Galaxy Simulation Comparison Project Steering Committee

Piero Madau & Joel R. Primack, UCSC, Co-Chairs
Tom Abel, Stanford
Nick Gnedin, Chicago/Fermilab
Lucio Mayer, University of Zurich
Romain Teyssier, Saclay & Zurich
James Wadsley, McMaster

Ji-hoon Kim, UCSC (Coordinator)

94 astrophysicists using 10 codes have joined AGORA

www.AGORAsimulations.org

AGORA High-Resolution Simulation Comparison

Initial Conditions for Simulations

MUSIC galaxy masses at $z \sim 0$: $\sim 10^{10}, 10^{11}, 10^{12}, 10^{13}\, M_\odot$

with both quiet and busy merging trees

isolation criteria agreed for Lagrangian regions

Isolated Spiral Galaxy at $z \sim 1$: $\sim 10^{12}\, M_\odot$

Astrophysics that all groups will include

UV background (Haardt-Madau 2012)

cooling function (based on ENZO and Eris cooling)

Tools to compare simulations based on *yt*, to be available for all codes used in AGORA

Images and SEDs for all timesteps from *yt* ➠ *Sunrise*

www.AGORAsimulations.org

www.AGORAsimulations.org

AGORA Task-Oriented Working Groups

	Working Group	Objectives and Tasks
T1	Common Astrophysics	UV background, metal-dependent cooling, IMF, metal yields
T2	ICs: Isolated	common initial conditions for isolated low-z disk galaxies
T3	ICs: Cosmological	common initial conditions for cosmological zoom-in simulations
T4	Common Analysis	support `yt` and other analysis tools, define quantitative and physically meaningful comparisons across simulations

AGORA Science Working Groups

	Working Group	Science Questions (includes, but not limited to)
S1	Isolated Galaxies and Subgrid Physics	tune the subgrid physics across platforms to produce similar results for similar astrophysical assumptions
S2	Dwarf Galaxies	simulate $\sim 10^{10} M_\odot$ halos, compare results across all platforms
S3	Dark Matter	radial profile, shape, substructure, core-cusp problem
S4	Satellite Galaxies	effects of environment, UV background, tidal disruption
S5	Galactic Characteristics	surface brightness, stellar properties, metallicity, images, SEDs
S6	Outflows	outflows, circumgalactic medium, metal absorption systems
S7	High-redshift Galaxies	cold flows, clumpiness, kinematics, Lyman-limit systems
S8	Interstellar Medium	galactic interstellar medium, thermodynamics
S9	Massive Black Holes	black hole growth and feedback in galactic context
S10	Lyα Absorption and Emission	prediction of Lyα maps for simulated galaxies and their environments including effects of radiative transfer

THE *AGORA* HIGH-RESOLUTION GALAXY SIMULATIONS COMPARISON PROJECT

JI-HOON KIM[1], TOM ABEL[2], OSCAR AGERTZ[3,4], GREG L. BRYAN[5], DANIEL CEVERINO[6], CHARLOTTE CHRISTENSEN[7], CHARLIE CONROY[1], AVISHAI DEKEL[8], NICKOLAY Y. GNEDIN[3,9,10], NATHAN J. GOLDBAUM[1], JAVIERA GUEDES[11], OLIVER HAHN[11], ALEXANDER HOBBS[11], PHILIP F. HOPKINS[12,13], CAMERON B. HUMMELS[7], FRANCESCA IANNUZZI[14], DUŠAN KEREŠ[15], ANATOLY KLYPIN[16], ANDREY V. KRAVTSOV[3,10], MARK R. KRUMHOLZ[1], MICHAEL KUHLEN[1,13], SAMUEL N. LEITNER[17], PIERO MADAU[1], LUCIO MAYER[18], CHRISTOPHER E. MOODY[1], KENTARO NAGAMINE[19,20], MICHAEL L. NORMAN[15], JOSE OÑORBE[21], BRIAN W. O'SHEA[22], ANNALISA PILLEPICH[1], JOEL R. PRIMACK[23], THOMAS QUINN[24], JUSTIN I. READ[4], BRANT E. ROBERTSON[7], MIGUEL ROCHA[21], DOUGLAS H. RUDD[10, 25], SIJING SHEN[1], BRITTON D. SMITH[22], ALEXANDER S. SZALAY[26], ROMAIN TEYSSIER[18], ROBERT THOMPSON[7, 19], KEITA TODOROKI[19], MATTHEW J. TURK[5], JAMES W. WADSLEY[27], JOHN H. WISE[28], AND ADI ZOLOTOV[8] FOR THE *AGORA* COLLABORATION[29]

ApJS 210, 1 (2014)

ABSTRACT

We introduce the Assembling Galaxies Of Resolved Anatomy (AGORA) project, a comprehensive numerical study of well-resolved galaxies within the ΛCDM cosmology. Cosmological hydrodynamic simulations with force resolutions of ∼100 proper pc or better will be run with a variety of code platforms to follow the hierarchical growth, star formation history, morphological transformation, and the cycle of baryons in and out of eight galaxies with halo masses $M_{\rm vir} \simeq 10^{10}$, 10^{11}, 10^{12}, and $10^{13}\ M_\odot$ at $z = 0$ and two different ("violent" and "quiescent") assembly histories. The numerical techniques and implementations used in this project include the smoothed particle hydrodynamics codes GADGET and GASOLINE, and the adaptive mesh refinement codes ART, ENZO, and RAMSES. The codes share common initial conditions and common astrophysics packages including UV background, metal-dependent radiative cooling, metal and energy yields of supernovae, and stellar initial mass function. These are described in detail in the present paper. Subgrid star formation and feedback prescriptions will be tuned to provide a realistic interstellar and circumgalactic medium using a non-cosmological disk galaxy simulation. Cosmological runs will be systematically compared with each other using a common analysis toolkit and validated against observations to verify that the solutions are robust—i.e., that the astrophysical assumptions are responsible for any success, rather than artifacts of particular implementations. The goals of the AGORA project are, broadly speaking, to raise the realism and predictive power of galaxy simulations and the understanding of the feedback processes that regulate galaxy "metabolism." The initial conditions for the AGORA galaxies as well as simulation outputs at various epochs will be made publicly available to the community. The proof-of-concept dark-matter-only test of the formation of a galactic halo with a $z = 0$ mass of $M_{\rm vir} \simeq 1.7 \times 10^{11}\ M_\odot$ by nine different versions of the participating codes is also presented to validate the infrastructure of the project.

G-M_{20} Nonparametric Morphology Measures Help Identify $0<z<1.5$ Galaxy Mergers

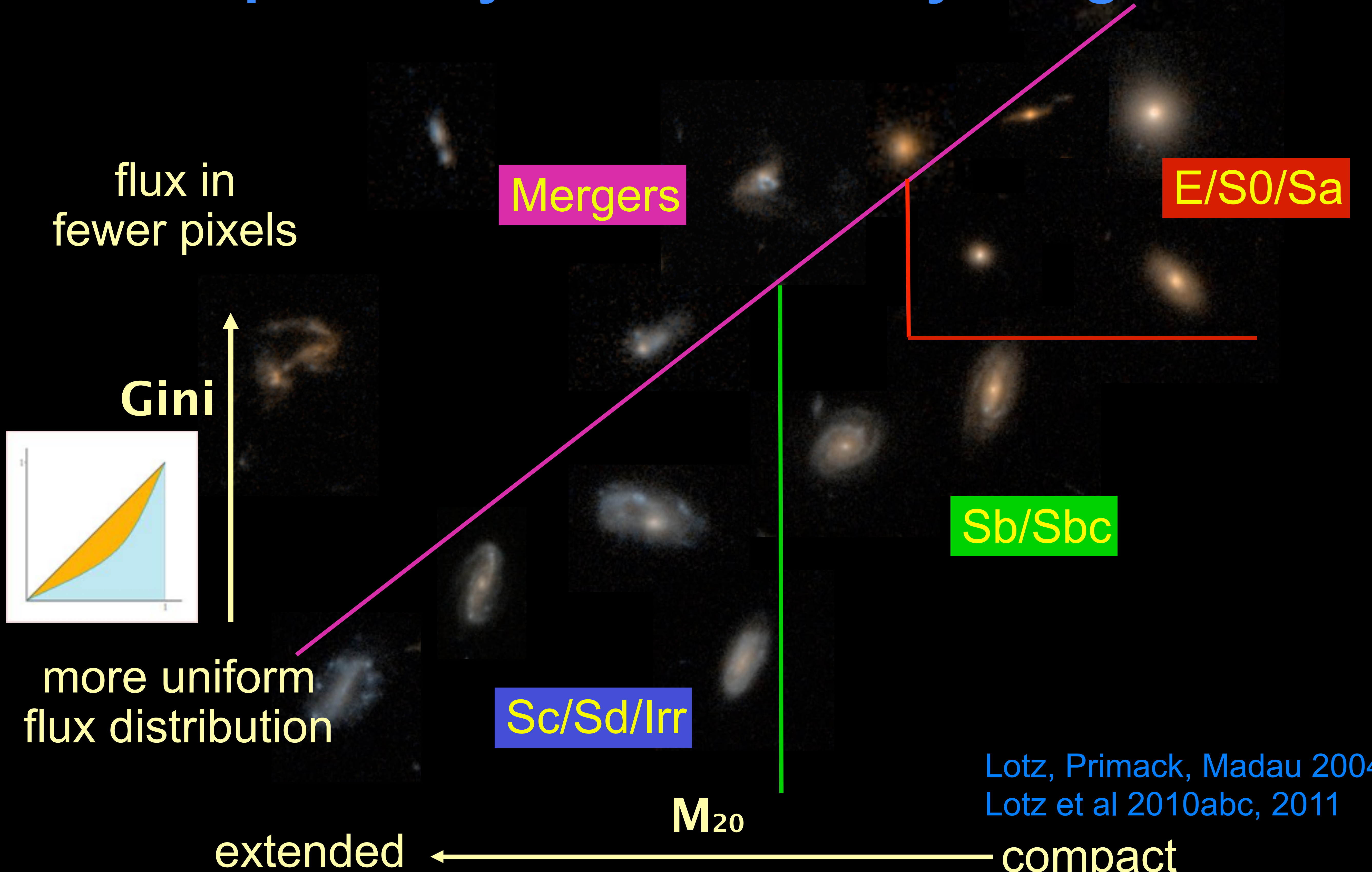

Lotz, Primack, Madau 2004
Lotz et al 2010abc, 2011

THE MAJOR AND MINOR GALAXY MERGER RATES AT Z < 1.5

Jennifer M. Lotz, Patrik Jonsson, T.J. Cox, Darren Croton, Joel R. Primack, Rachel S. Somerville, and Kyle Stewart

Astrophysical Journal 2011

Calculating the galaxy merger rate requires both a census of galaxies identified as merger candidates, and a cosmologically-averaged ‘observability’ timescale $\langle T_{obs}(z)\rangle$ for identifying galaxy mergers. While many have counted galaxy mergers using a variety of techniques, $\langle T_{obs}(z)\rangle$ for these techniques have been poorly constrained. We address this problem by calibrating three merger rate estimators (pairs, asymmetry, and G-M_{20}) with a suite of hydrodynamic merger simulations and three galaxy formation models. When our physically-motivated timescales are adopted, the observed galaxy merger rates become largely consistent. The theoretical predictions are in good agreement with the observed major merger rates.

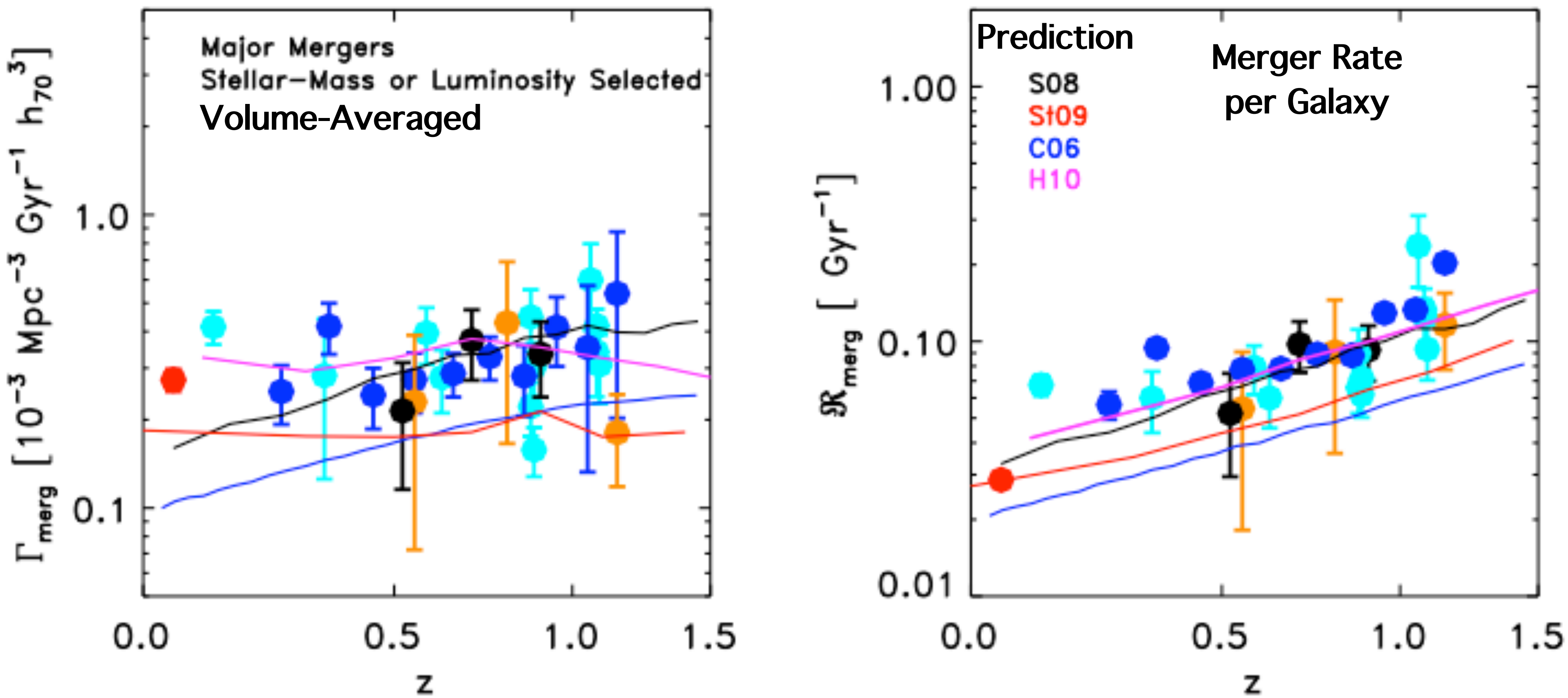

Observed Galaxy Merger Rates v. Theoretical Predictions. The volume-averaged (left) and fractional major merger (right) rates given by stellar-mass and luminosity-selected close pairs are compared to the major merger rates given by the S08 (black lines), St09 (red lines), C06 (blue line), and Hopkins et al. 2010b (magenta lines) models for 1:1 - 1:4 stellar mass ratio mergers and galaxies with $M_{star} > 10^{10}\,M_\odot$.

GALAXY EVOLUTION

From June 2014 *Sky & Telescope* article

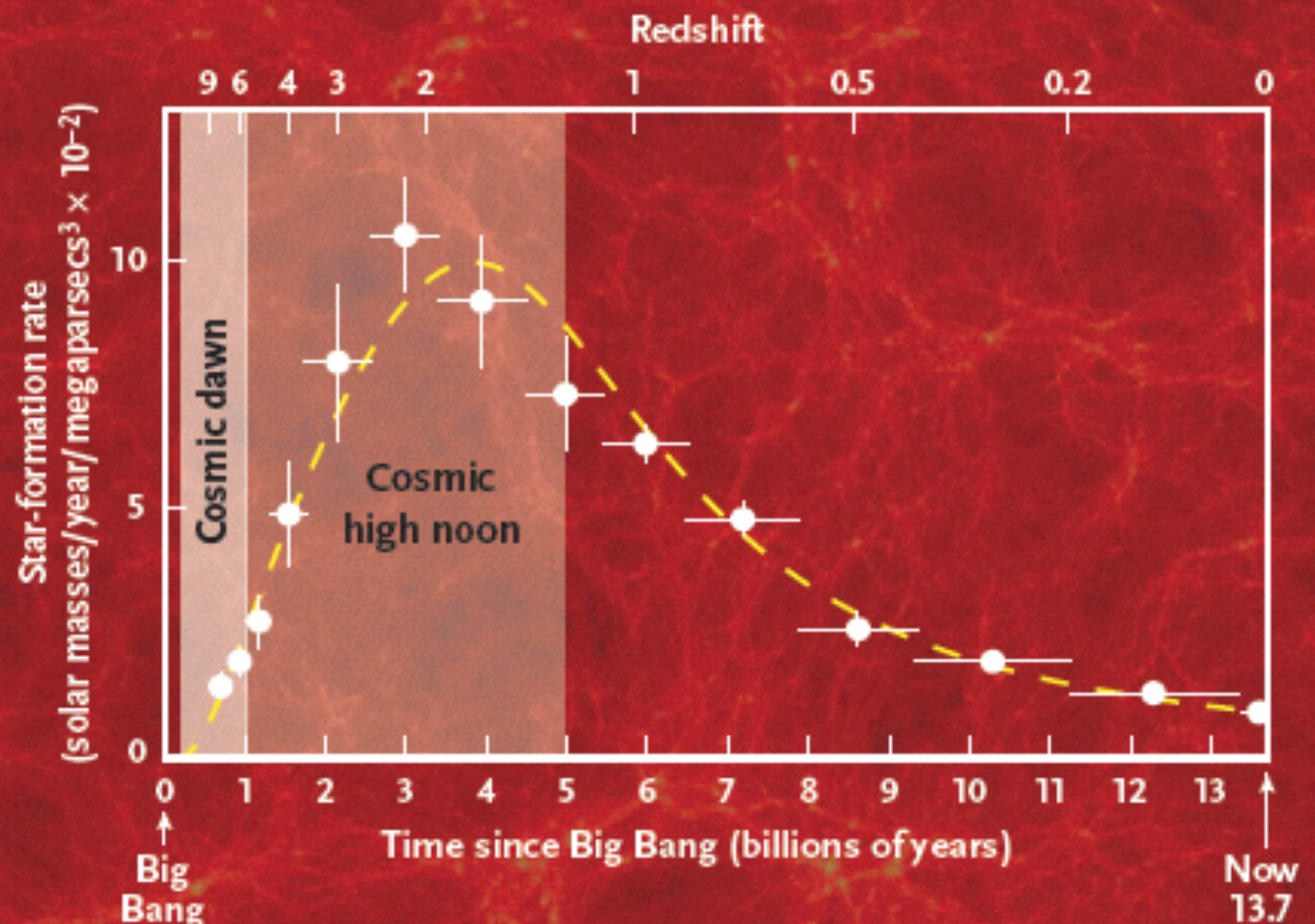

STARBIRTH RATE Using data from many surveys, including CANDELS, astronomers have plotted the rate of star formation through cosmic history. The rate climbed rapidly at cosmic dawn and peaked at cosmic high noon.

GALAXY EVOLUTION

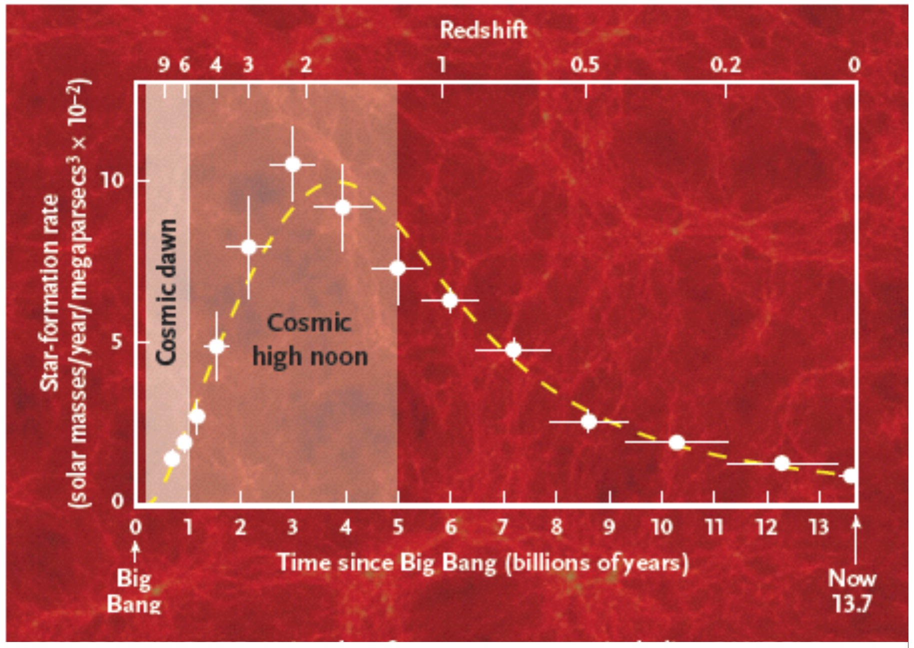

Star formation rate density vs. Redshift z (Madau Plot)

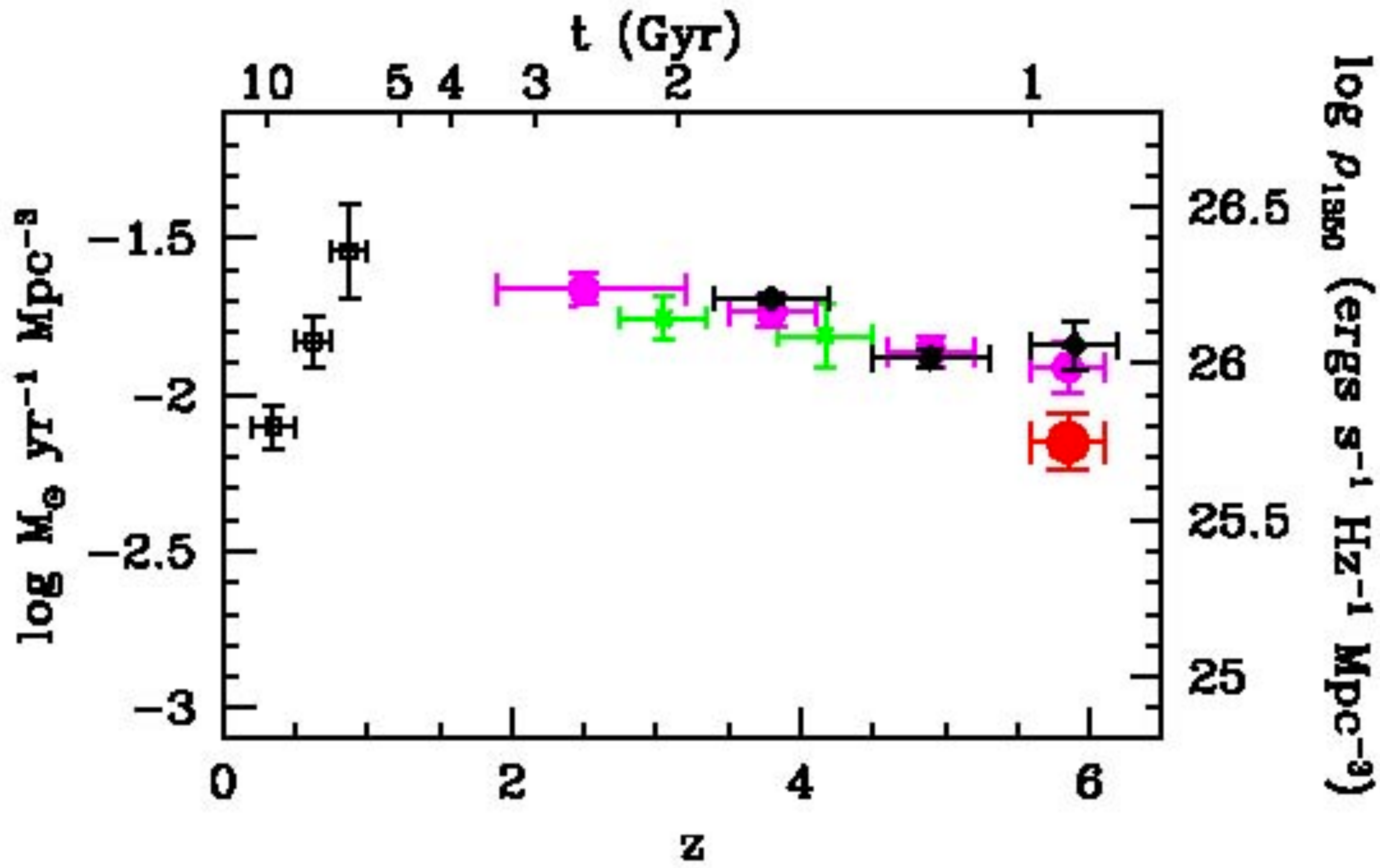

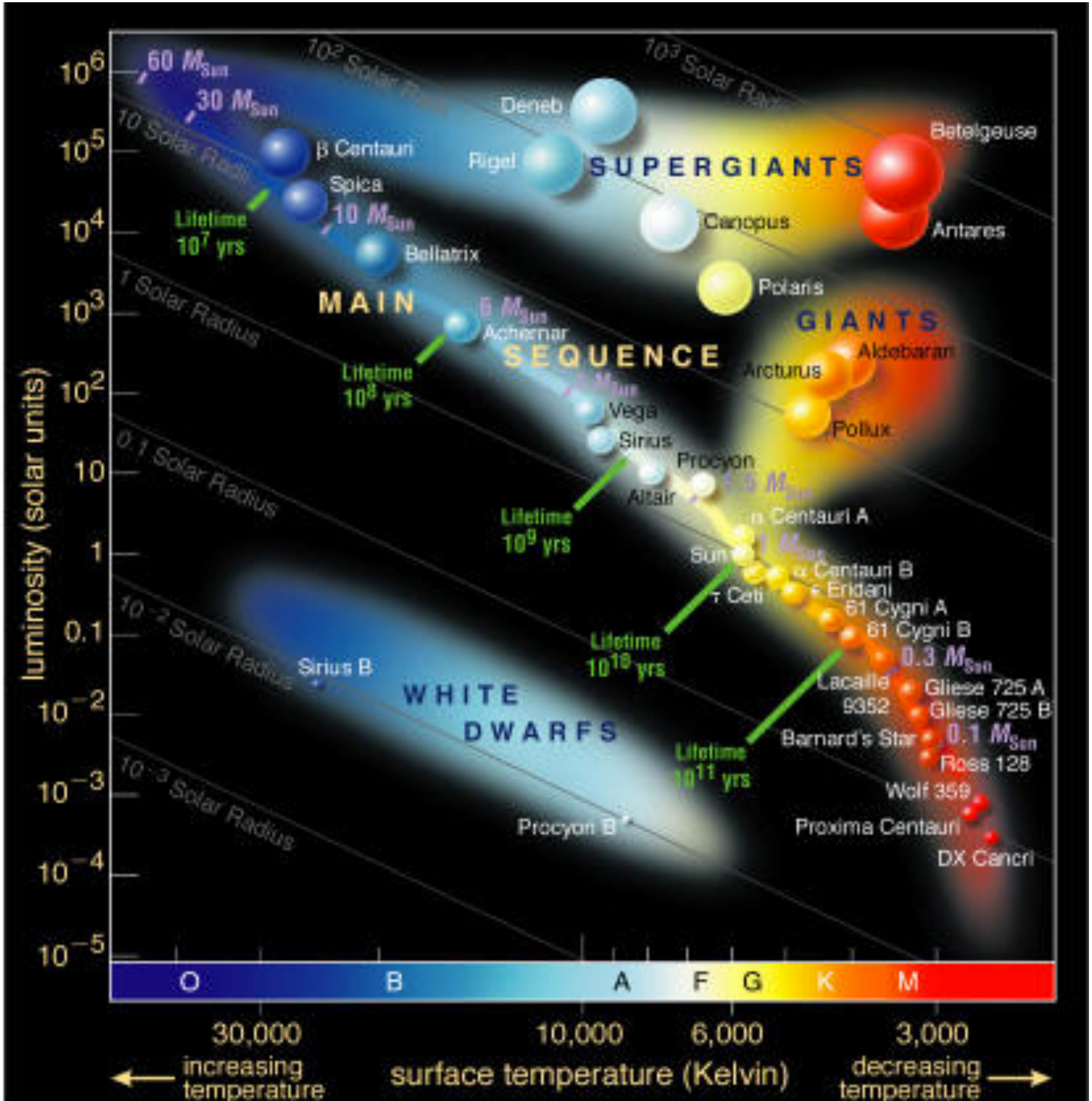

The STELLAR MAIN SEQUENCE

Mass is the key parameter, and lifetime and color depend mainly on mass — although other factors such as metallicity also play a role.

The GALAXY MAIN SEQUENCE

According to standard ΛCDM, galaxies were assembled via chaotic hierarchical mergers between massive cold dark matter halos, in which baryonic star forming matter was embedded. One would therefore expect the properties of individual galaxies to be determined by numerous independent factors such as star forming history, merger history, mass, angular momentum, size and environment. It is therefore surprising to find that **galaxies actually appear to form an (almost) one parameter family in which galaxy mass is the dominant factor.**

Mass - Age

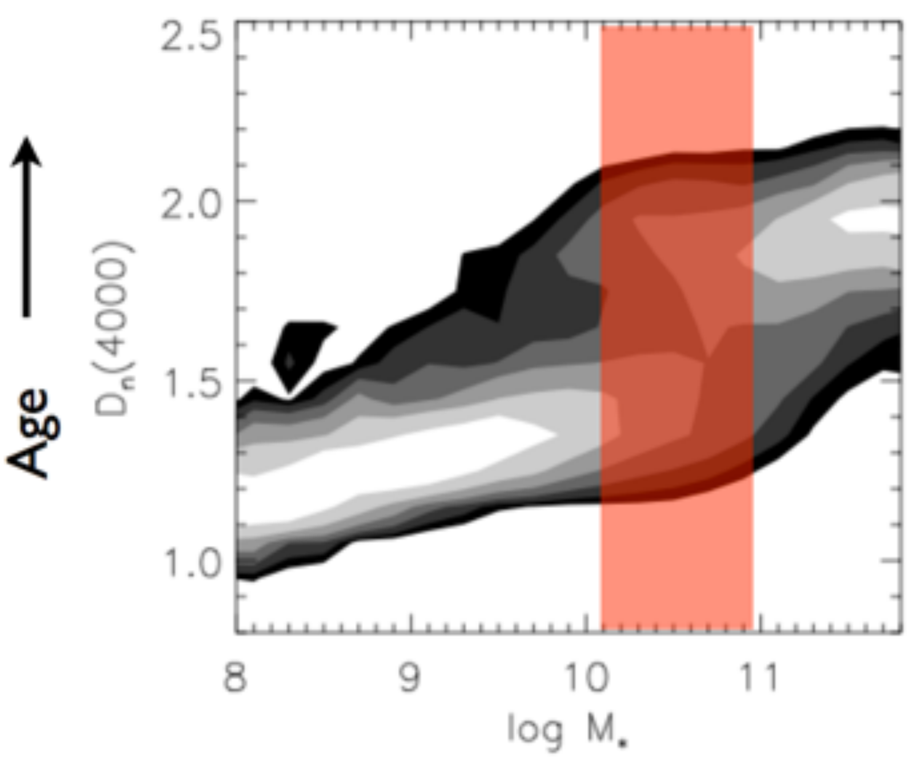

Guinevere Kauffmann+03

Mass - Metallicity

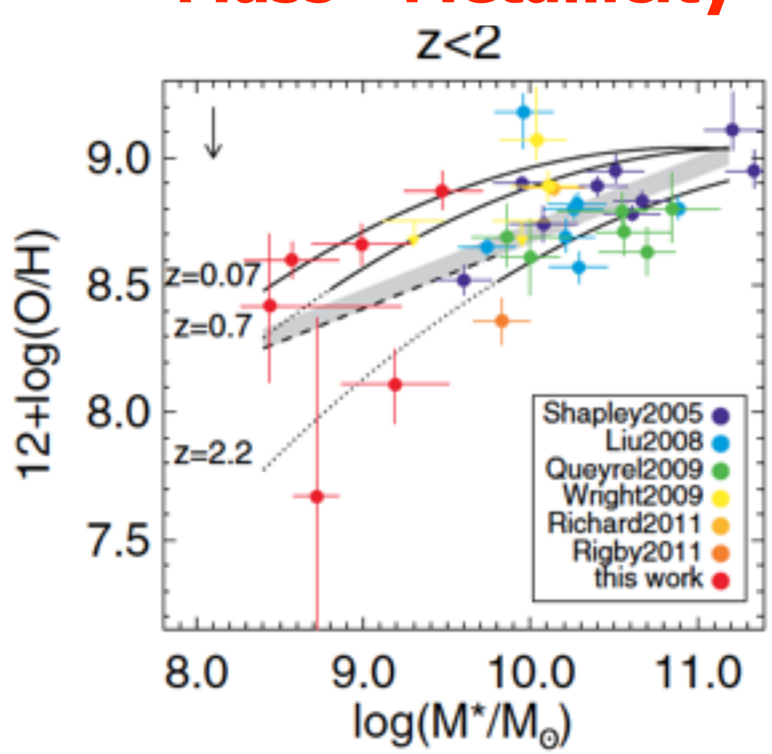

Eva Wuyts+12

Mass - Star Form. Rate

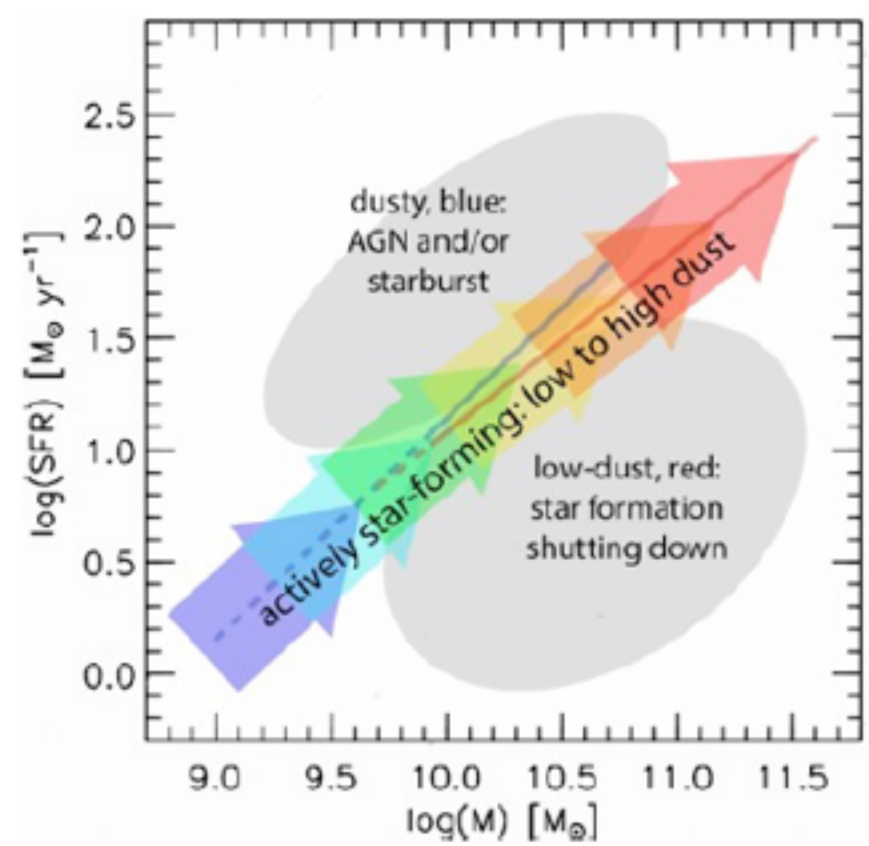

Katherine Whitaker+12

The Astrophysical Journal, 660: L43–L46, 2007 May 1

STAR FORMATION IN AEGIS FIELD GALAXIES SINCE z = 1.1: THE DOMINANCE OF GRADUALLY DECLINING STAR FORMATION, AND THE MAIN SEQUENCE OF STAR-FORMING GALAXIES

K. G. Noeske,[1] B. J. Weiner,[2] S. M. Faber,[1] C. Papovich,[2] D. C. Koo,[1] R. S. Somerville,[3] K. Bundy,[4] C. J. Conselice,[5] J. A. Newman,[6,7] D. Schiminovich,[8] E. Le Floc'h,[2] A. L. Coil,[2,7] G. H. Rieke,[2] J. M. Lotz,[9] J. R. Primack,[10] P. Barmby,[11] M. C. Cooper,[12] M. Davis,[12] R. S. Ellis,[4] G. G. Fazio,[11] P. Guhathakurta,[1] J. Huang,[11] S. A. Kassin,[1] D. C. Martin,[4] A. C. Phillips,[1] R. M. Rich,[13] T. A. Small,[4] C. N. A. Willmer,[2] and G. Wilson[14]

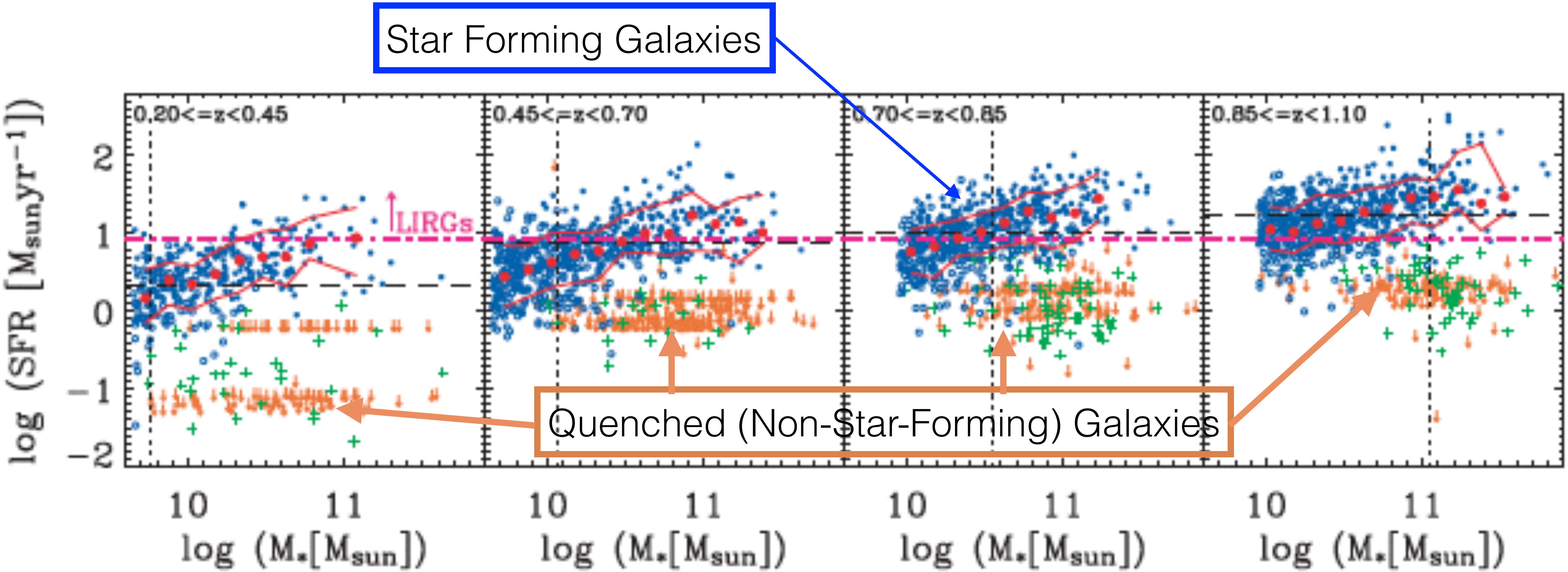

Fig. 1.—SFR vs. M_* for 2905 galaxies in the Extended Groth Strip, in the M_* range where the data are >80% complete; see § 2. The dotted vertical line marks >95% completeness. *Filled blue circles*: Combined SFRs from MIPS 24 μm and DEEP2 emission lines. *Open blue circles*: No 24 μm detection, blue $U-B$ colors, SFR from extinction-corrected emission lines. *Green plus signs*: Same as open blue circles, but red $U-B$ colors, mostly LINER/AGN candidates (§ 3). *Orange downward arrows*: No robust detection of f(24 μm) or emission lines; conservative SFR upper limits shown. There is a distinct sequence formed by fiducial SF galaxies (*open and filled circles*); galaxies with little or no SF lie below this sequence. Red circles show the median of log (SFR) in mass bins of 0.15 dex for MS galaxies (*blue circles*). Red lines include 34% of the MS galaxies above and 34% below the median of log (SFR), $\pm 1\,\sigma$ in the case of a normal distribution. *Horizontal black dashed line*: SFR corresponding to the 24 μm 80% completeness limit at the center of each z bin; 24 μm–detected galaxies above the magenta dot-dashed line are LIRGs (§ 4.2).

The Astrophysical Journal Letters, 754:L29 (6pp), 2012 August 1

THE STAR FORMATION MASS SEQUENCE OUT TO $z = 2.5$

Katherine E. Whitaker[1], Pieter G. van Dokkum[1], Gabriel Brammer[2], and Marijn Franx[3]

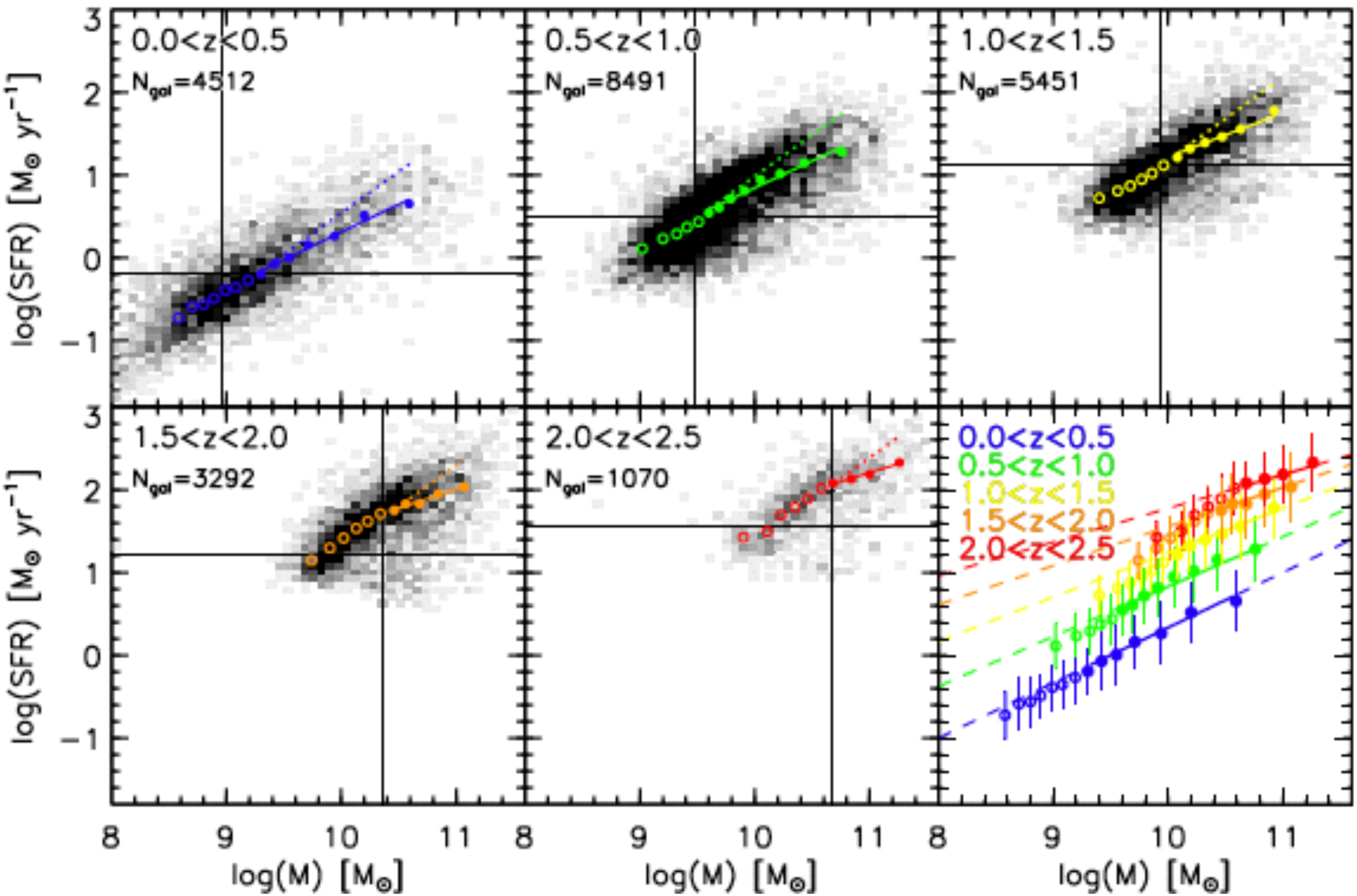

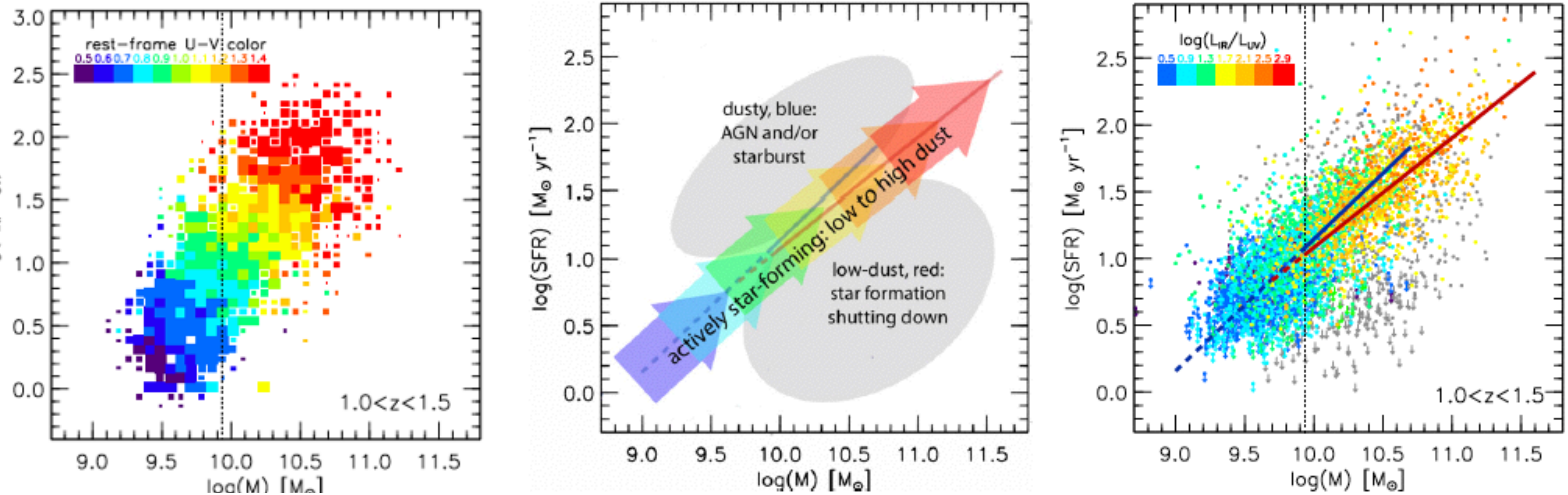

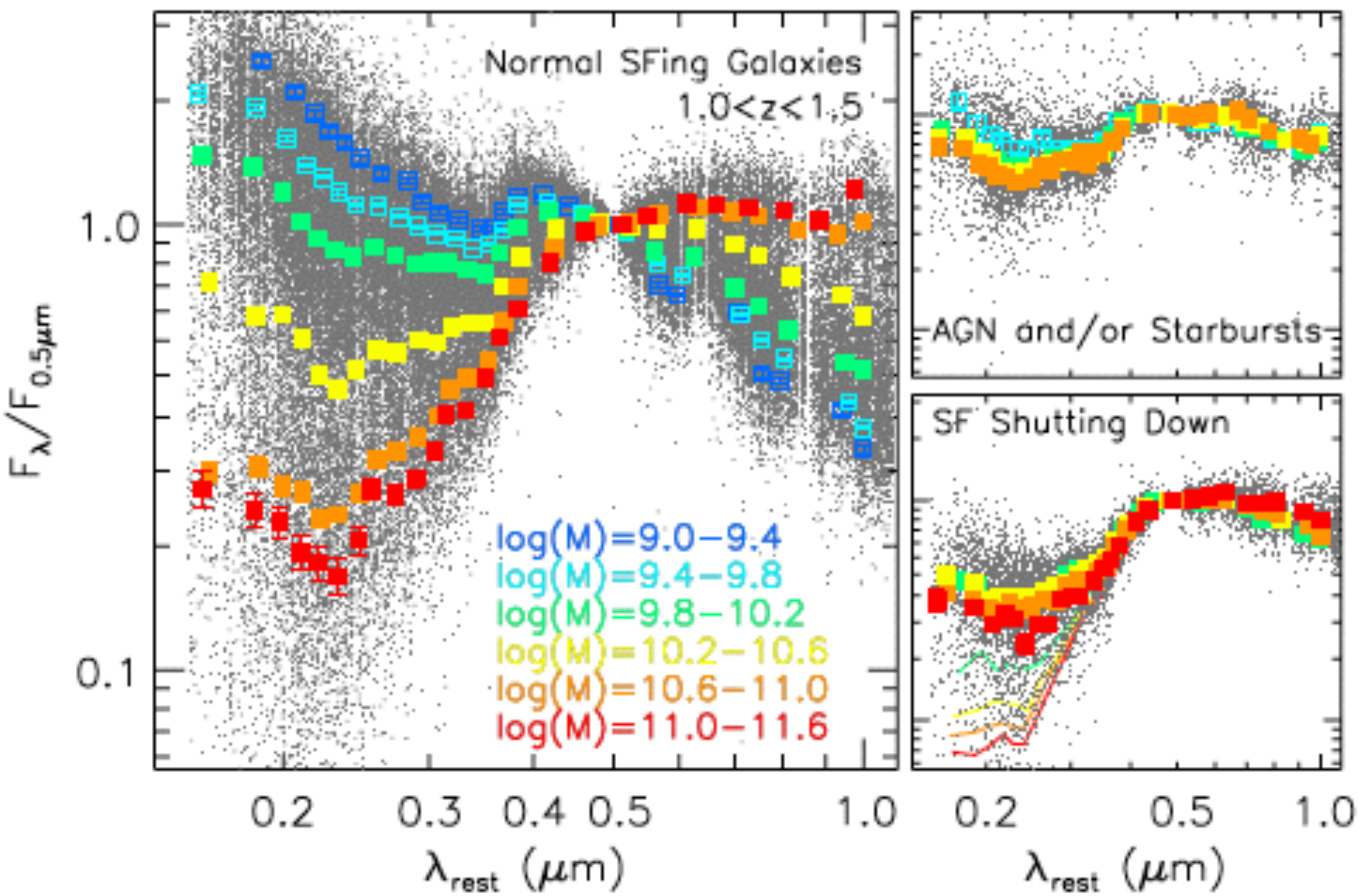

Rest-frame composite SEDs of galaxies on the “normal” star formation sequence (left) show increasing levels of dust attenuation with stellar mass. The spectral shape of dusty, blue galaxies appears to be independent of stellar mass (upper right). Galaxies in the process of shutting off star formation (bottom right) show larger amounts of rest-frame UV emission relative to quiescent galaxies at the same stellar mass and redshift (solid lines).

Katherine Whitaker+12

The GALAXY MAIN SEQUENCE

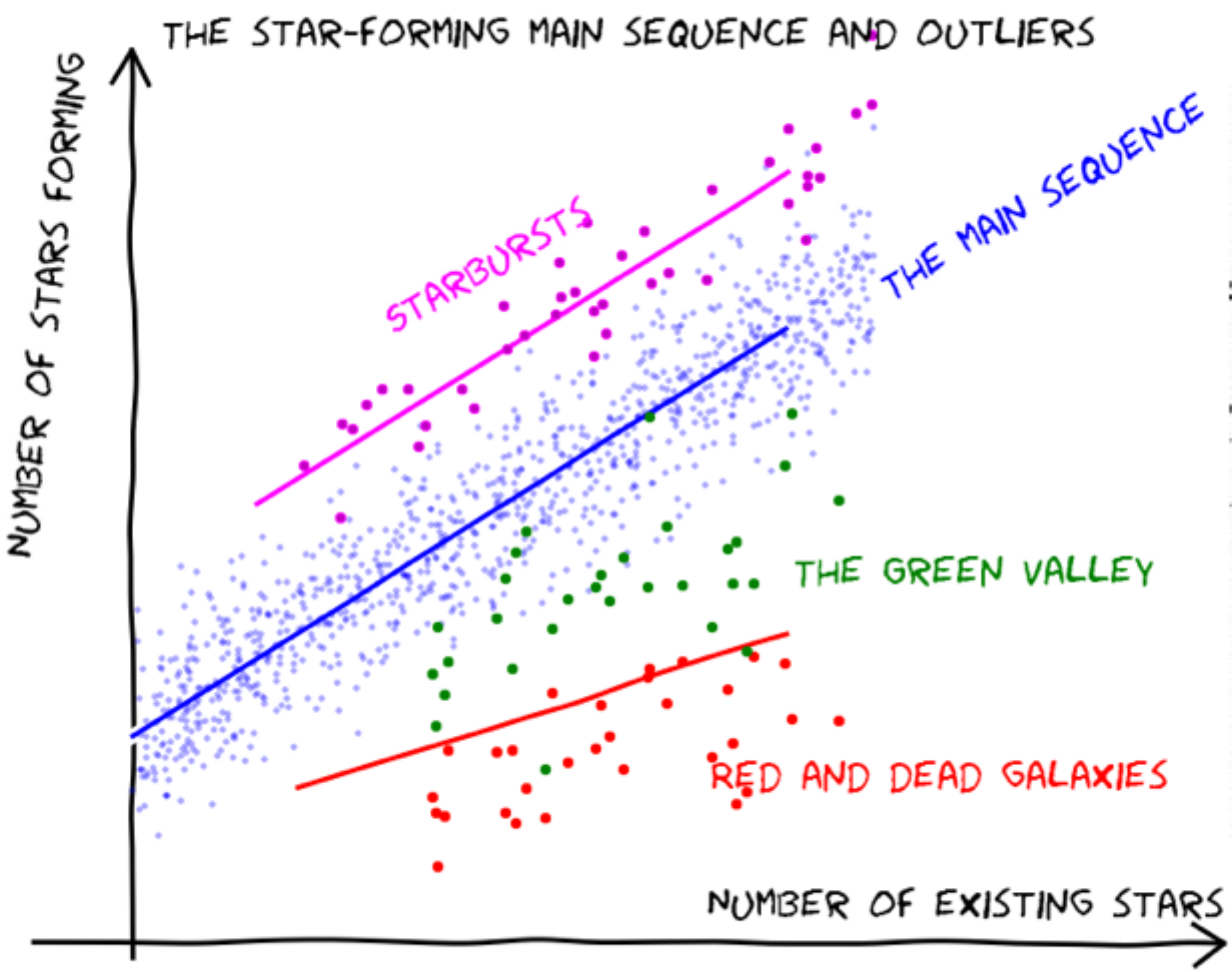

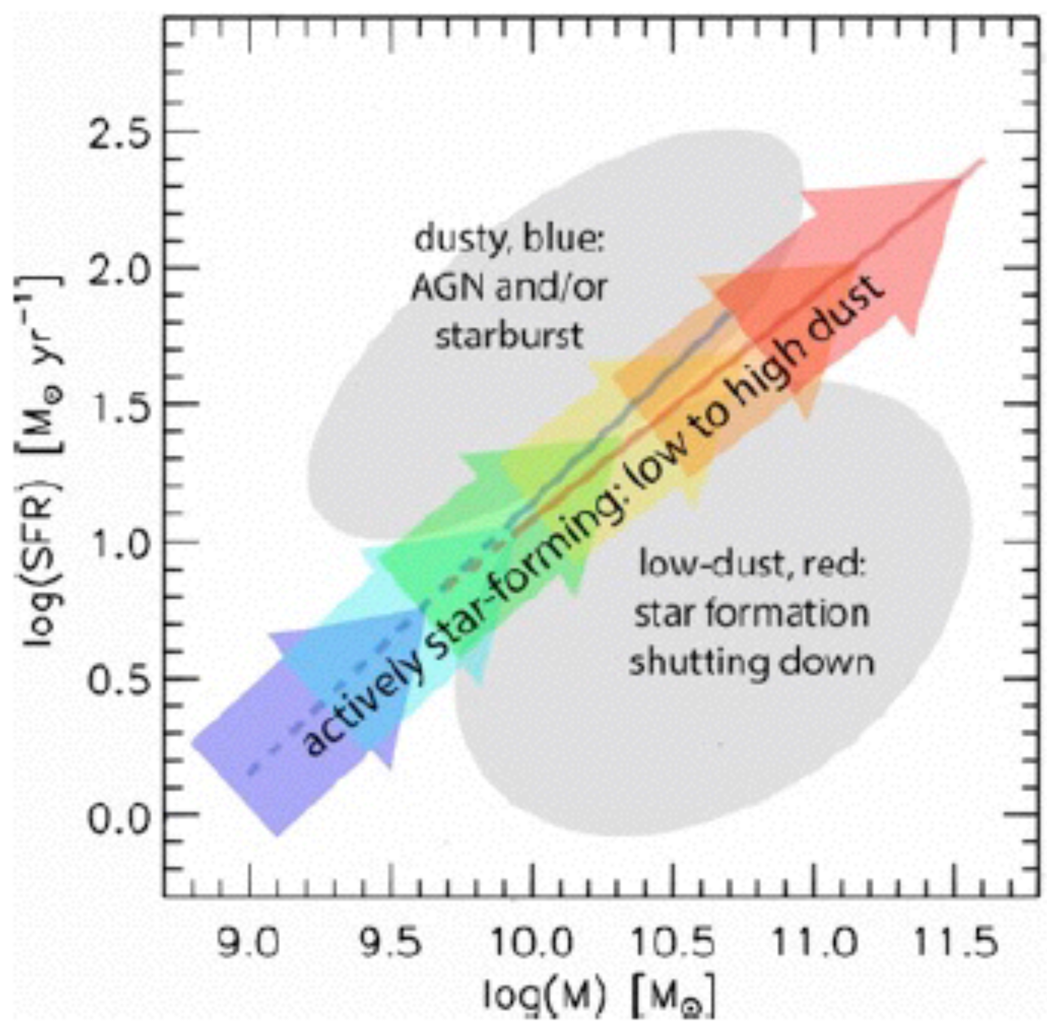

Whitaker et al. 2012

Most galaxies seem to form stars at a rate that is proportional to the number of stars that they already have. This the **main sequence** **of star-forming galaxies. Other galaxies fall off the sequence. The red and dead ones or quenched or quiescent ones aren't forming many stars at all. On the other hand there are some galaxies forming stars at much higher rates, which we call starbursts. Then there are a few galaxies that are still forming stars, but at lower rates than on the main sequence. These populate the green valley, although shutting down star formation isn't the only way to end up with greenish colors, so the green valley is sort of a hodgepodge of various kinds of galaxies.**

Local and high-z galaxies follow a "main sequence" of star formation (SFR ∽ mass) which is found to be very similar (modulo normalization):

at low and high redshift

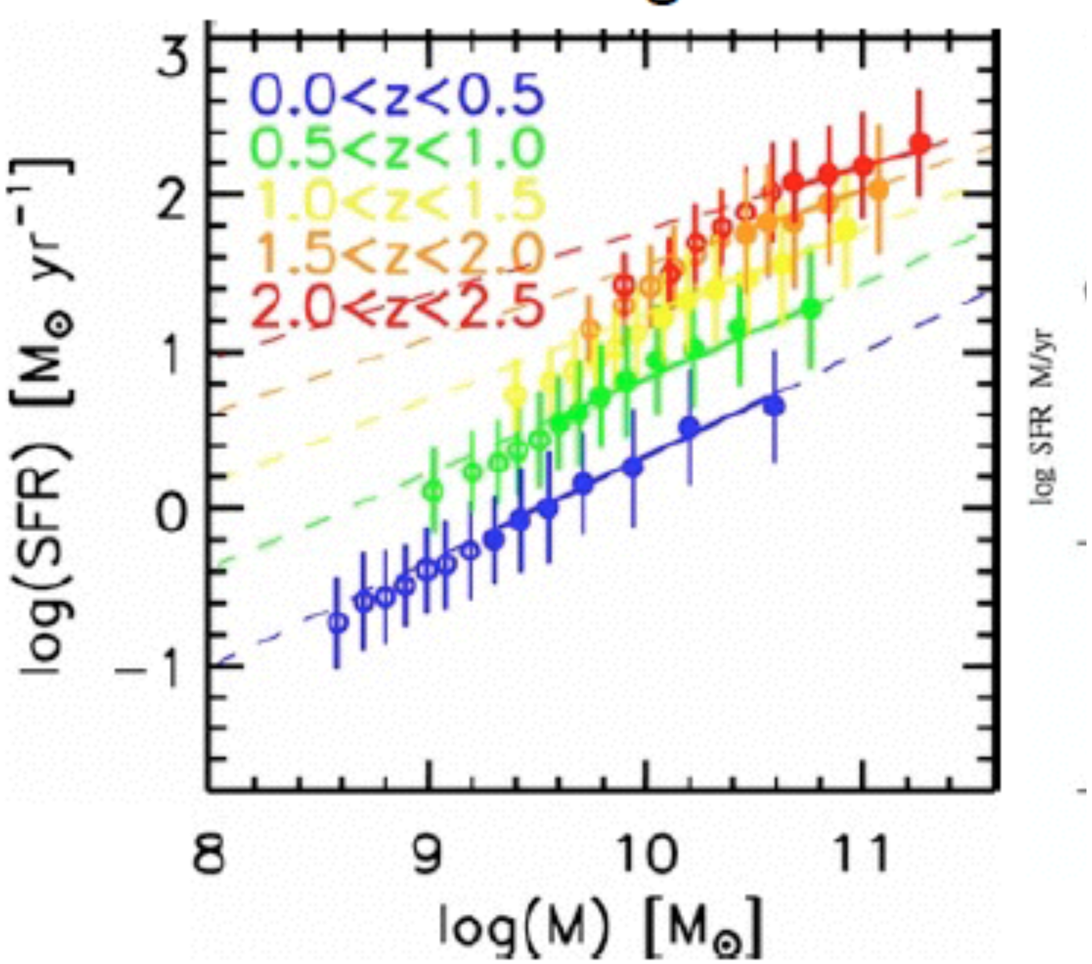

Katherine Whitaker+12

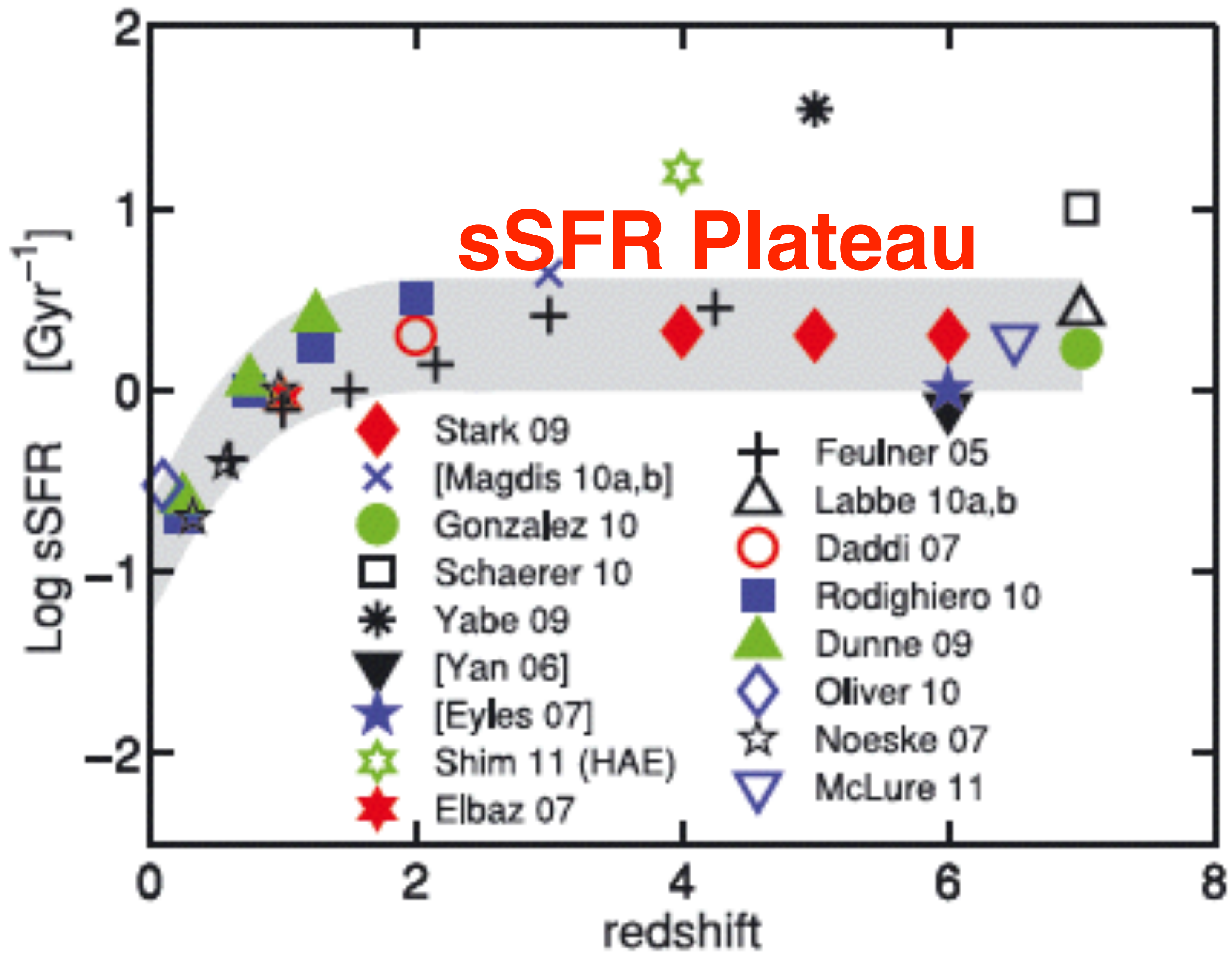

Simone Weinmann+12

Dividing the Star Formation Rate (SFR) by the galaxy's stellar mass gives the Specific Star Formation Rate (sSFR), which flattens the lines on the above plot.

There isn't much change in sSFR from z=1.5-2 to z=2-2.5, or out to z~7.

Local and high-z galaxies follow a "main sequence" of star formation (SFR ∽ mass) which is found to be very similar (modulo normalization):

at low and high redshift

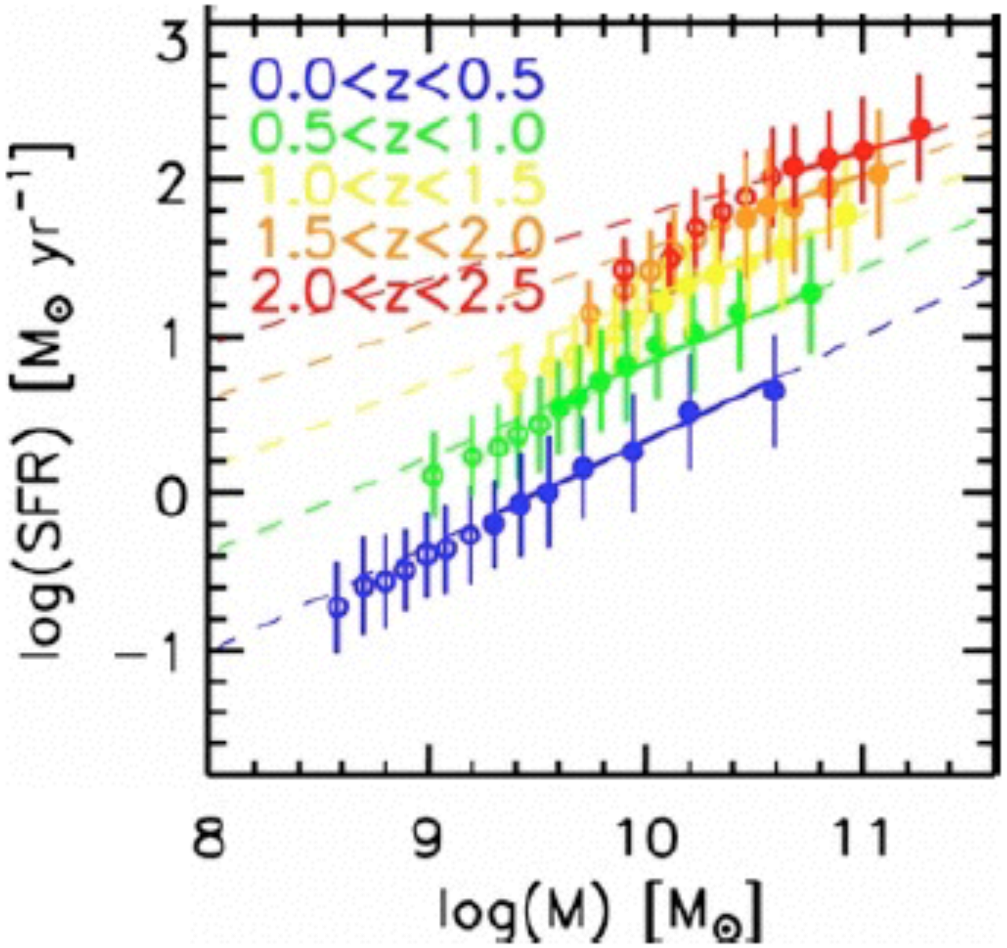

Katherine Whitaker+12

in different environments

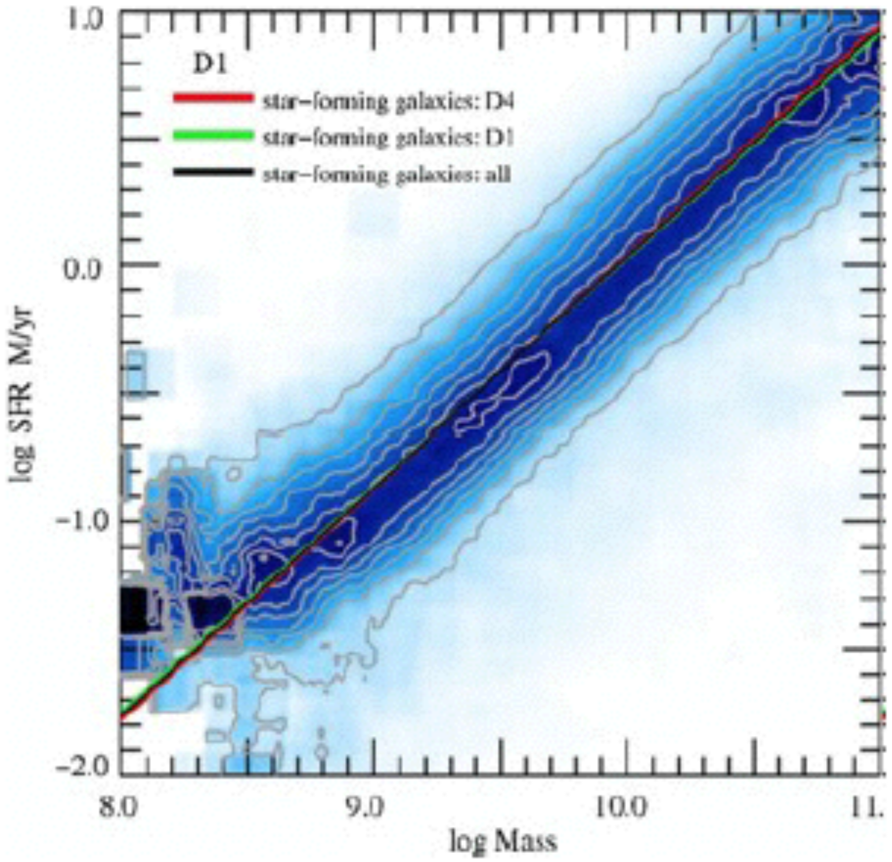

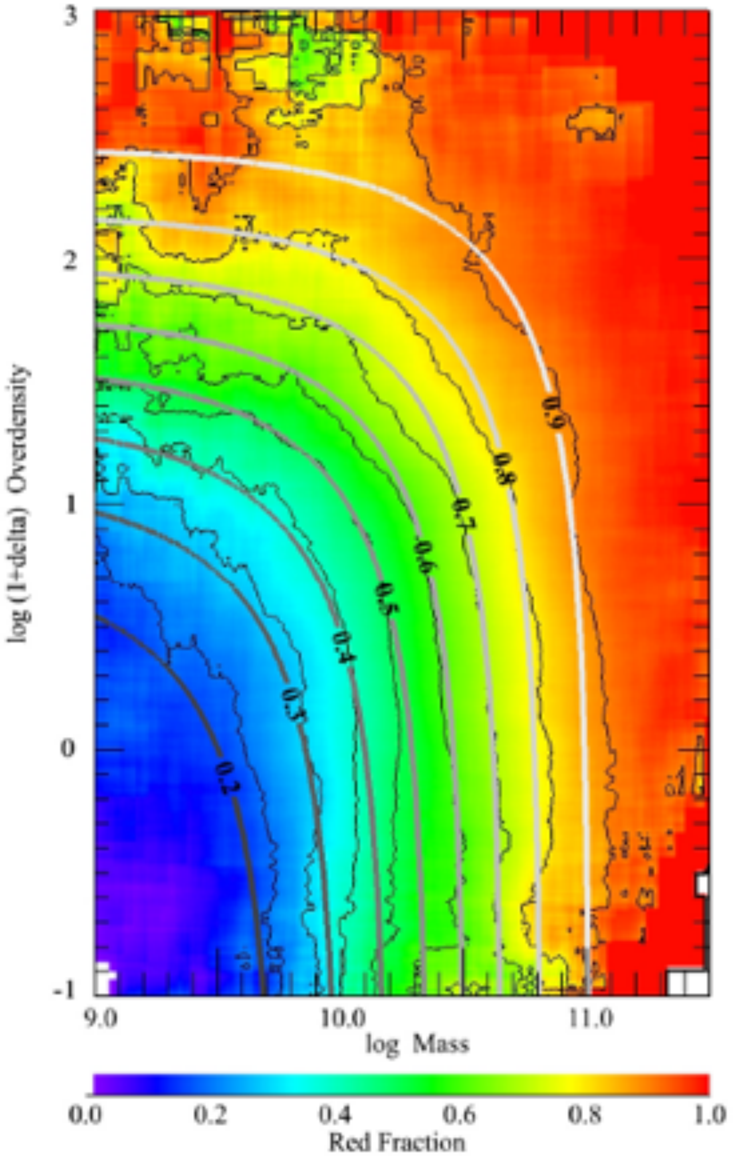

Fig 6: The red fraction in SDSS as functions of stellar mass and environme

Peng et al. 2010

Mass and environment as drivers of galaxy evolution in SDSS and zCOSMOS and the origin of the Schechter function

Y. Peng, S. Lilly, et al. 2010

In SDSS we demonstrate the clear separability of the *differential* effects of stellar mass and environment on the fraction of galaxies that are actively forming stars compared with those which are passive. The differential effects of the environment do not depend on the mass of the galaxies and, vice versa, the differential effects of mass do not depend on the environment. This suggests two different effects may be operating, which we refer to as "mass quenching" and "environment quenching".

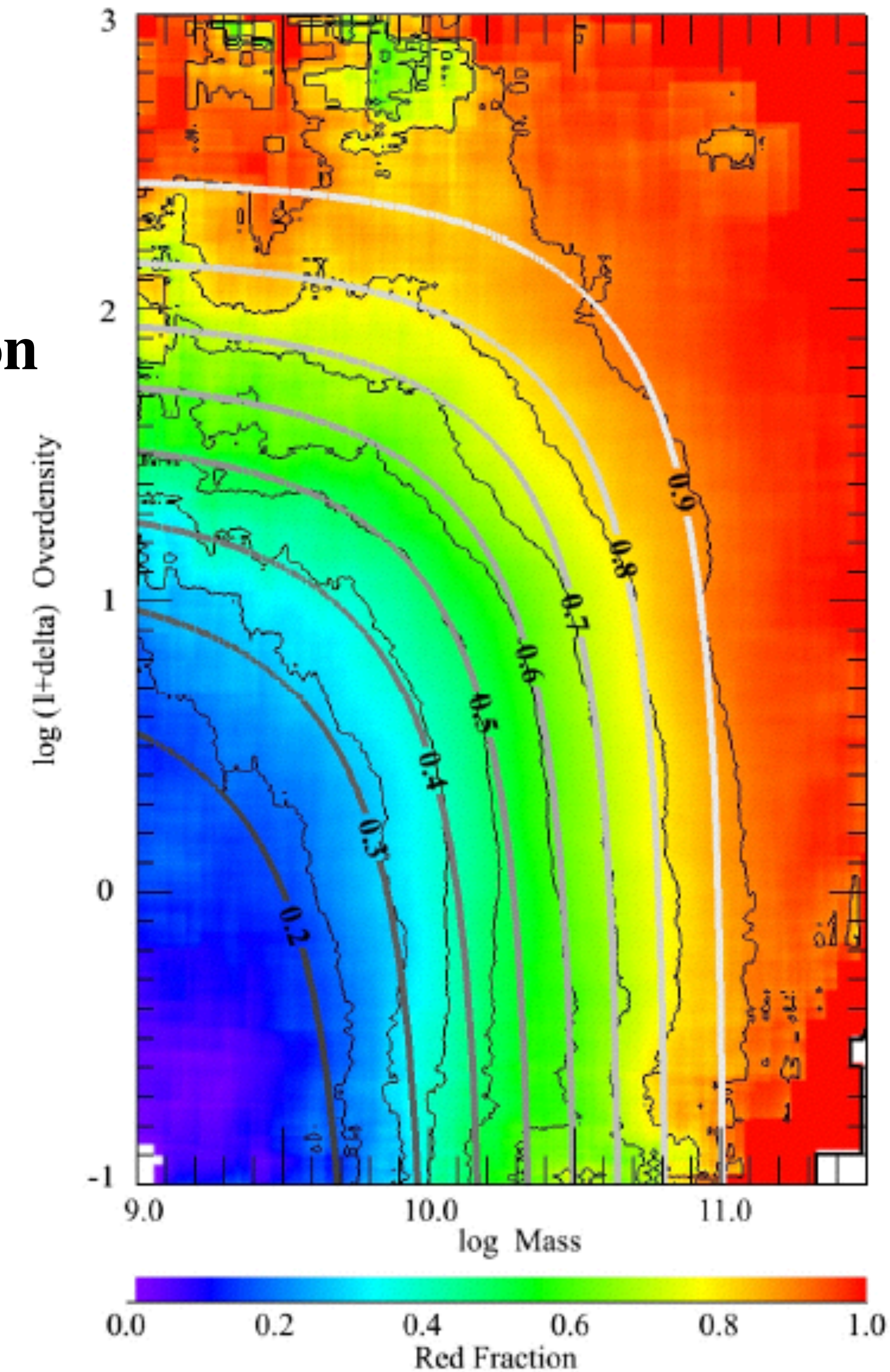

Fig 6: The red fraction in SDSS as functions of stellar mass and environment.

The Astrophysical Journal, 778:23 (9pp), 2013 November 20

THE INTRINSIC SCATTER ALONG THE MAIN SEQUENCE OF STAR-FORMING GALAXIES AT $z \sim 0.7$

Kexin Guo[1,2], Xian Zhong Zheng[1], and Hai Fu[3]

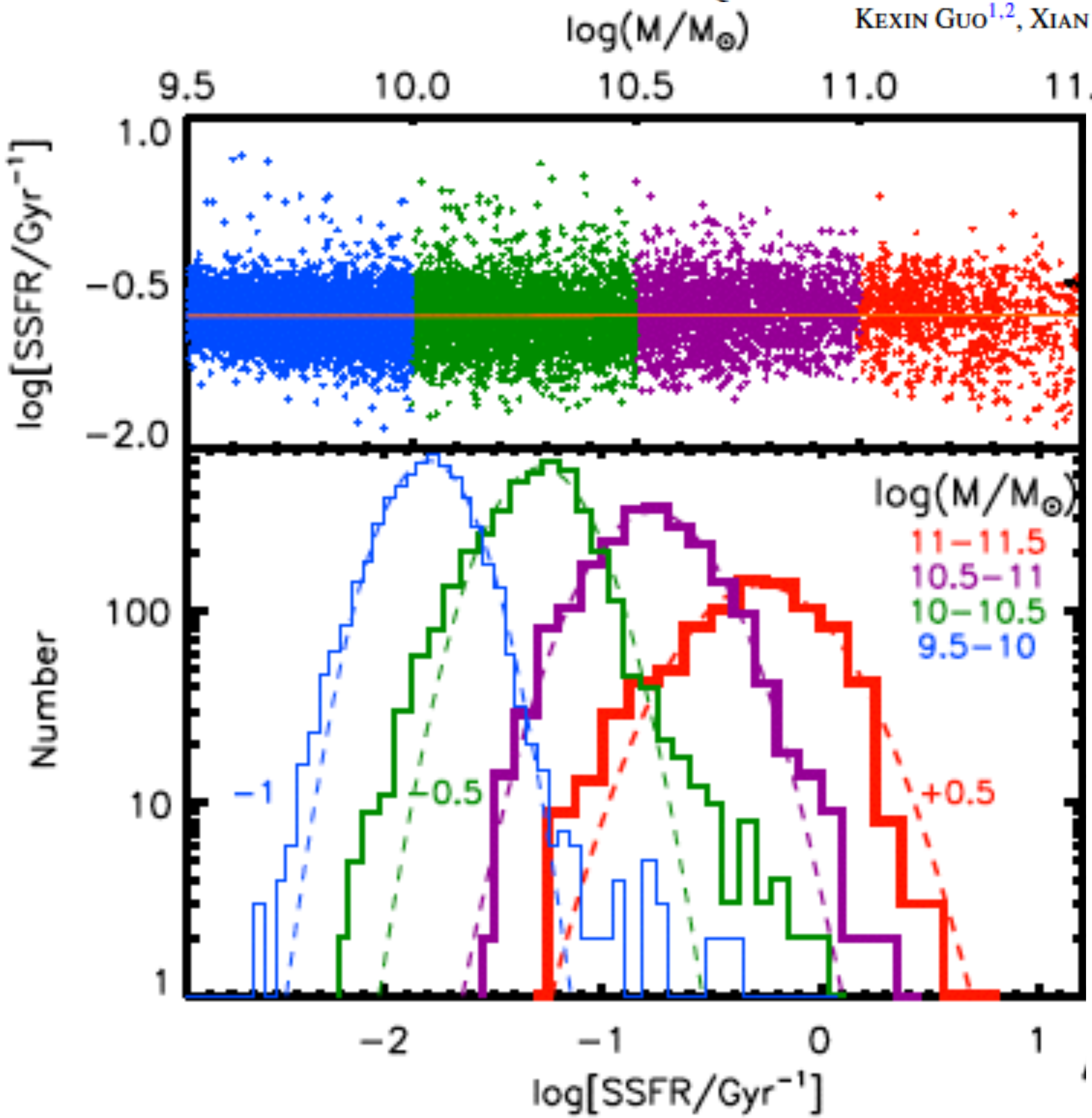

Intrinsic scatter of the main sequence increases with galaxy stellar mass, indicating more violent star formation in more massive galaxies.

GALAXY COLOR CORRELATES WITH INNER MASS SURFACE DENSITY Σ^*_{1kpc}

$$I(r) = \exp(-r^{1/n_{Sersic}})$$

Disks: $n_{Sersic} \approx 1$

Spheroids: $n_{Sersic} \approx 4$

$$\Sigma^*_{1kpc} = \left(\begin{array}{c}\text{stellar mass}\\ \text{in central kpc}\end{array}\right)$$

Global Sersic index

Inner Mass Surface Density

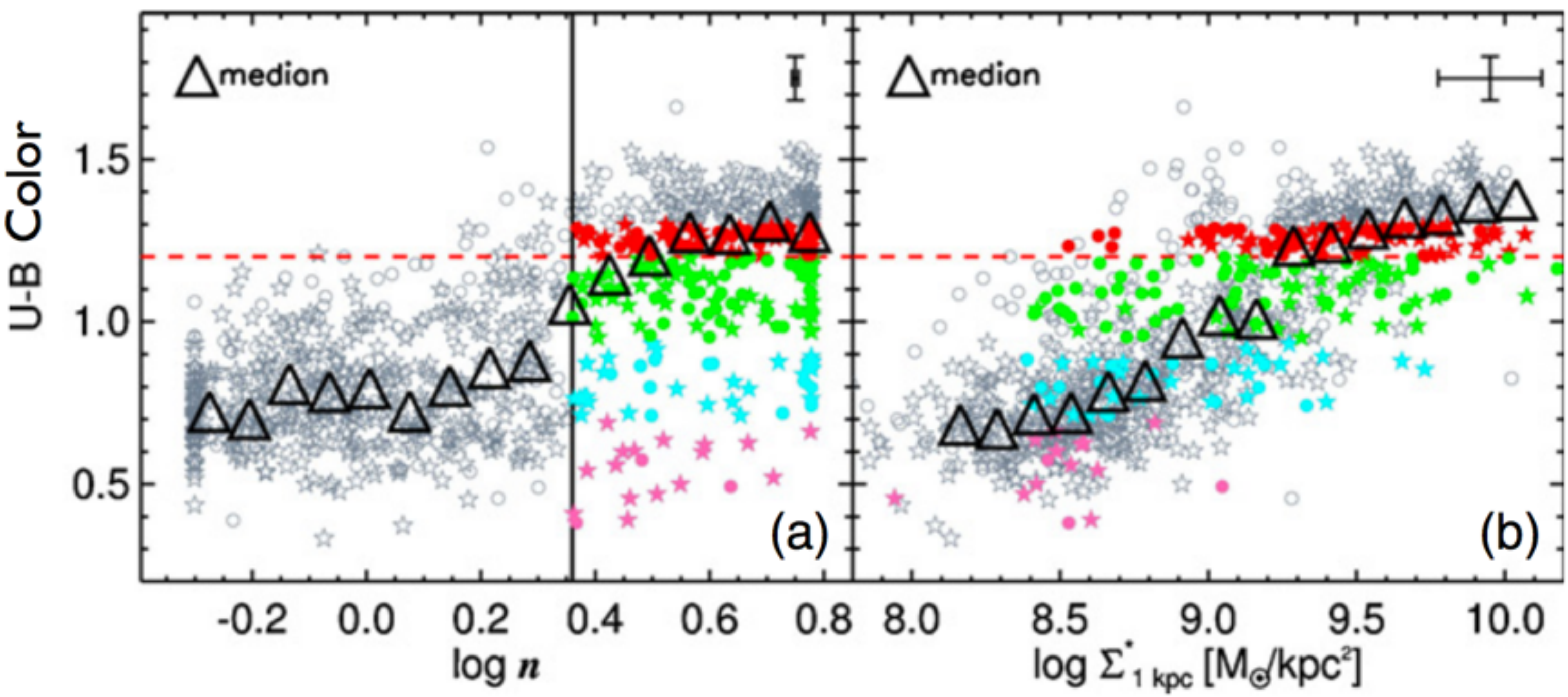

Cheung+12

Galaxies at z~0.8 (AEGIS survey)

Astro/Phys 224 Spring 2014

Origin and Evolution of the Universe

Week 8

Galaxy Evolution; Small Scale Issues

Joel Primack

University of California, Santa Cruz

galaxies on 'star forming (main) sequence' are disks with $\Sigma_{\text{star form}}$ & n_{Sersic} increasing above sequence

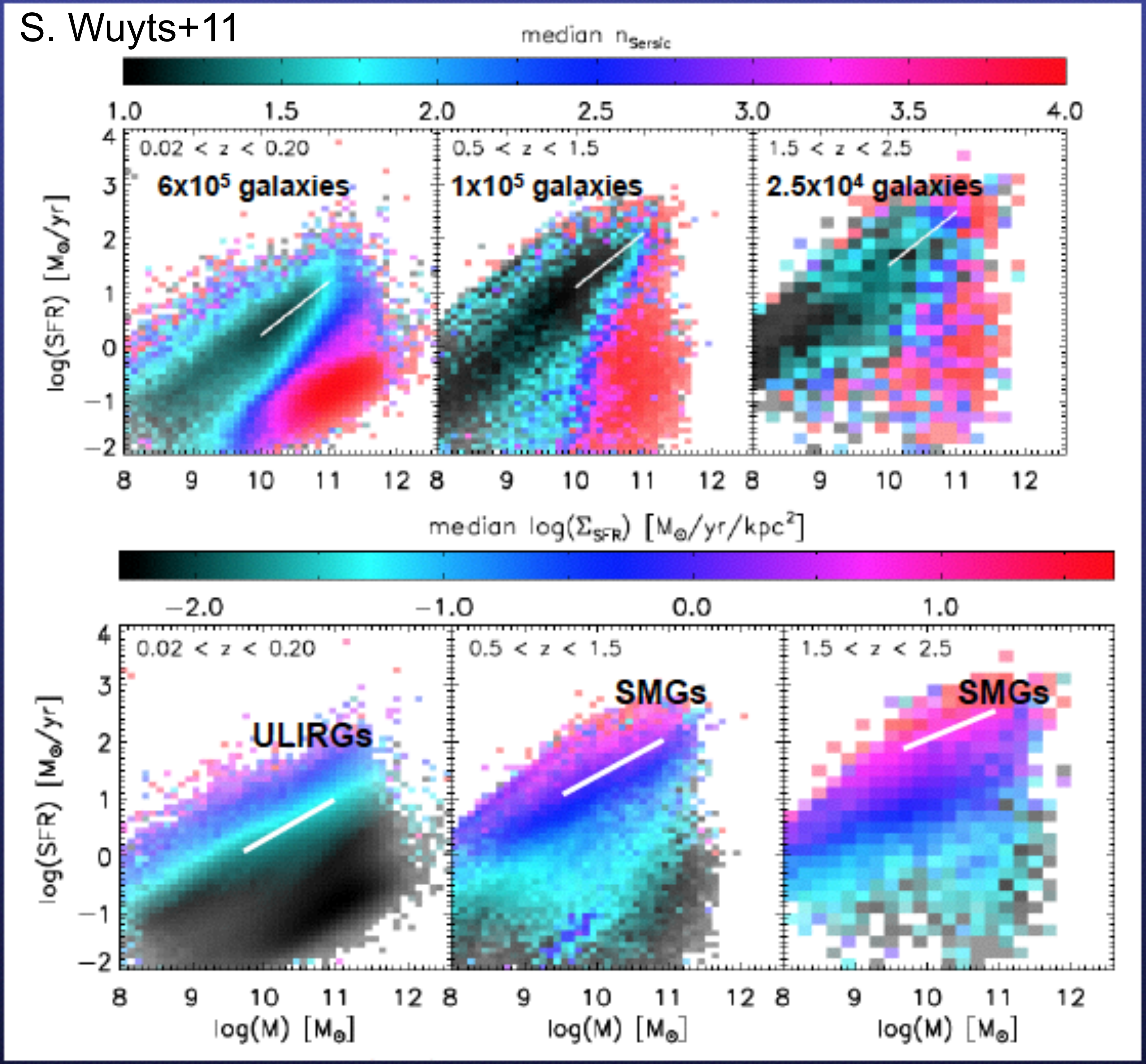

$I(r)=\exp(-r^{1/n_{\text{Sersic}}})$

Disks: $n_{\text{Sersic}} \approx 1$

Spheroids: $n_{\text{Sersic}} \approx 4$

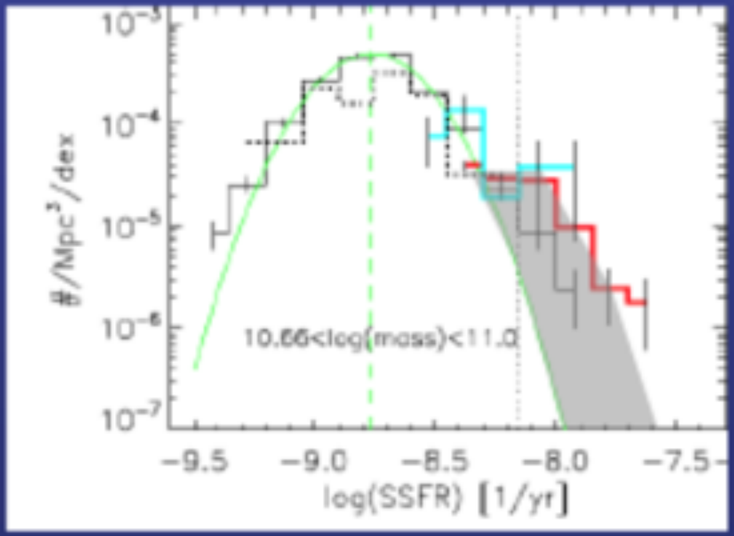

Rodighiero et al. 2011 (PEP):
off-ms galaxies account for ~10% of cosmic star formation at z~2

Correlation between luminosity and dustiness

LIRG: $L_{FIR} \geq 10^{11} L_{\odot}$ ULIRG: $L_{FIR} \geq 10^{12} L_{\odot}$ HLIRG: $L_{FIR} \geq 10^{13} L_{\odot}$

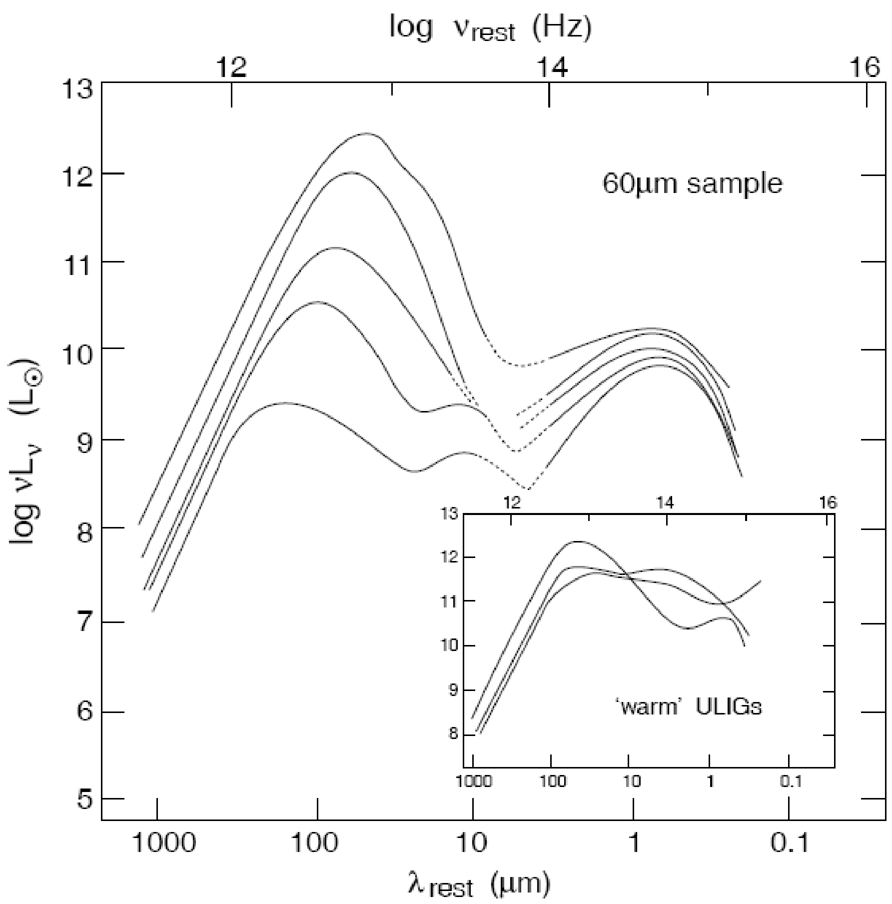

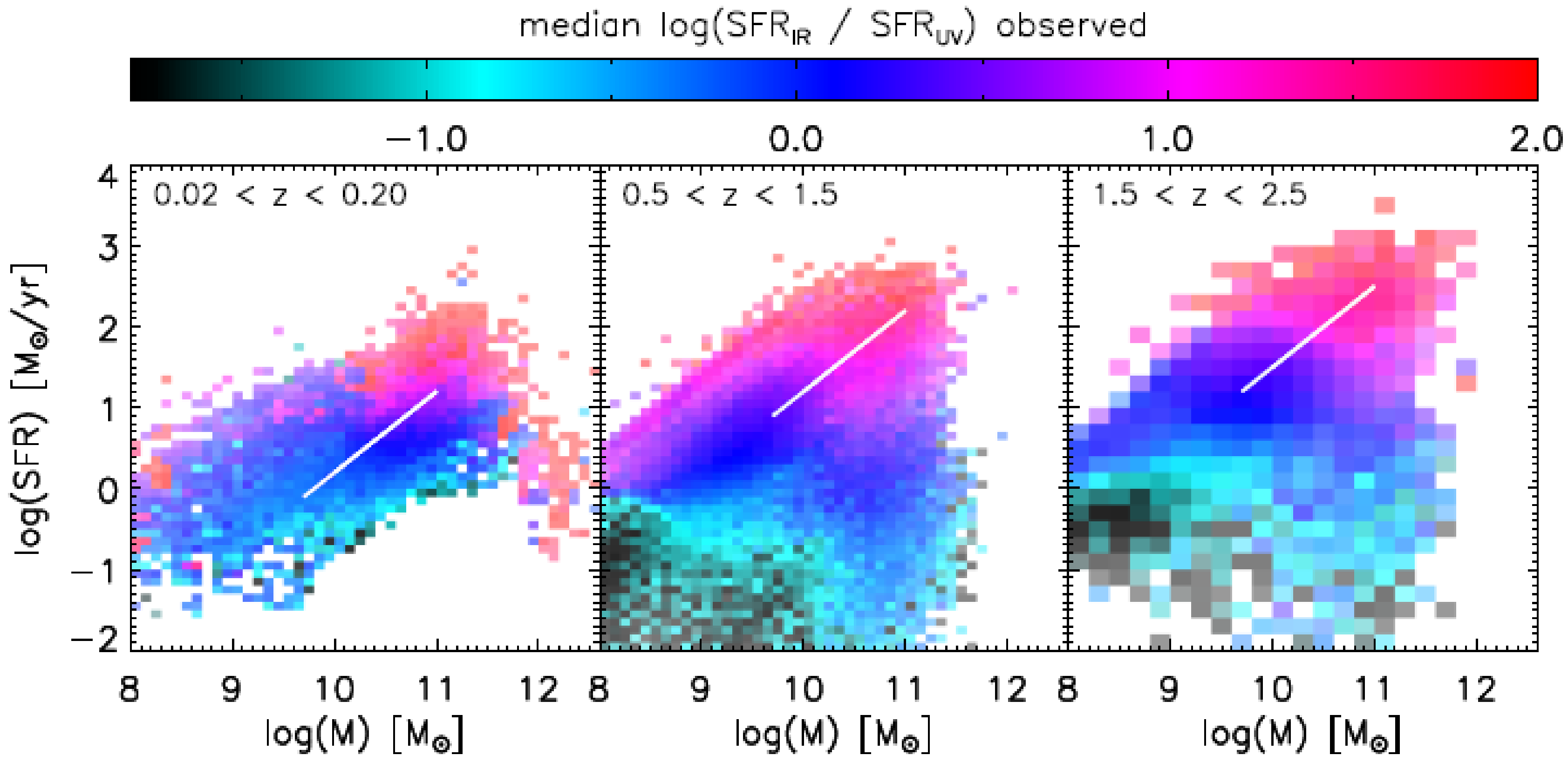

more luminous and massive galaxies are (much) more obscured: for starbursts and (U)LIRGs a de-reddening of the UV-emission does not succeed: the central starburst is behind a 'black screen' and the UV emission comes from a lower obscuration component; even de-reddened Hα fails by about a factor of 10; ULIRGs/starbursts often have 'post-starburst' UV/optical SEDs while the real starburst is completely hidden

Sanders & Mirabel 1996, Meurer et al. 1999,Wuyts et al. 2011

Herschel far-IR

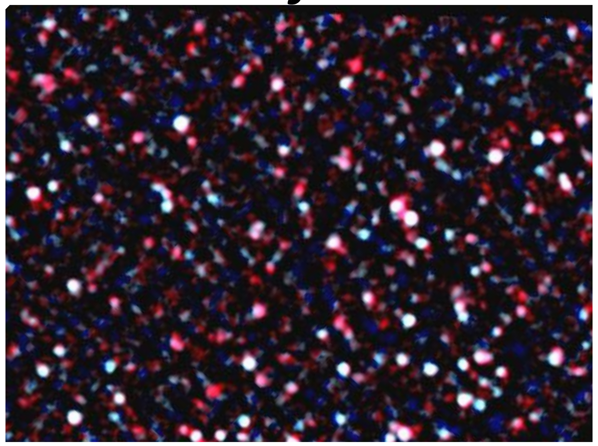

Spitzer mid-IR

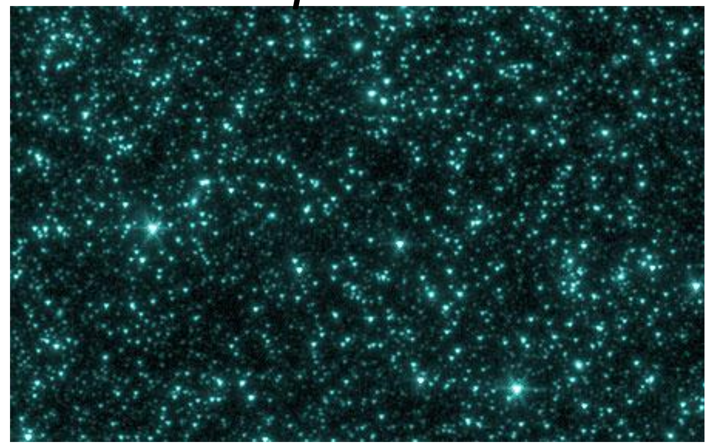

HST-optical/UV

0.850-1.2mm

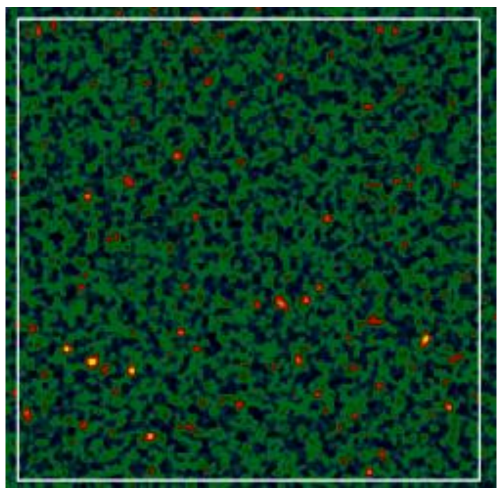

in the future: ALMA, CCAT..

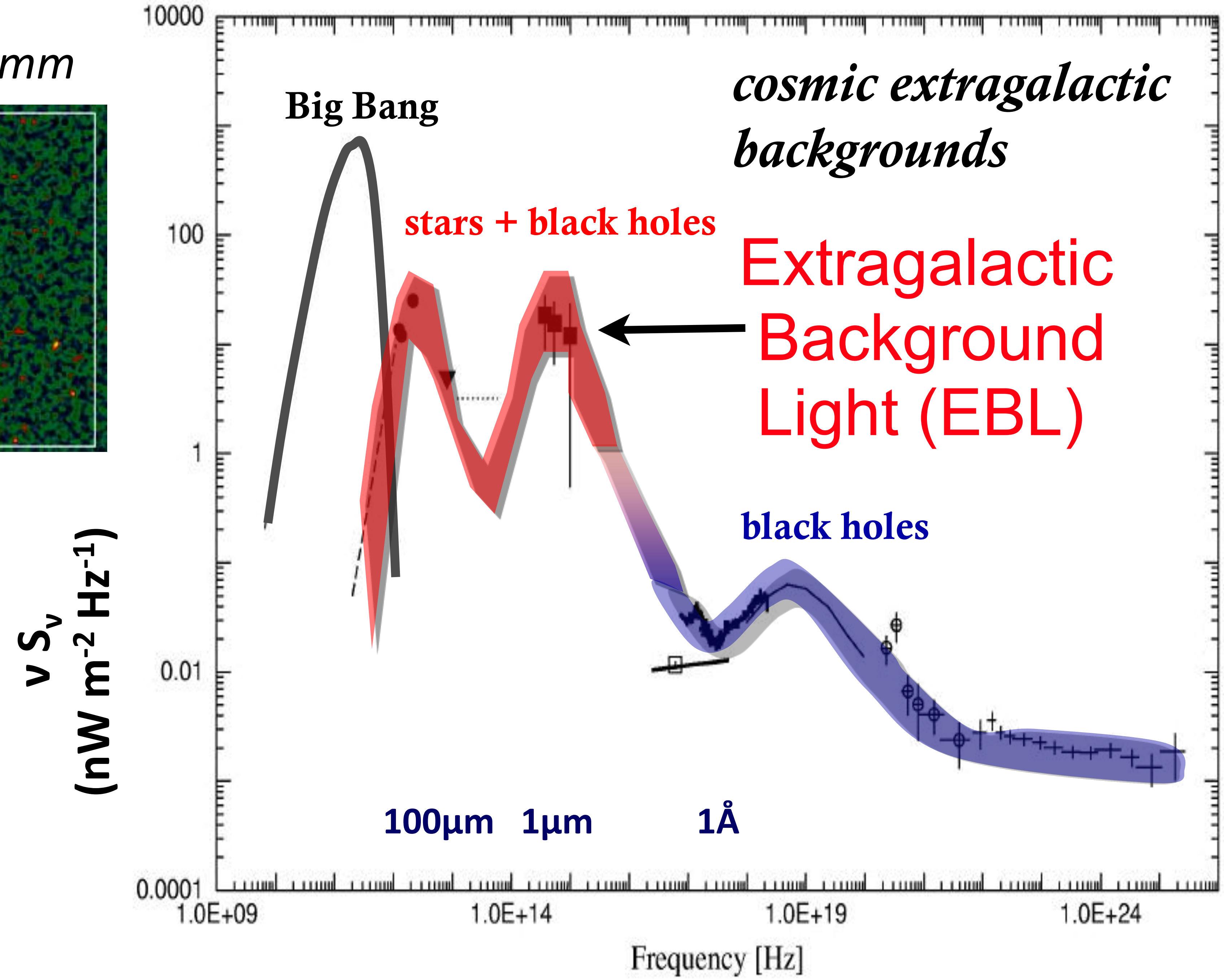

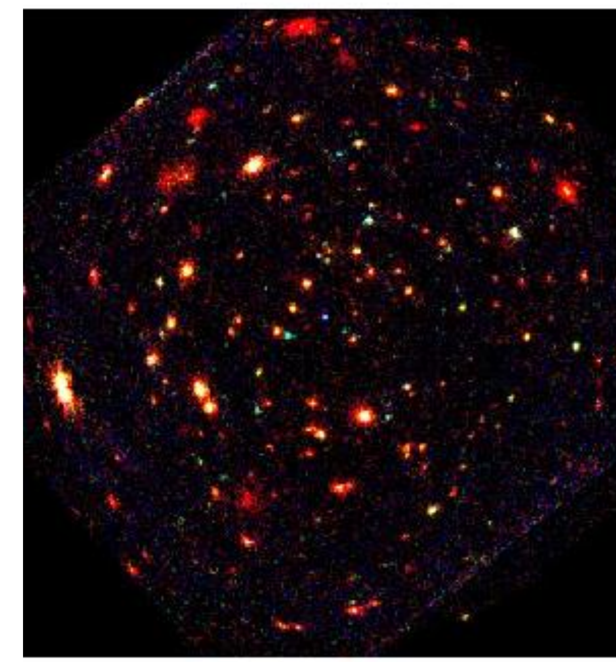

Chandra/XMM –X-ray

Extragalactic Background Light (EBL)

- The usual plot of $\lambda I_\lambda = dI/d \log \lambda$ vs. $\log \lambda$ shows directly the ENERGY DENSITY $\rho_\lambda = (4\pi/c)\, \lambda I_\lambda$ in the EBL:

  $$1 \text{ nW/m}^2\text{/sr} = 10^{-6} \text{ erg/s/cm}^2\text{/sr} = 2.6\times10^{-4} \text{ eV/cm}^3$$

  Total EBL $\Omega_{EBL}{}^{obs} = (4\pi/c)\, I_{EBL}/(\rho_{crit}\, c^2) = 2.0 \times10^{-4}\, I_{EBL}\, h_{70}{}^{-2}$

  The estimated $I_{EBL}{}^{obs}$= 60-100 nW/m^2/sr translates to

  $$\Omega_{EBL}{}^{obs} =(3\text{-}5) \times10^{-6} \quad (\text{about } 5\% \text{ of } \Omega_{CMB})$$

- Local galaxies typically have $E_{FIR}/E_{opt} \approx 0.3$, while the EBL has E_{FIR}/E_{opt} = 1-2. **This implies that most high-redshift radiation was emitted in the far IR.**

Spectral Energy Distribution (SED) vs. L_{IR}

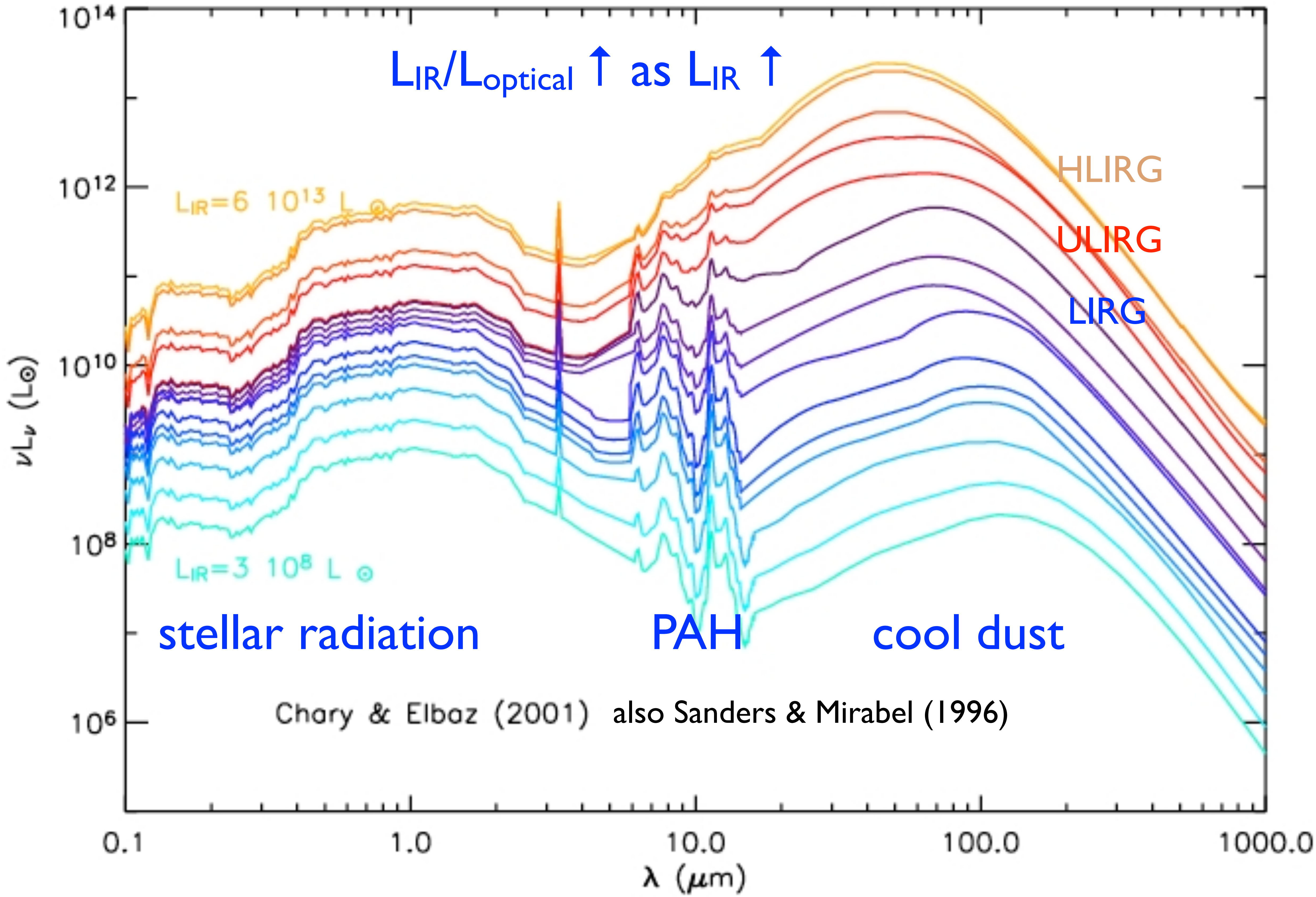

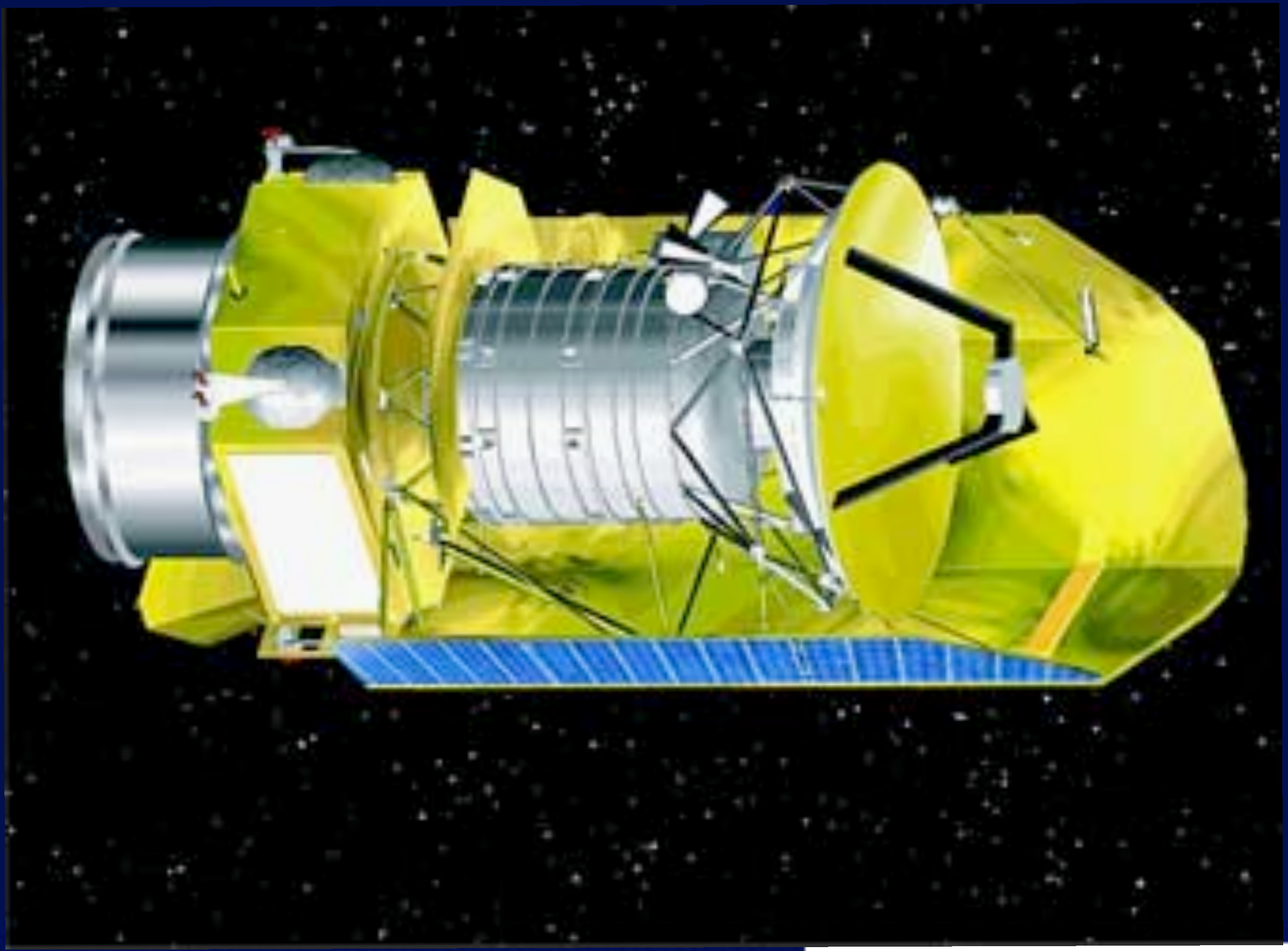

The Herschel Space Observatory has shown that there are two types of galaxy SEDs. Herschel was a space observatory built and operated by the European Space Agency (ESA) in L2. It was active from 2009 to 2013, and was the largest infrared telescope ever launched, carrying a single 3.5-meter (11.5 ft) mirror and instruments sensitive to the far infrared and submillimetre wavebands (55–672 μm).

Elbaz et al. 2010, 2011, Hwang et al. 2011, Nordon et al. 2010, 2011

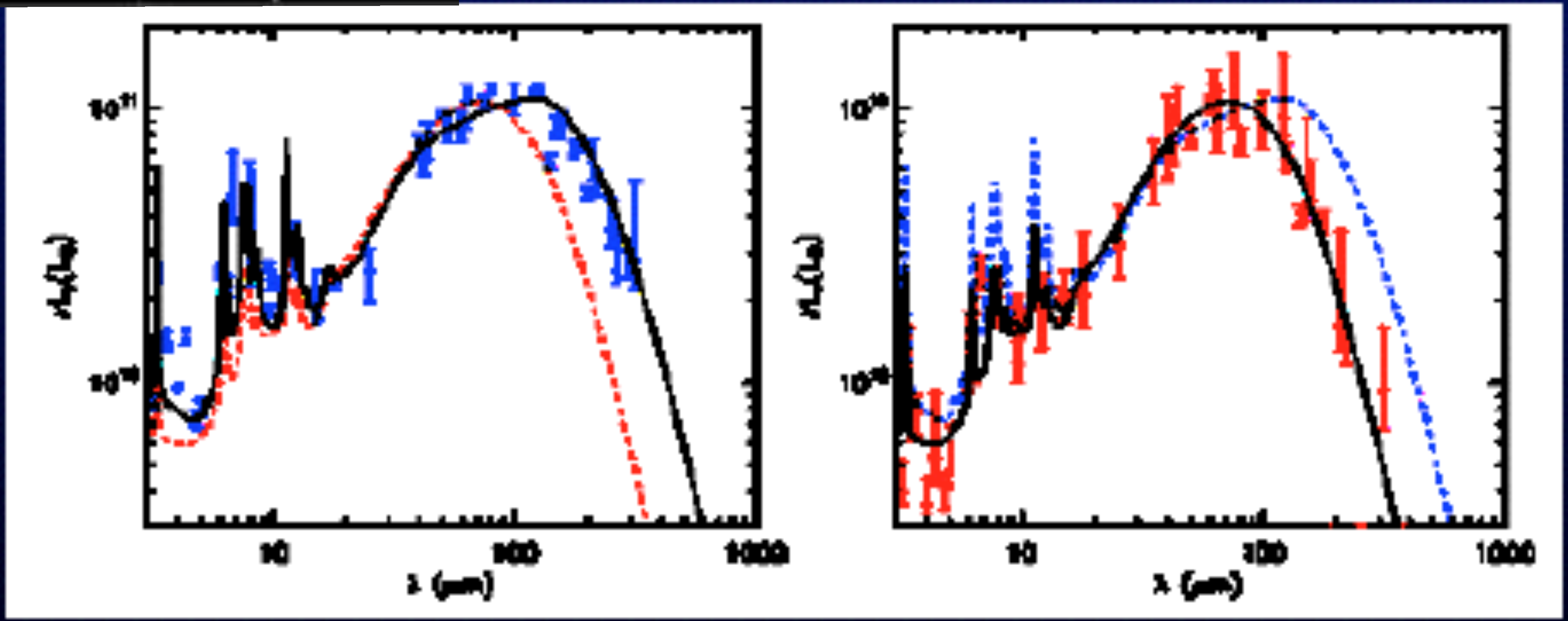

main-sequence galaxies across z have remarkably uniform infrared spectral energy distributions

off-main-sequence galaxies across z are warmer and have much lower PAH emission

Define IR8 ≡ $L_{IR}/L8$

A&A 533, A119 (2011)

$L_{IR}=10^{11}\ L_{\odot}$ Galaxies:

Main Sequence brighter than Starbursts in PAH and submm

IR8 ≈ 4±1.6 (1σ) IR8≳8

D. Elbaz et al.: GOODS–*Herschel*: an infrared main sequence for star-forming galaxies

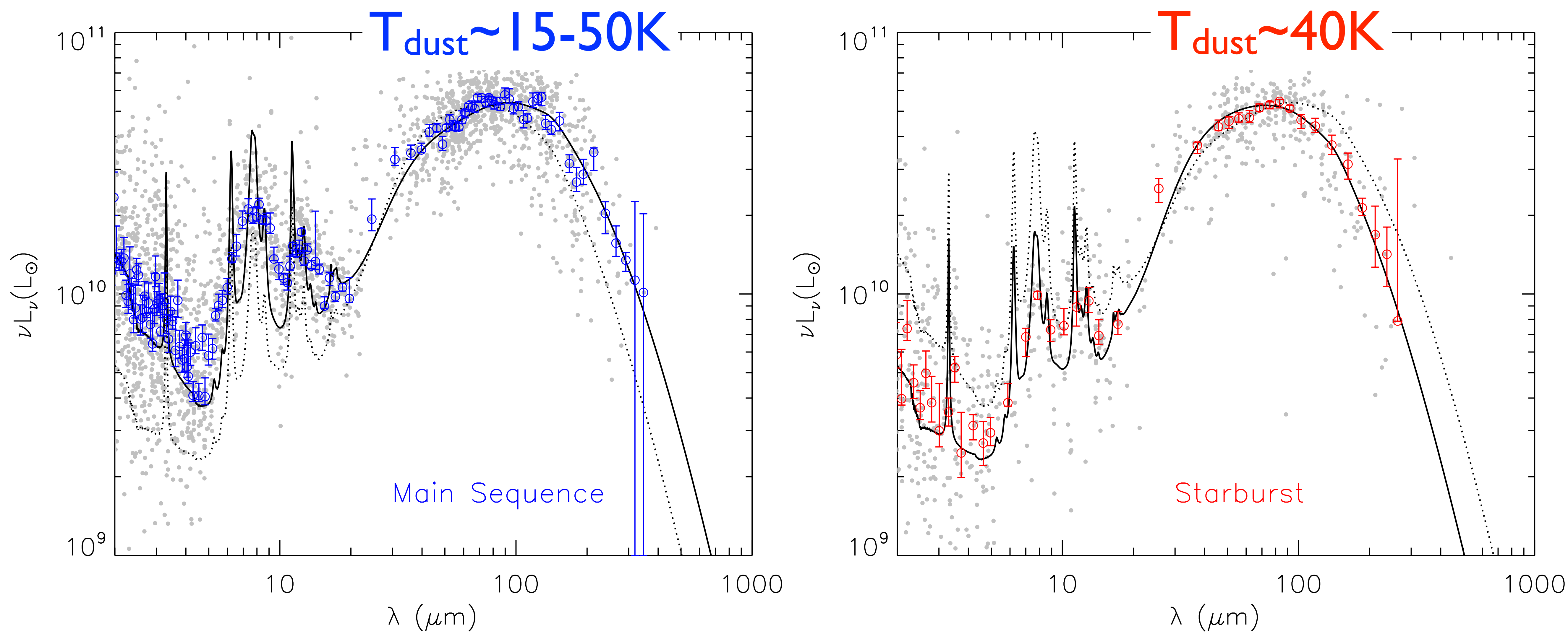

Fig. 21. Composite spectral energy distribution of the typical main sequence galaxy (*left*; IR8 = 4 ± 2, see Eq. (5)) and starburst (*right*; IR8 > 8, i.e., above 2σ). Light grey dots: individual GOODS–*Herschel* galaxies normalized to $L_{\rm IR}^{\rm tot} = 10^{11}\ L_{\odot}$. The large filled symbols with error bars are the median and associated uncertainty of the MS (*left figure*, blue dots) and SB (*right figure*, red dots) galaxies computed in intervals of wavelengths defined to contain a fixed number of 25 ± 5 galaxies. The uncertainty on the median values is derived from the 16th and 84th percentiles around the median divided by the square root of the number of galaxies. The model fit to each SED is shown with a solid black line while the opposing SED (MS or SB) is shown with a dotted black line for comparison.

See also Magdis+12 for Herschel SED templates

EBL Evolution Calculated from Observations Using AEGIS Multiwavelength Data

Alberto DomÍnguez, Joel Primack, et al. (MNRAS, 2011)

$$j_i(\lambda, z) = j_i^{faint} + j_i^{mid} + j_i^{bright} =$$

$$= \int_{M_1}^{M_2} \Phi(M_K, z) f_i T_i(M_K, \lambda) dM_K +$$

$$+ \int_{M_2}^{M_3} \Phi(M_K, z) m_i T_i(M_K, \lambda) dM_K +$$

$$+ \int_{M_3}^{M_4} \Phi(M_K, z) b_i T_i(M_K, \lambda) dM_K$$

Spectral energy distributions
SWIRE template library, Polletta+ 07

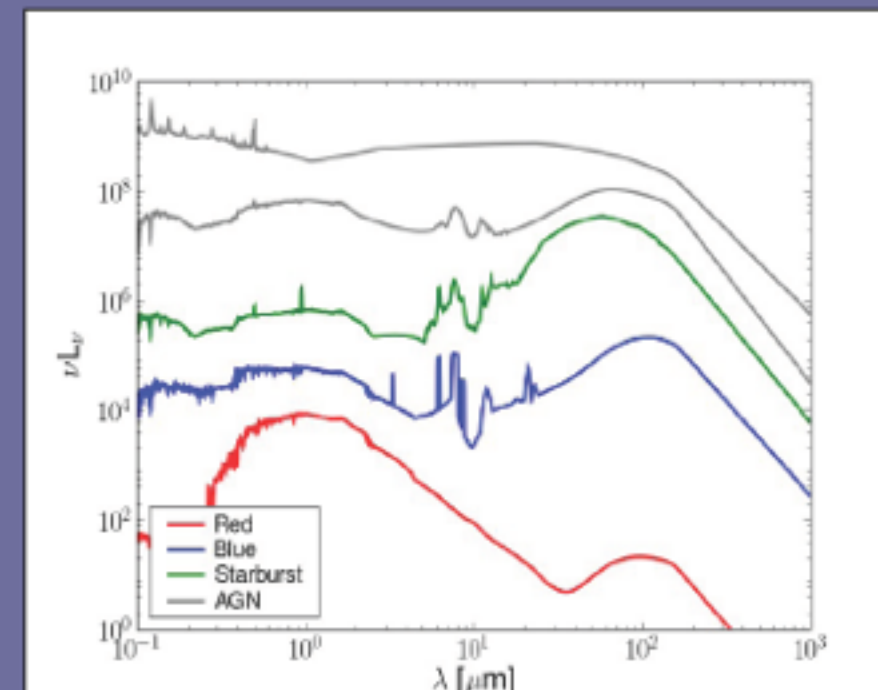

Luminosity function
observed K-band, Cirasuolo+ 09

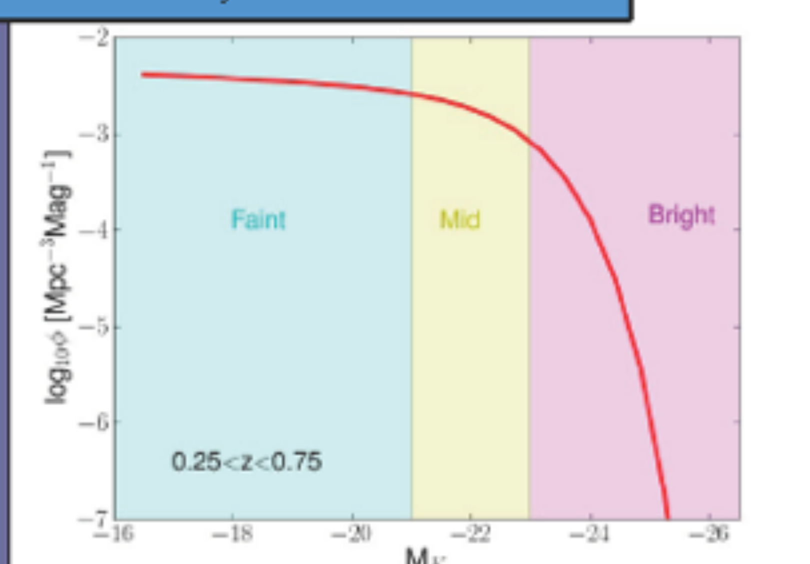

Spectral-type fractions

$$\lambda I_\lambda(z) = \frac{c}{4\pi} \int_z^{z_{max}} j_{total}[\lambda(1+z)/(1+z'), z'] \left| \frac{dt}{dz'} \right| dz'$$

http://aegis.ucolick.org/

Local Extragalactic Background Light

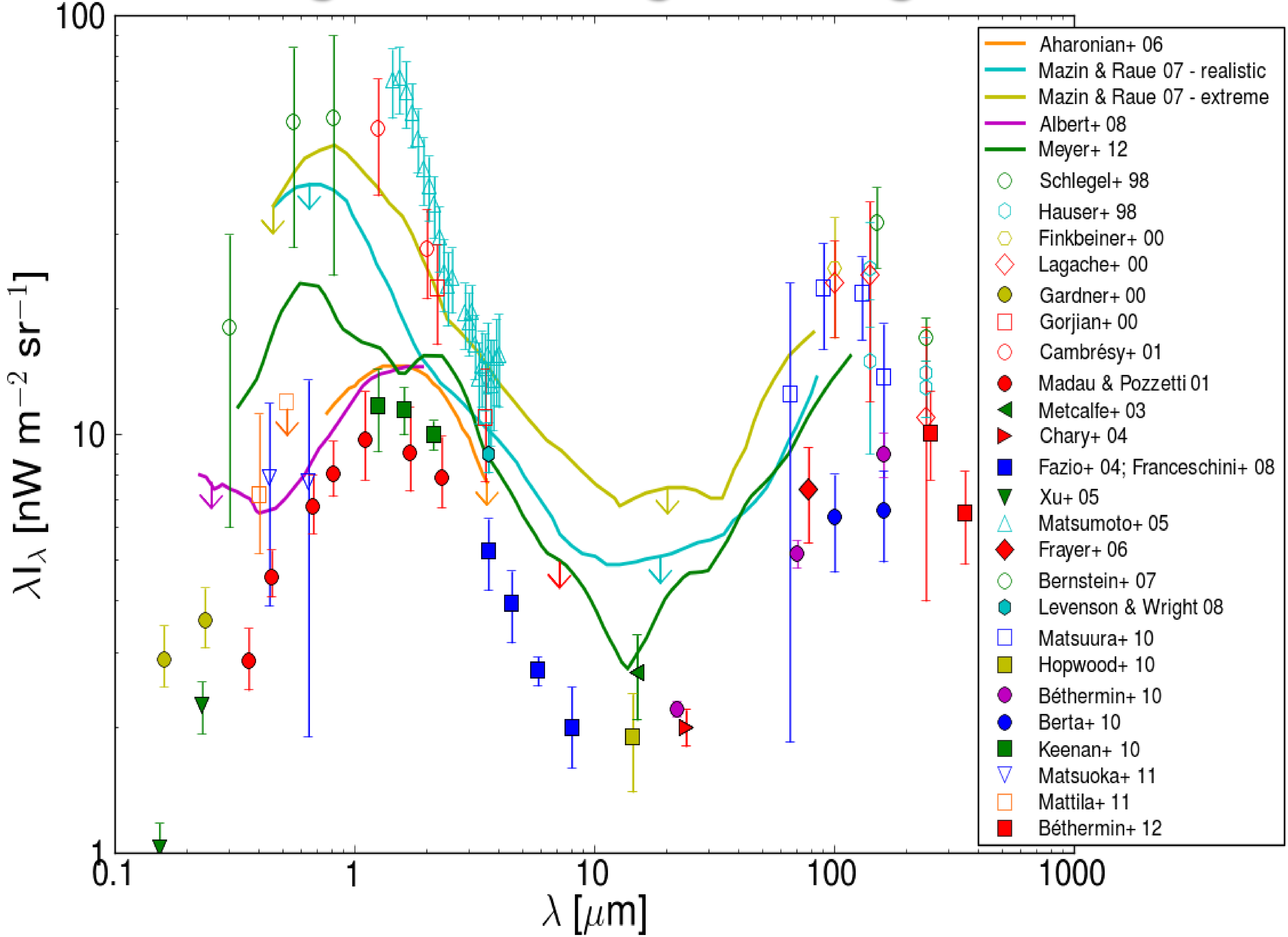

Local Extragalactic Background Light

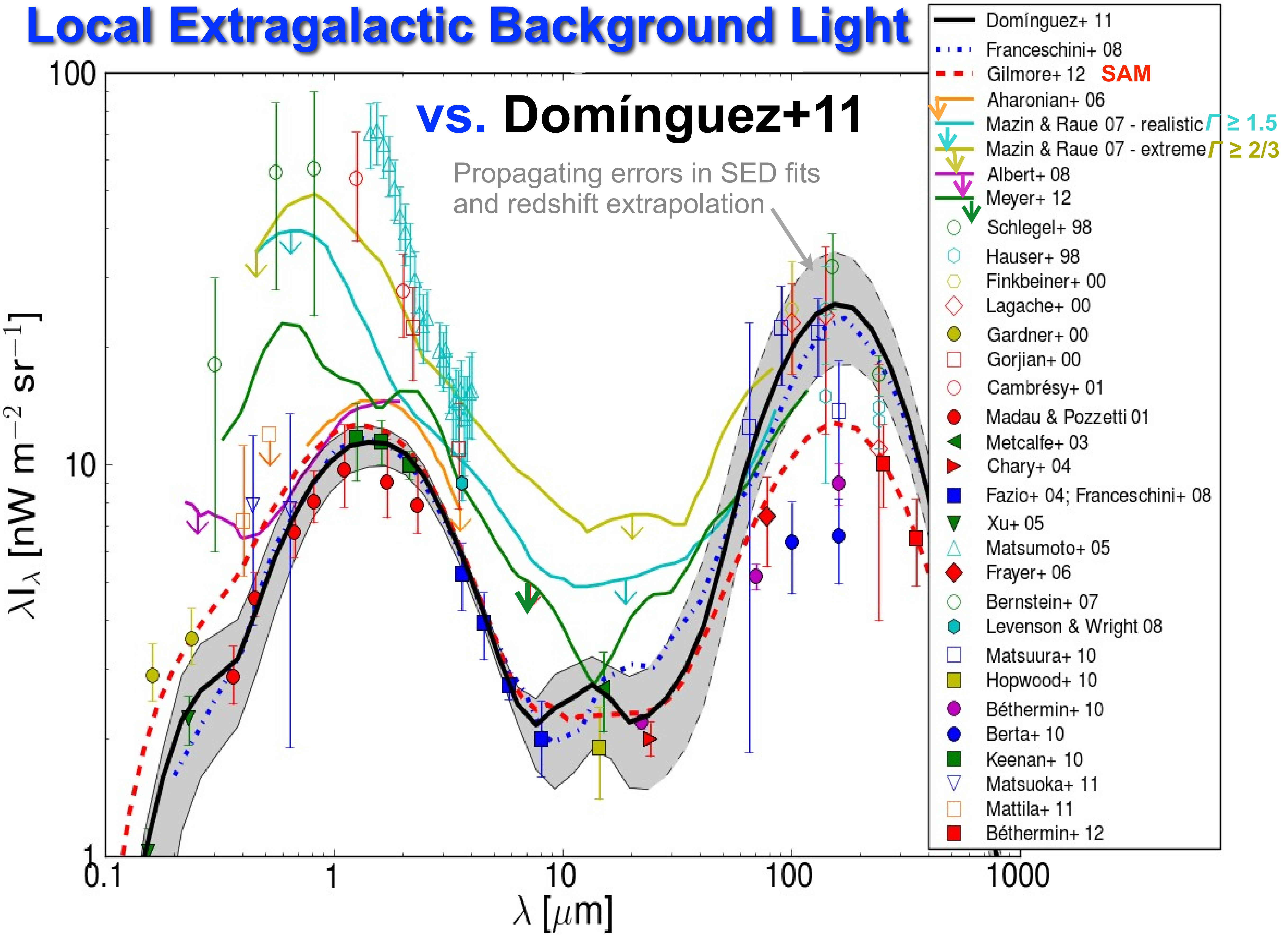

Local Extragalactic Background Light

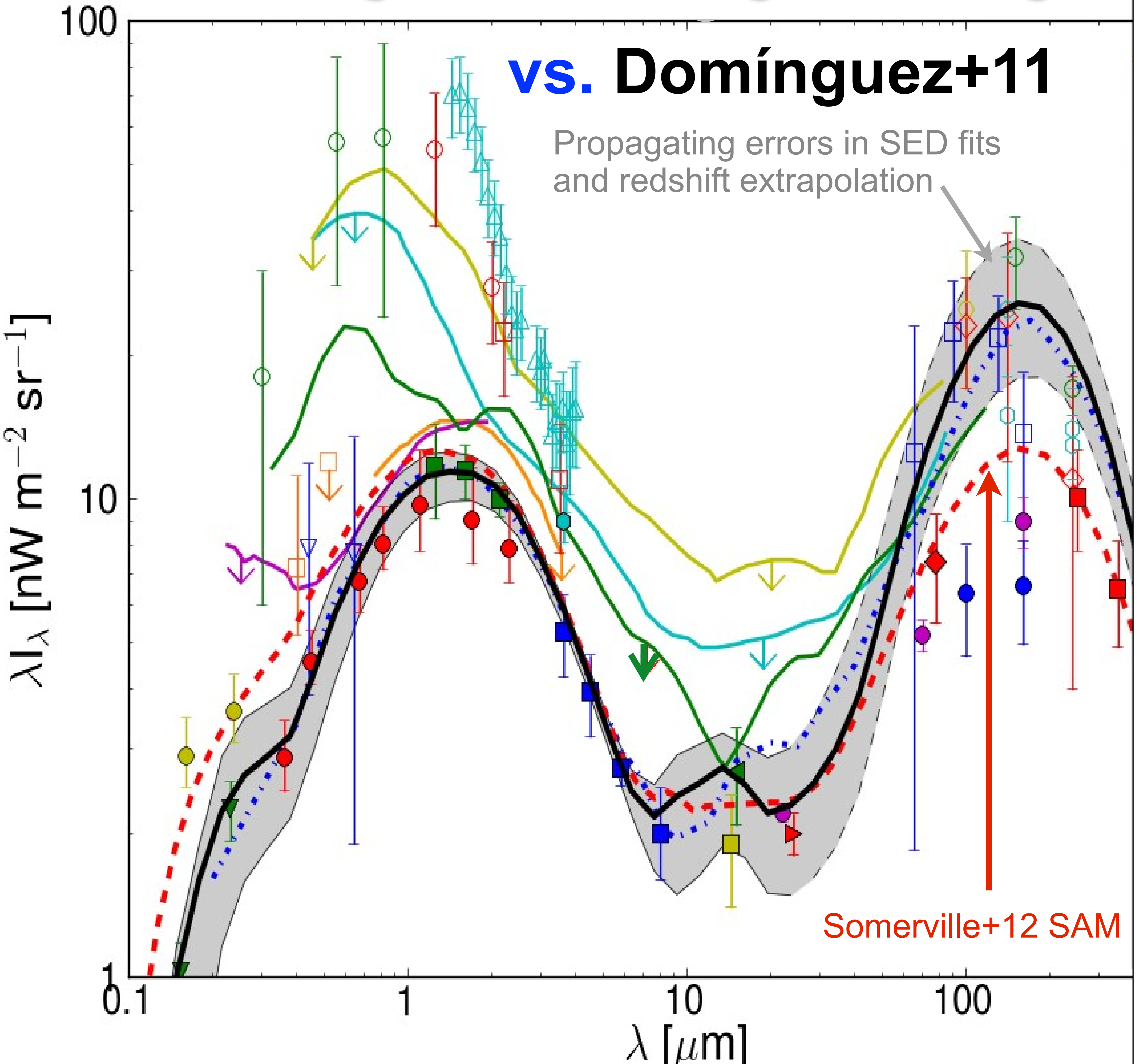

Note that the IR EBL is at least as high as the optical EBL. Since few nearby galaxies are strong IR emitters, this IR must have come from higher redshift and been diluted by cosmic expansion. Thus most of the radiation emitted at higher z must have been emitted at long wavelengths by dust.

Note also that the Somerville+12 SAM gives much less Far IR EBL than the direct measurement by Dominguez+11. This SAM's greatest discrepancy compared with observations is at long wavelengths. That should be improved using Chris Hayward's new *Sunrise* modeling of ULIRGs.

Some Results from Somerville+12 SAM

Number Counts in UV, b, i, z, K Bands

Number Counts in 3.6, 8, 24, 70, 250, & 850 μm Bands

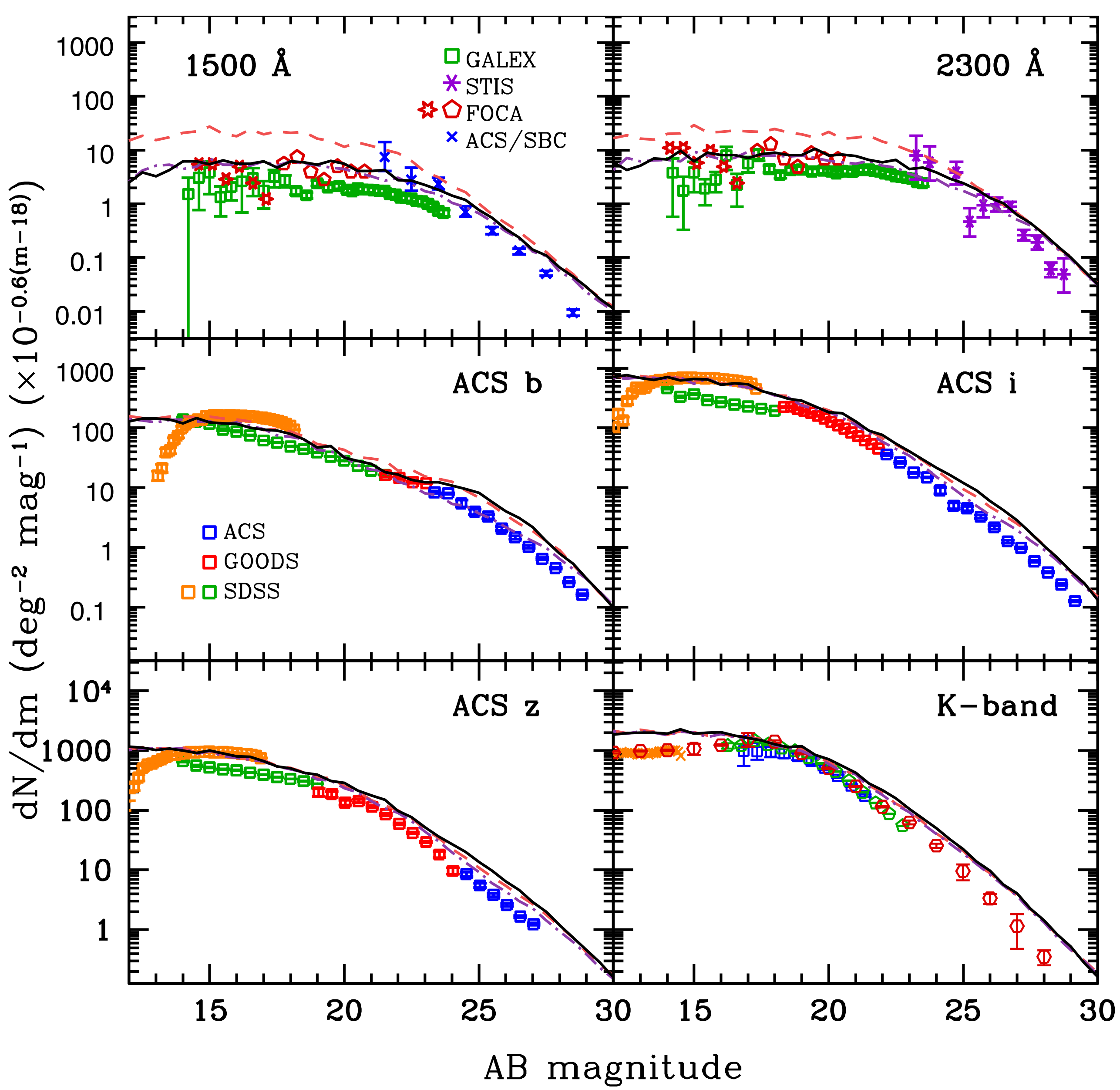

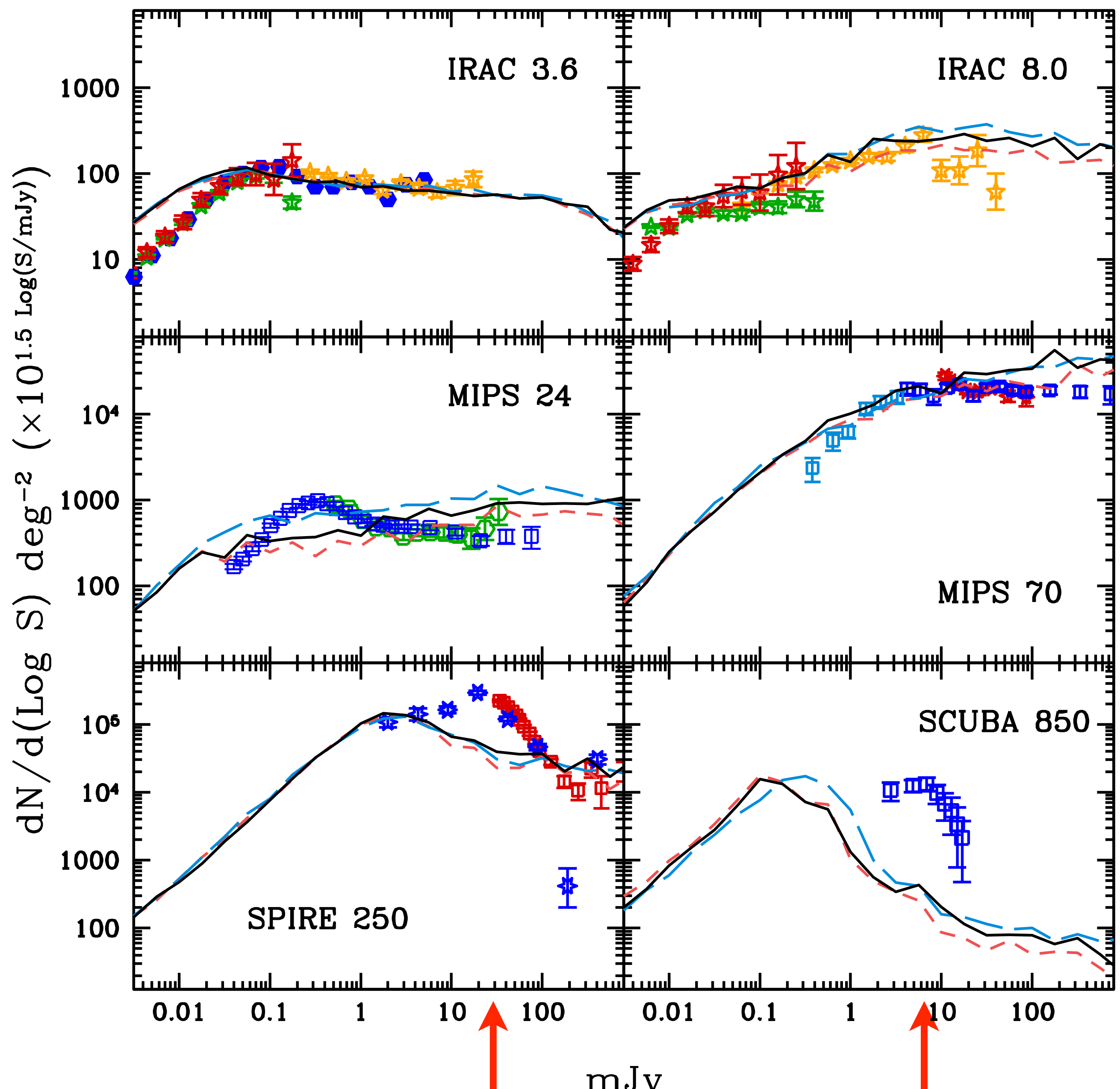

Somerville, Gilmore, Primack, & Dominguez (2012)

Far-IR Underpredictions

Conclusions from Chris Hayward's recent papers based on simulated galaxy mergers with *Sunrise* dust modeling:

- Submm galaxies are a heterogeneous population, including coalescence phase of major gas-rich mergers, but also galaxies with much less star formation and cool dust

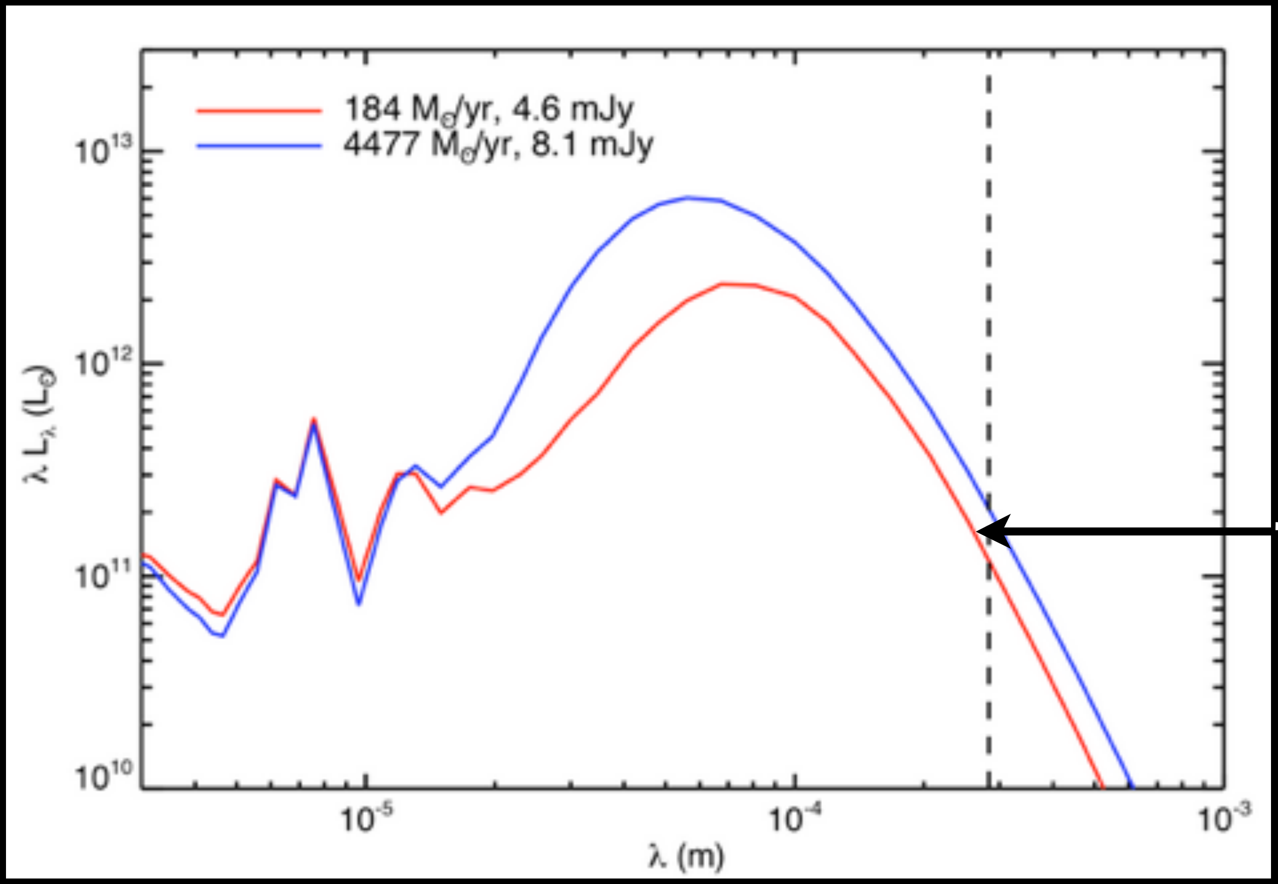

https://www.cfa.harvard.edu/~chayward/research.html

submm flux differ by less than a factor of 2

- significant contribution to single-dish counts from blended galaxy pairs

- Counts can be matched with standard IMF

Evolution of the EBL

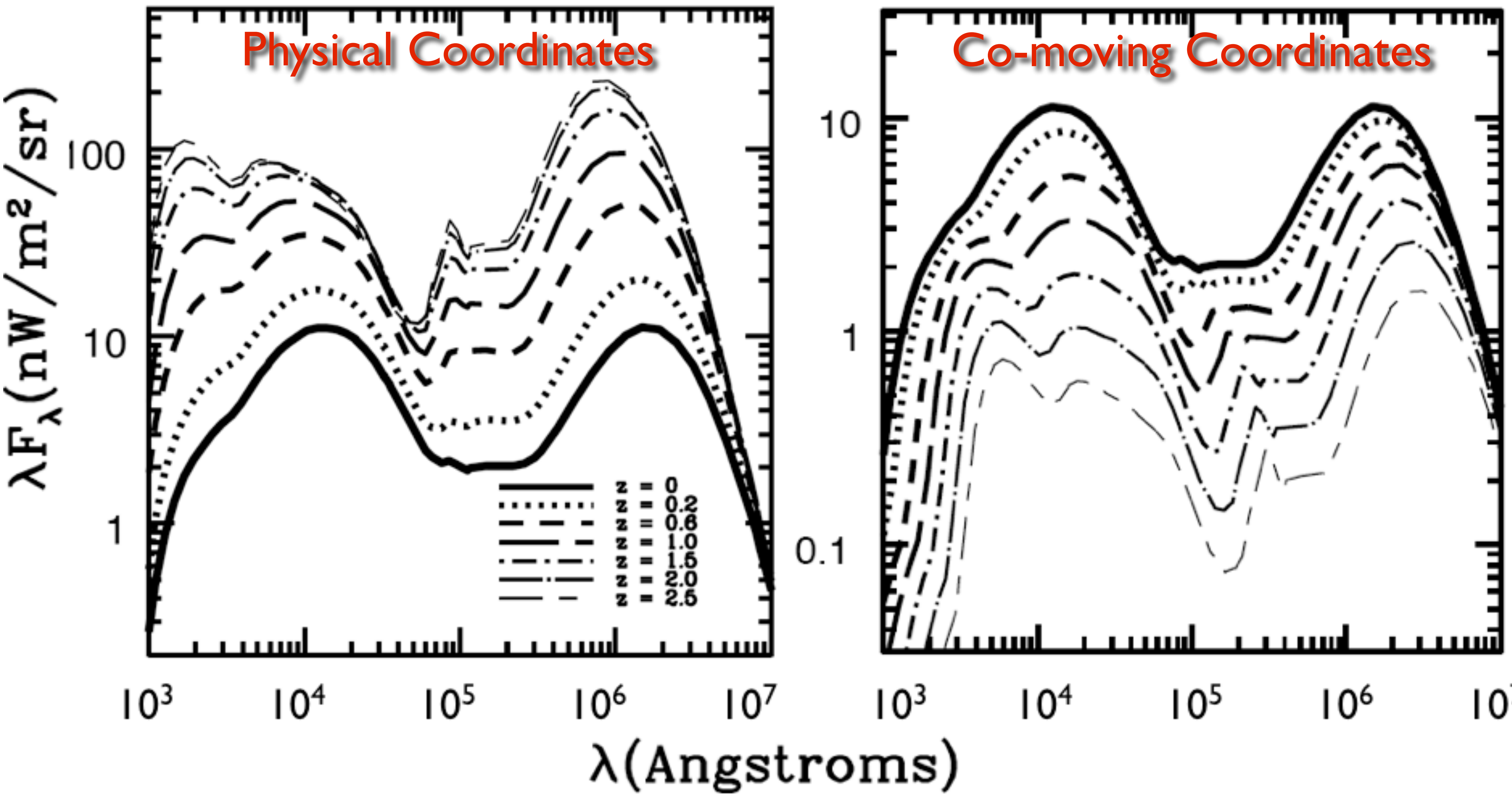

The evolution of the EBL in our WMAP5 Fiducial model. This is plotted on the left panel in standard units. The right panel shows the build-up of the present-day EBL by plotting the same quantities in comoving units. The redshifts from 0 to 2.5 are shown by the different line types in the key in the left panel.

Gilmore, Somerville, Primack, & Domínguez (2012)

Extragalactic Background Light (EBL)

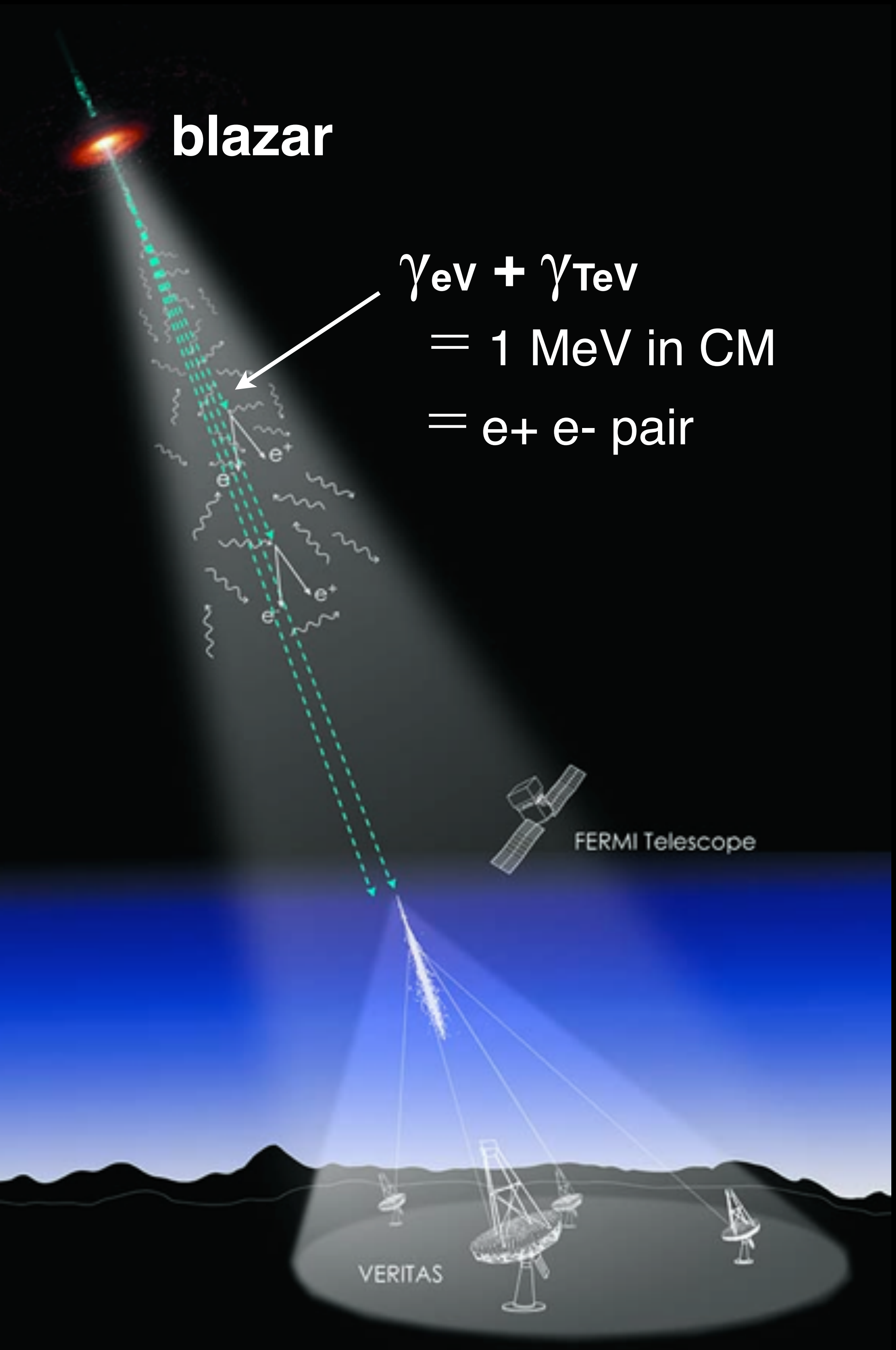

Data from (non-) attenuation of gamma rays from blazars and gamma ray bursts (GRBs) give upper limits on the EBL from the UV to the mid-IR that are only a little above the lower limits from observed galaxies. New data on attenuation of gamma rays from blazers now lead to statistically significant measurements of the cosmic gamma ray horizon (CGRH) as a function of source redshift and gamma ray energy that are independent of EBL models. These new measurements are consistent with recent EBL calculations based both on multiwavelength observations of thousands of galaxies and also on semi-analytic models of the evolving galaxy population. Such comparisons account for (almost) all the light, including that from galaxies too faint to see.


PILLAR OF STAR BIRTH
Carina Nebula in UV Visible Light
WFC3/UVIS


PILLAR OF STAR BIRTH
Carina Nebula in IR Light
Longer wavelength light
penetrates the dust better
Longer wavelength gamma rays
also penetrate the EBL better
WFC3/IR

Predicted Gamma Ray Attenuation

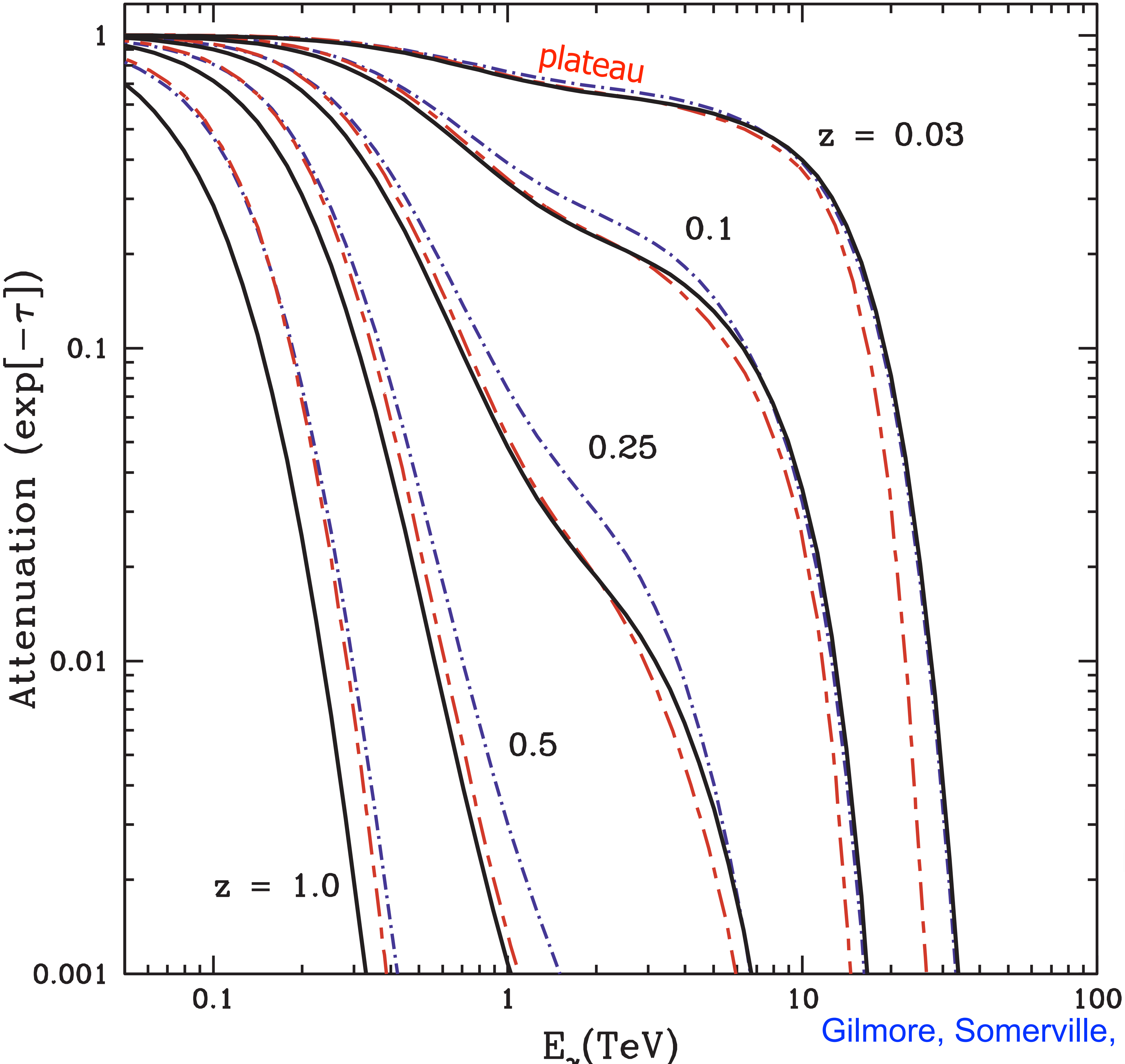

Increasing distance causes absorption features to increase in magnitude and appear at lower energies. The plateau seen between 1 and 10 TeV at low z is a product of the mid-IR valley in the EBL spectrum.

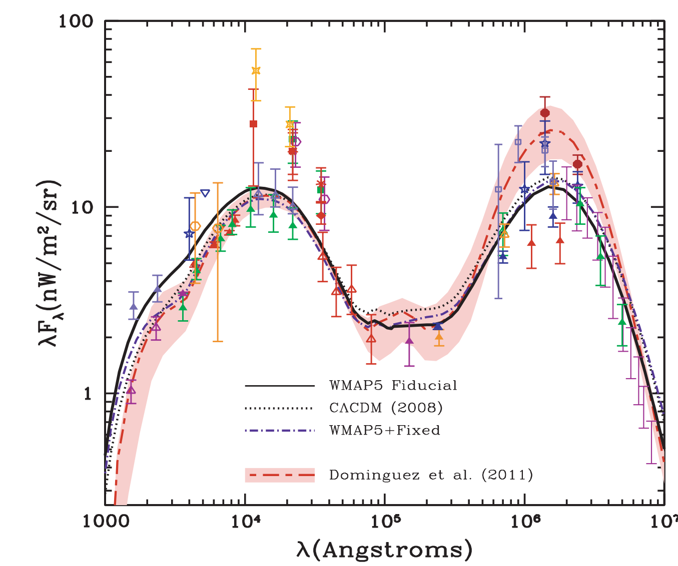

WMAP5 Fiducial
WMAP5 Fixed
Domiínguez+11

Gilmore, Somerville, Primack, & Domínguez (2012)

Gamma Ray Attenuation due to γγ → e+e-

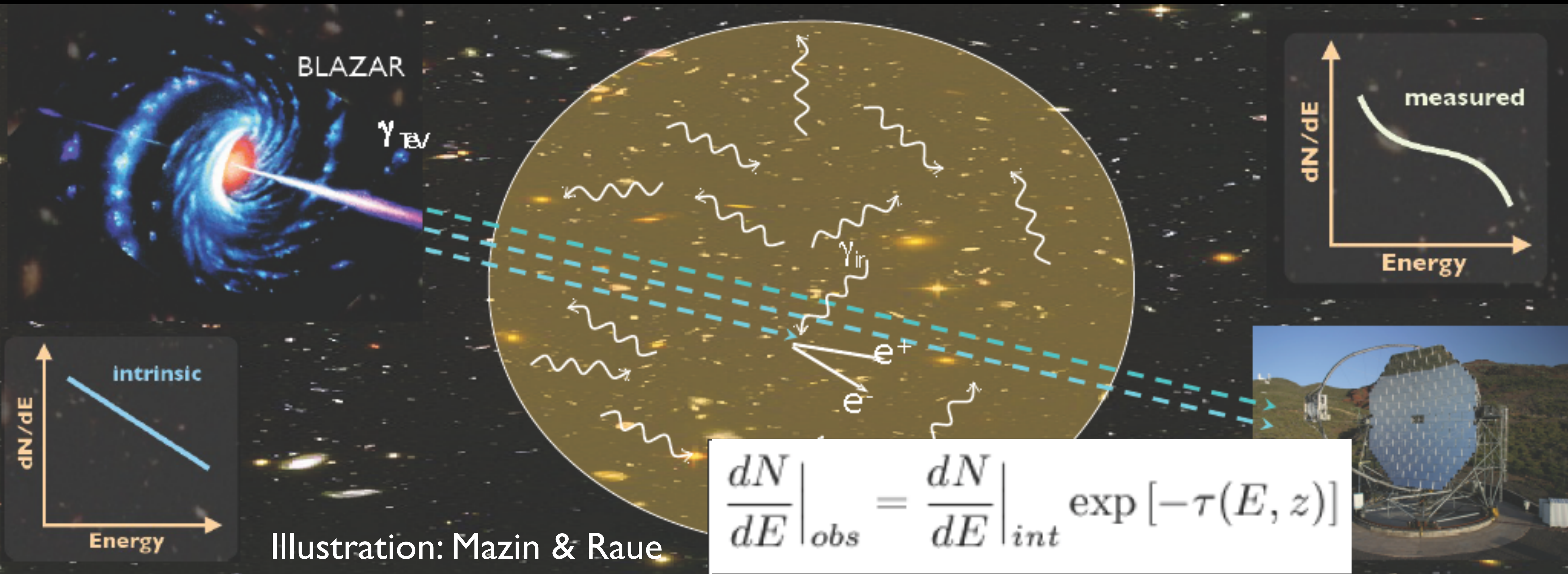

$$\left.\frac{dN}{dE}\right|_{obs} = \left.\frac{dN}{dE}\right|_{int} \exp\left[-\tau(E,z)\right]$$

If we know the intrinsic spectrum, we can infer the optical depth τ(*E*,*z*) from the observed spectrum. In practice, we typically *assume* that $dN/dE|_{int}$ is not harder than $E^{-\Gamma}$ with Γ = 1.5, since local sources have $\Gamma \geq 2$. More conservatively, we can assume that $\Gamma \geq 2/3$.

Local Extragalactic Background Light

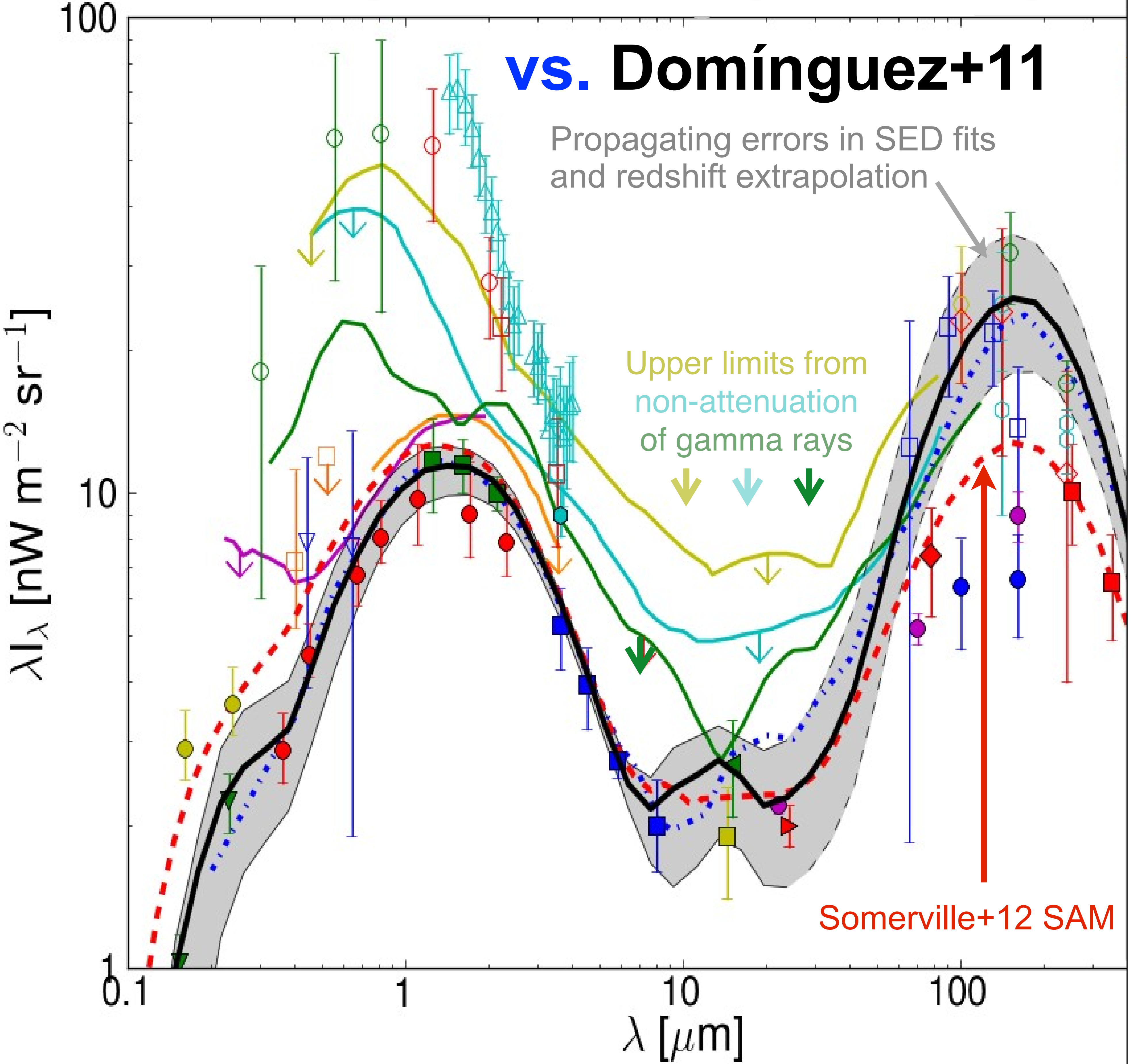

Note that the IR EBL is at least as high as the optical EBL. Since few nearby galaxies are strong IR emitters, this IR must have come from higher redshift and been diluted by cosmic expansion. Thus most of the radiation emitted at higher z must have been emitted at long wavelengths by dust.

Note also that the Somerville+12 SAM gives much less Far IR EBL than the direct measurement by Dominguez+11. This SAM's greatest discrepancy compared with observations is at long wavelengths. That should be improved using Chris Hayward's new *Sunrise* modeling of ULIRGs.

Predicted Gamma Ray Attenuation

The Cosmic Gamma Ray Horizon is the observed gamma ray energy as a function of redshift where the attenuation is 1/e = 0.368

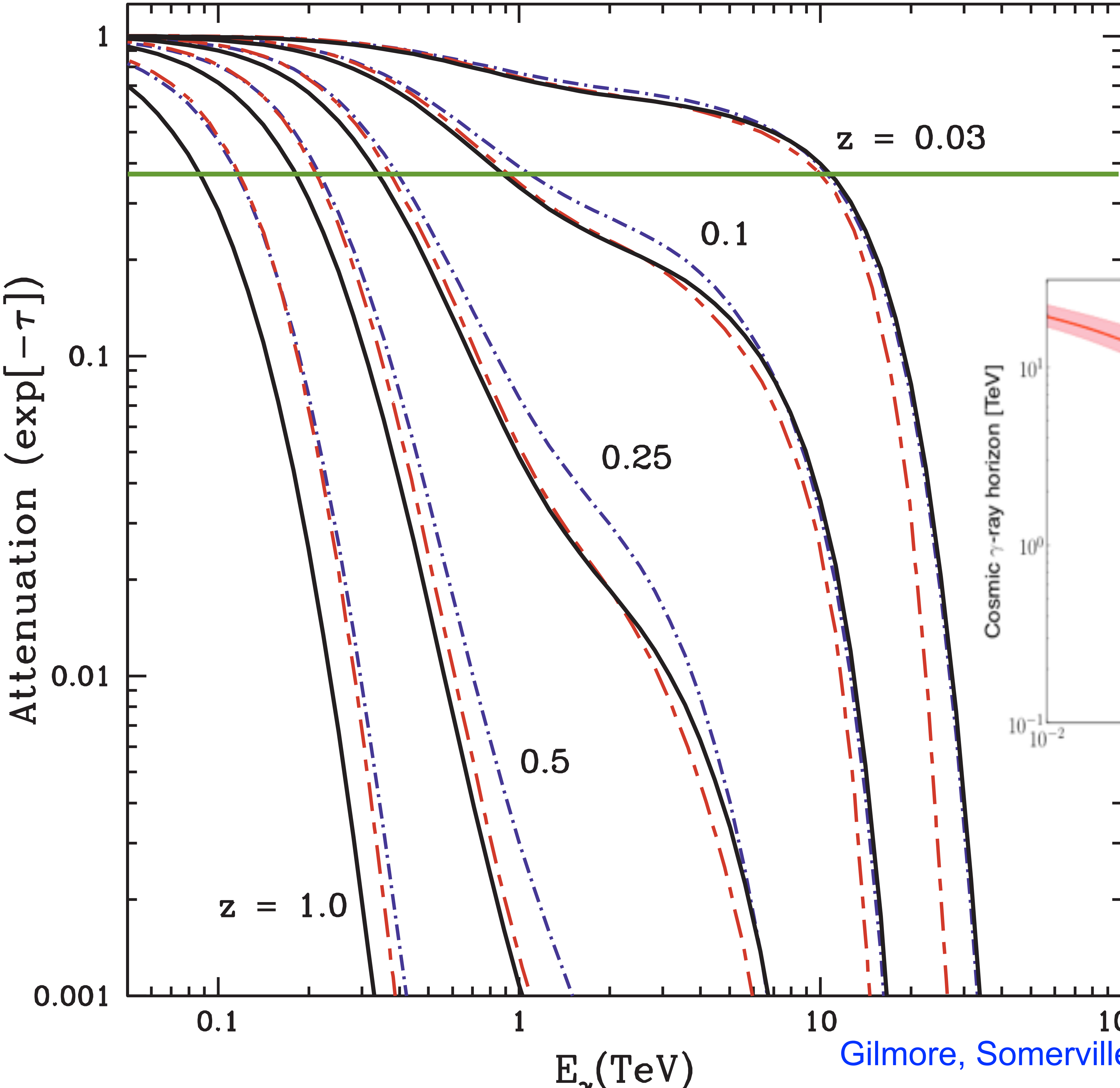

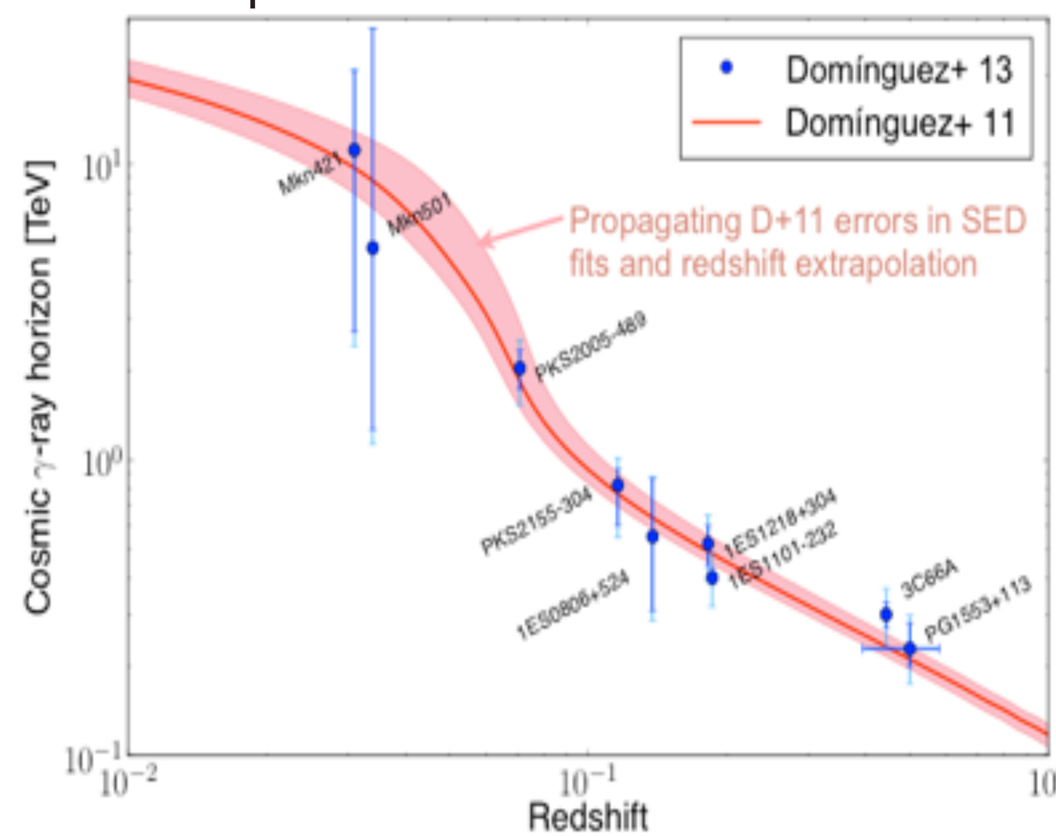

Gilmore, Somerville, Primack, & Domínguez (2012)

Cosmic Gamma-Ray Horizon

With a 50 GeV threshold, we see to z≈1.5-3 with less than 1/e attenuation!

100 GeV Threshold

50 GeV Threshold

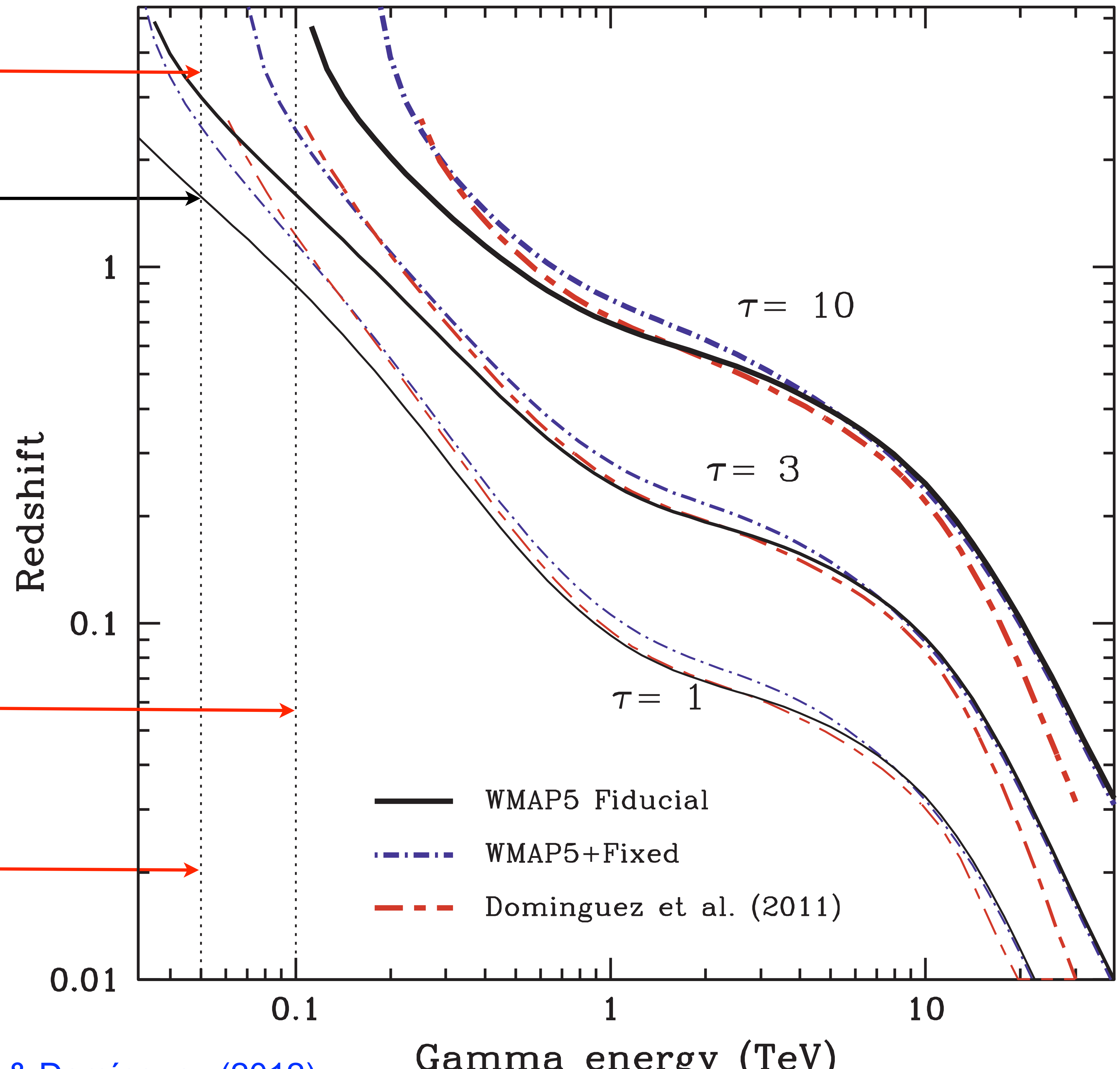

Gilmore, Somerville, Primack, & Domínguez (2012)

DETECTION OF THE COSMIC γ-RAY HORIZON FROM MULTIWAVELENGTH OBSERVATIONS OF BLAZARS

ApJ 770, 77 (2013)

A. Domínguez, J. D. Finke, F. Prada, J. R. Primack, F. S. Kitaura, B. Siana, D. Paneque

The first statistically significant detection of the cosmic γ-ray horizon (CGRH) that is independent of any extragalactic background light (EBL) model is presented. The CGRH is a fundamental quantity in cosmology. It gives an estimate of the opacity of the Universe to very-high energy (VHE) γ-ray photons due to photon-photon pair production with the EBL. The only estimations of the CGRH to date are predictions from EBL models and lower limits from γ-ray observations of cosmological blazars and γ-ray bursts. Here, we present synchrotron self-Compton models (SSC) of the spectral energy distributions of 15 blazars based on (almost) simultaneous observations from radio up to the highest energy γ-rays taken with the Fermi satellite. These SSC models predict the unattenuated VHE fluxes, which are compared with the observations by imaging atmospheric Cherenkov telescopes. This comparison provides an estimate of the optical depth of the EBL, which allows a derivation of the CGRH through a maximum likelihood analysis that is EBL-model independent. We find that the observed CGRH is compatible with the current knowledge of the EBL.

Cosmic Gamma-Ray Horizon Compared with EBL Models

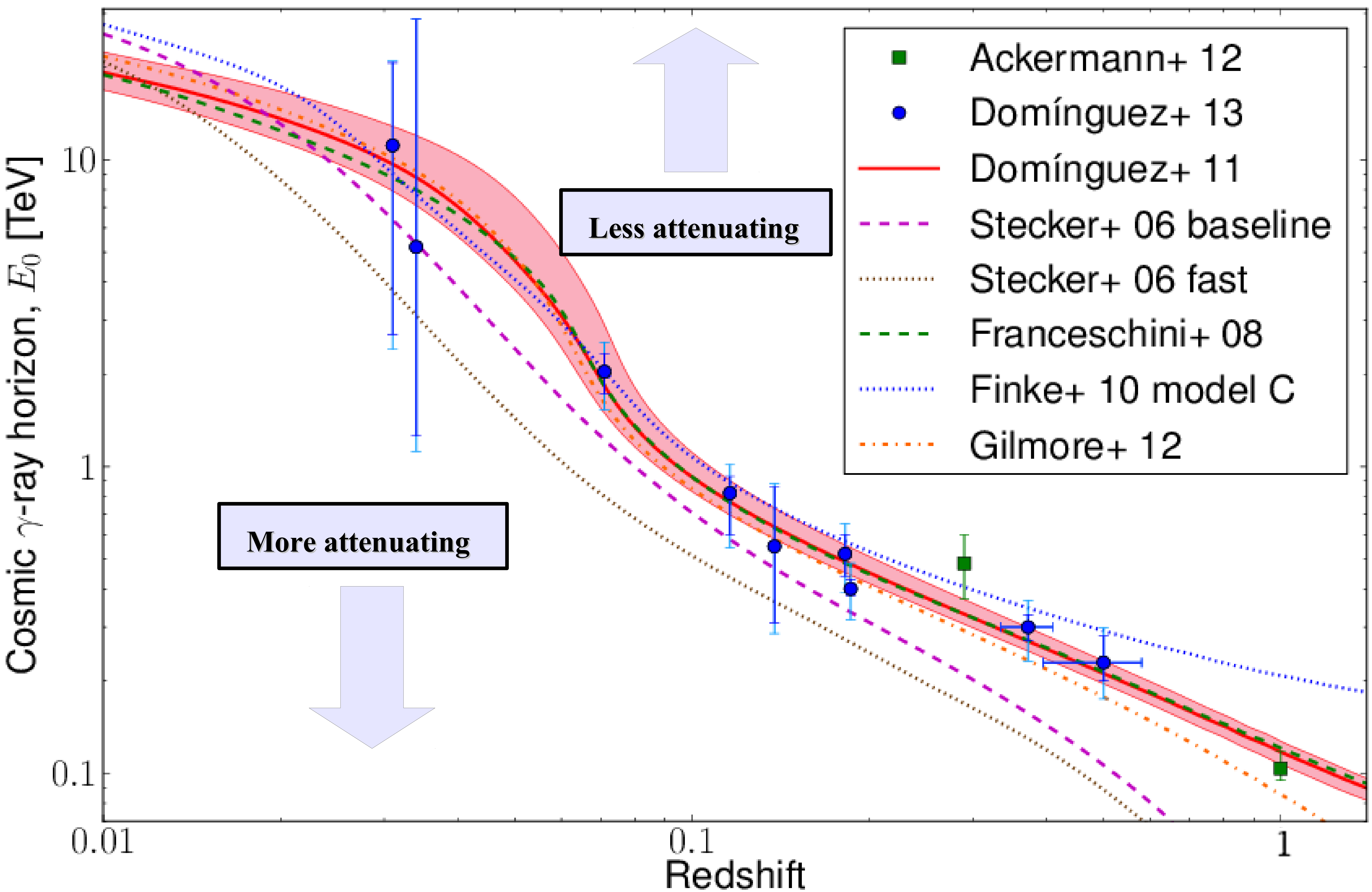

When and how did the first galaxies form?
How fast did they grow and build-up?

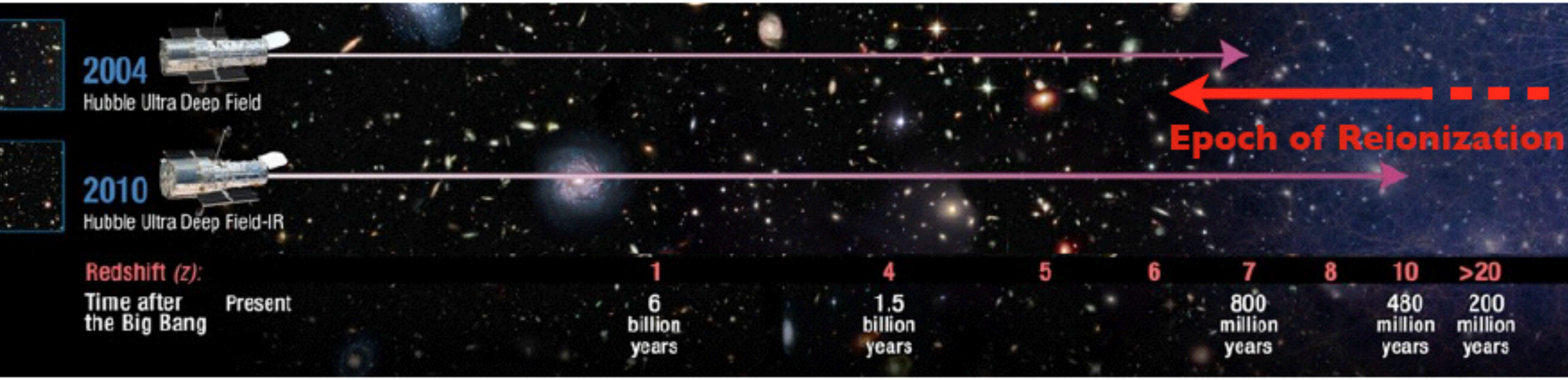

Thanks to WFC3/IR: now able to overcome z~6-7 “barrier”

Now have large samples (>300) of galaxies in heart of reionization at z>6

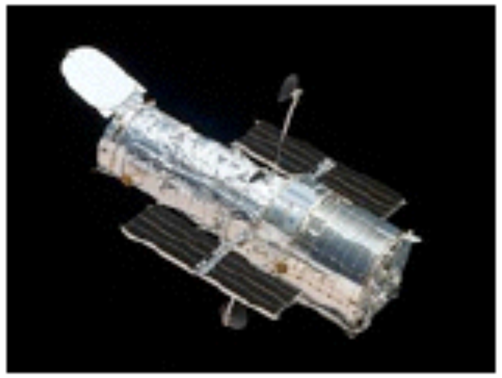

rest-UV SFRs

+

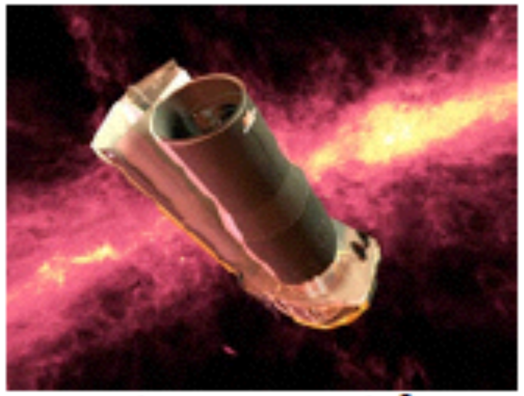

rest-optical Masses

How to Find Distant Galaxies

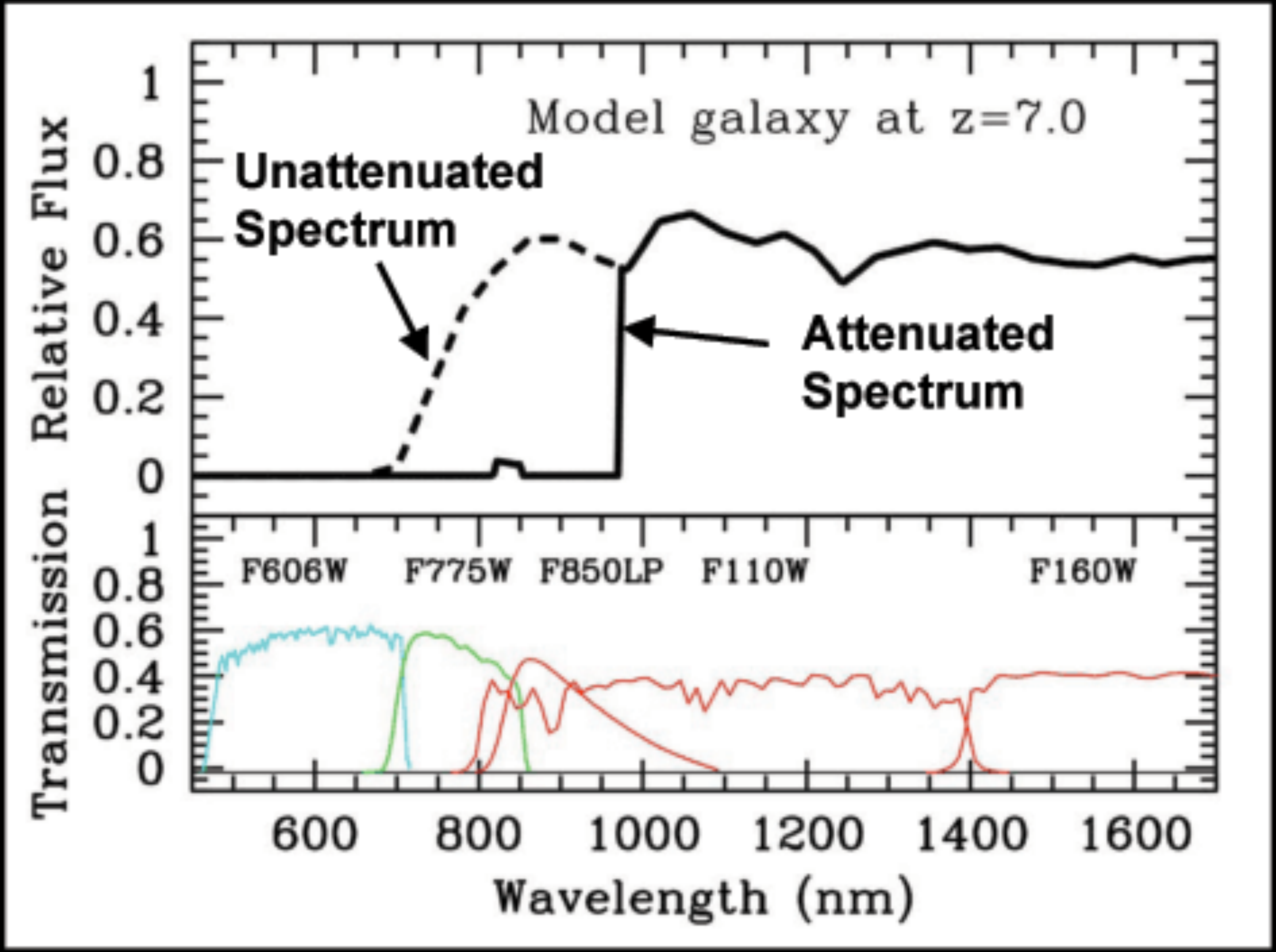

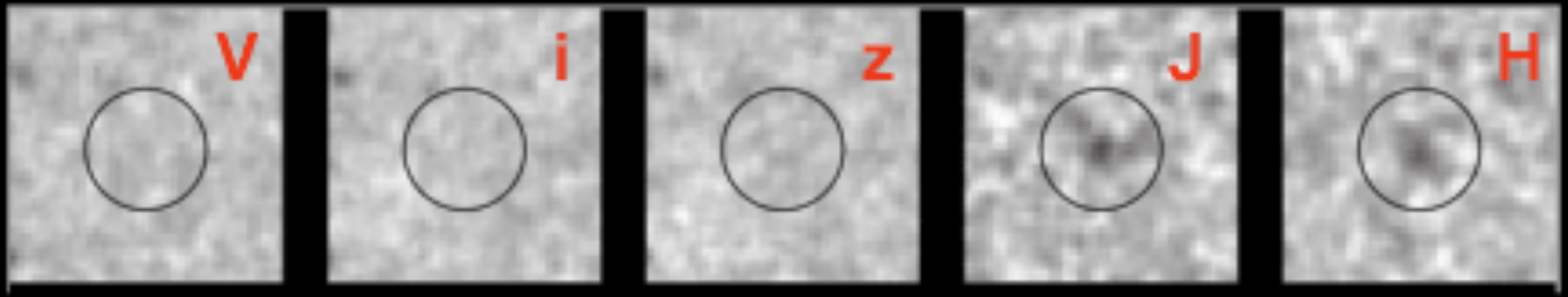

http://candels-collaboration.blogspot.com/2012/08/how-to-find-distant-galaxies.html

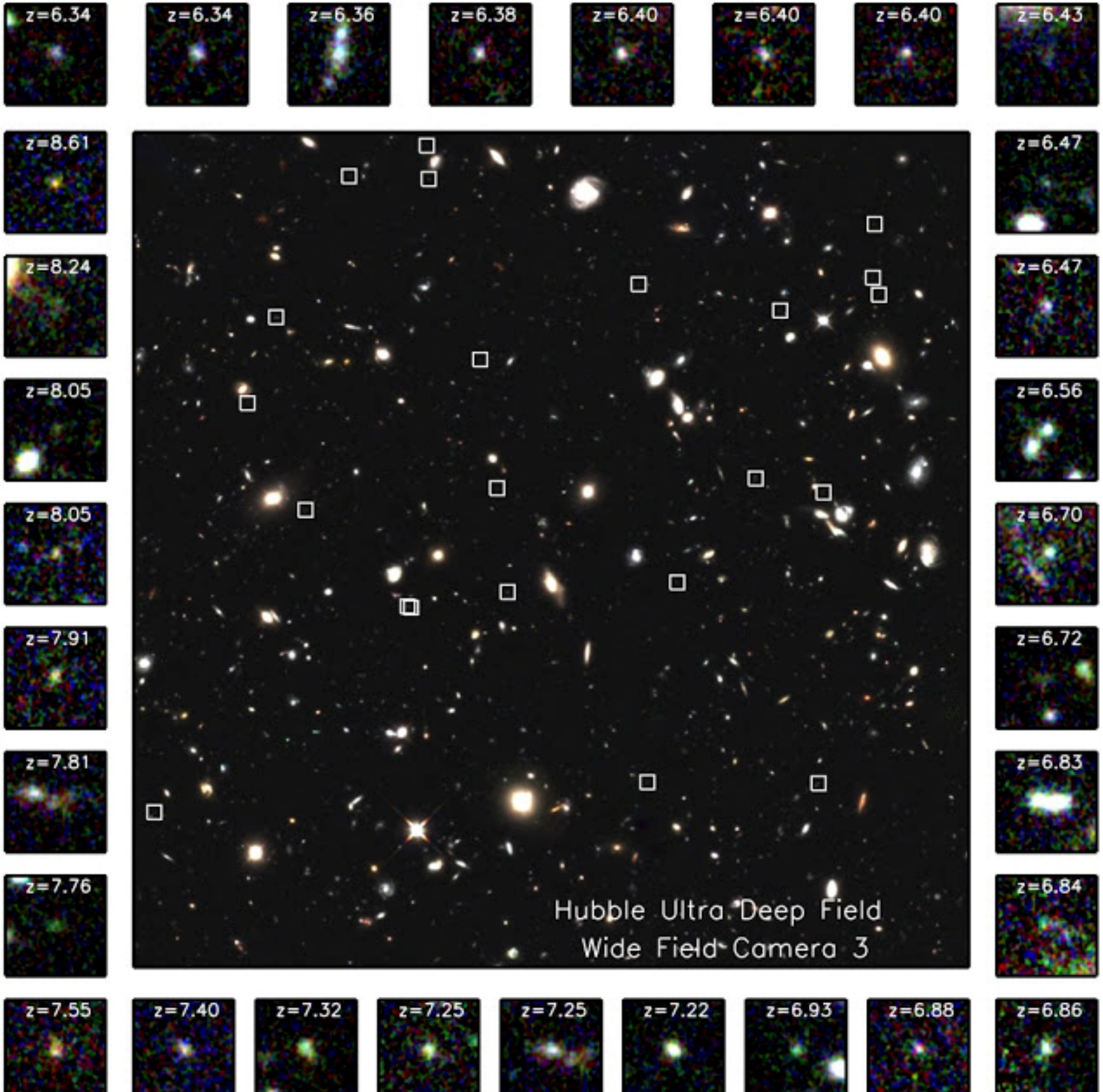

z=6.34
z=6.34
z=6.36
z=6.38
z=6.40
z=6.40
z=6.40
z=6.43
z=8.61
z=6.47
z=8.24
z=6.47
z=8.05
z=6.56
z=8.05
z=6.70
z=7.91
z=6.72
z=7.81
z=6.83
z=7.76
z=6.84
Hubble Ultra Deep Field
Wide Field Camera 3
z=7.55
z=7.40
z=7.32
z=7.25
z=7.25
z=7.22
z=6.93
z=6.88
z=6.86

WFC3/IR Data around GOODS-South

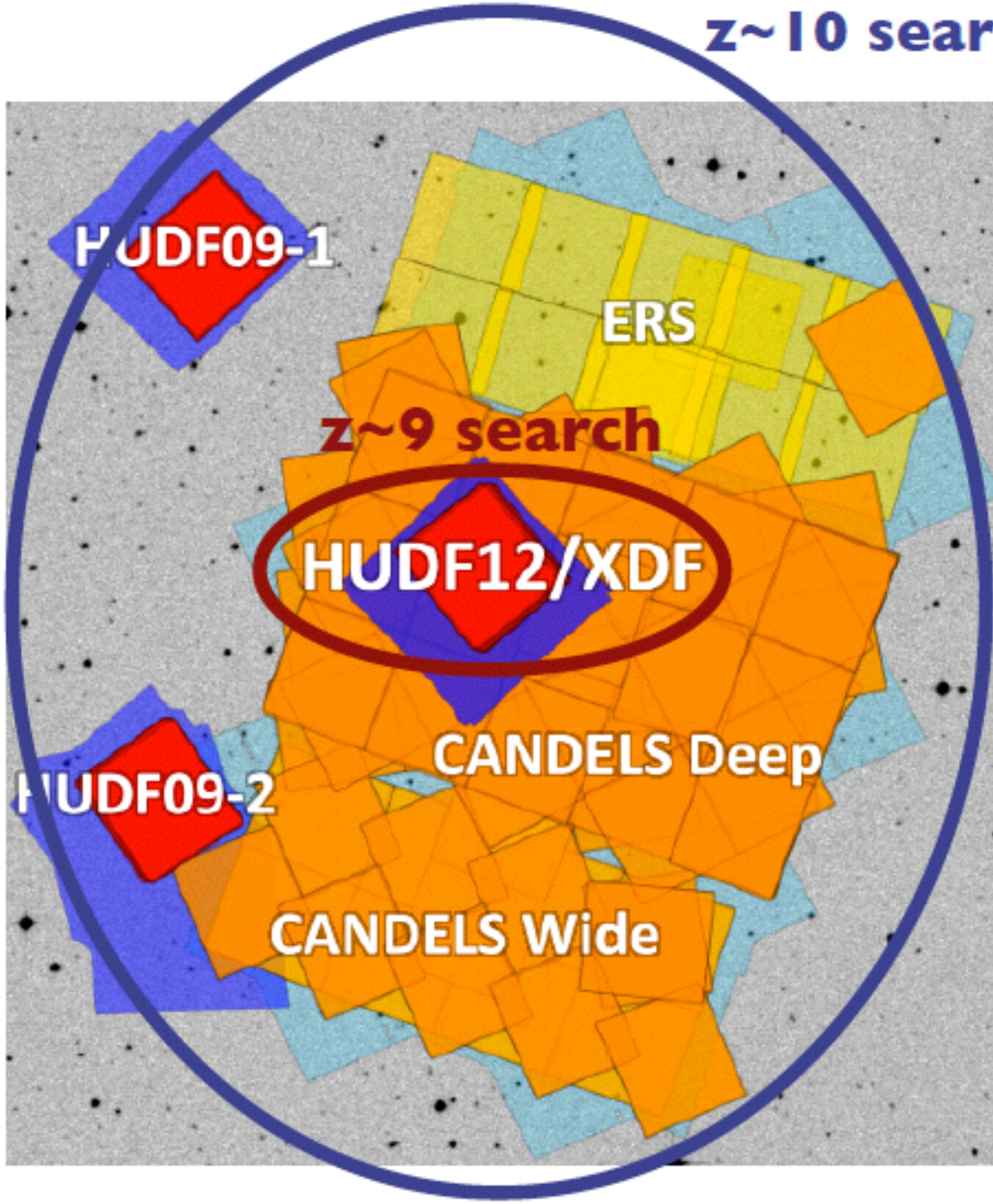

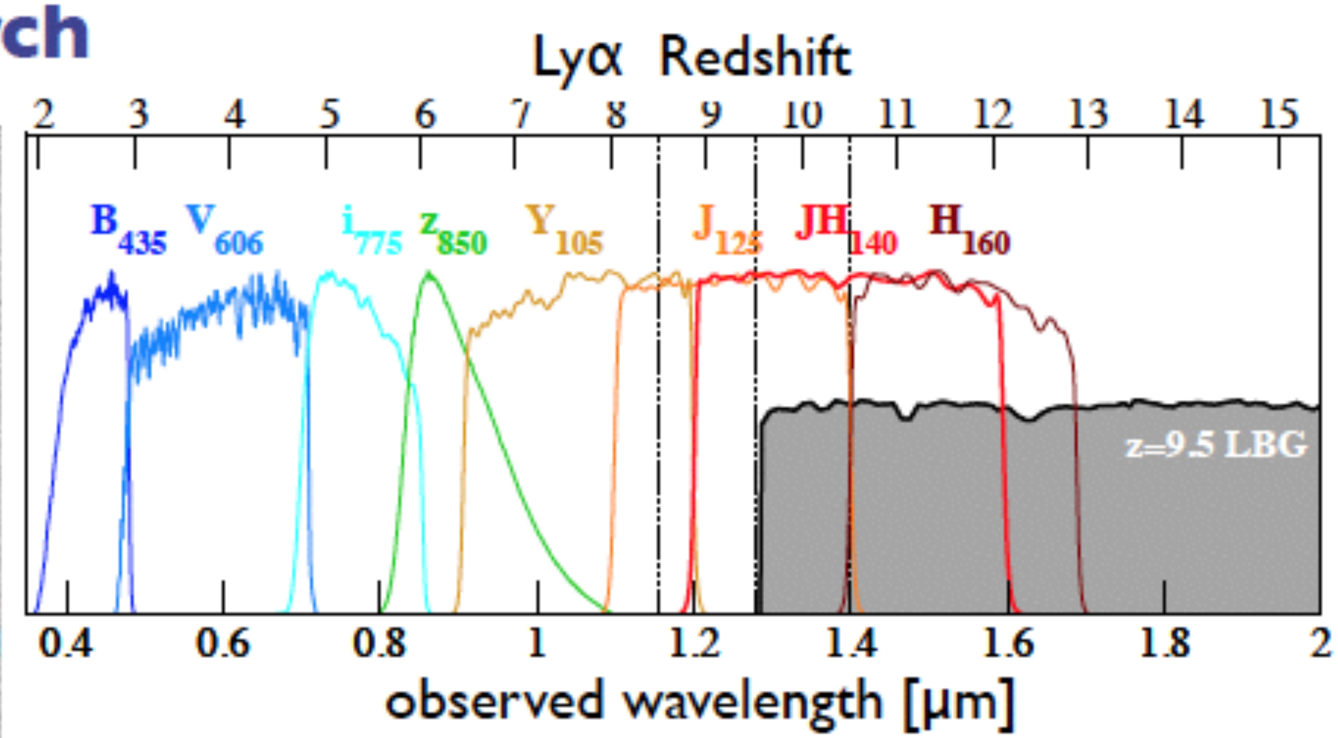

- Large amount of public optical (ACS) and NIR (WFC3) data
  - *HUDF12 & XDF*
  - ERS
  - CANDELS (Deep & Wide)
- Total of ~160 arcmin^2
- Reach to 27.5 - 30 AB mag
- Full data: can select z~10 galaxies
- HUDF12/XDF: can select z~9 galaxies

HUBBLE SPACE TELESCOPE

XDF • EXTREME DEEP FIELD

All optical ACS and WFC3/IR data over HUDF from 2003 to 2013 combined into eXtreme Deep Field (XDF)

Total of ~2Ms of HST data

Adds ~130 ACS orbits to the HUDF

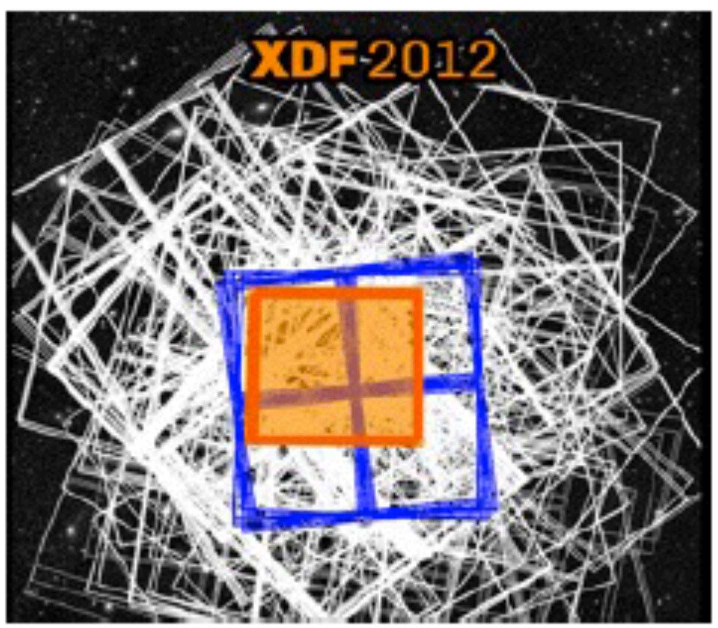

Reaches about 31mag at 5σ: deepest multi-color image ever taken

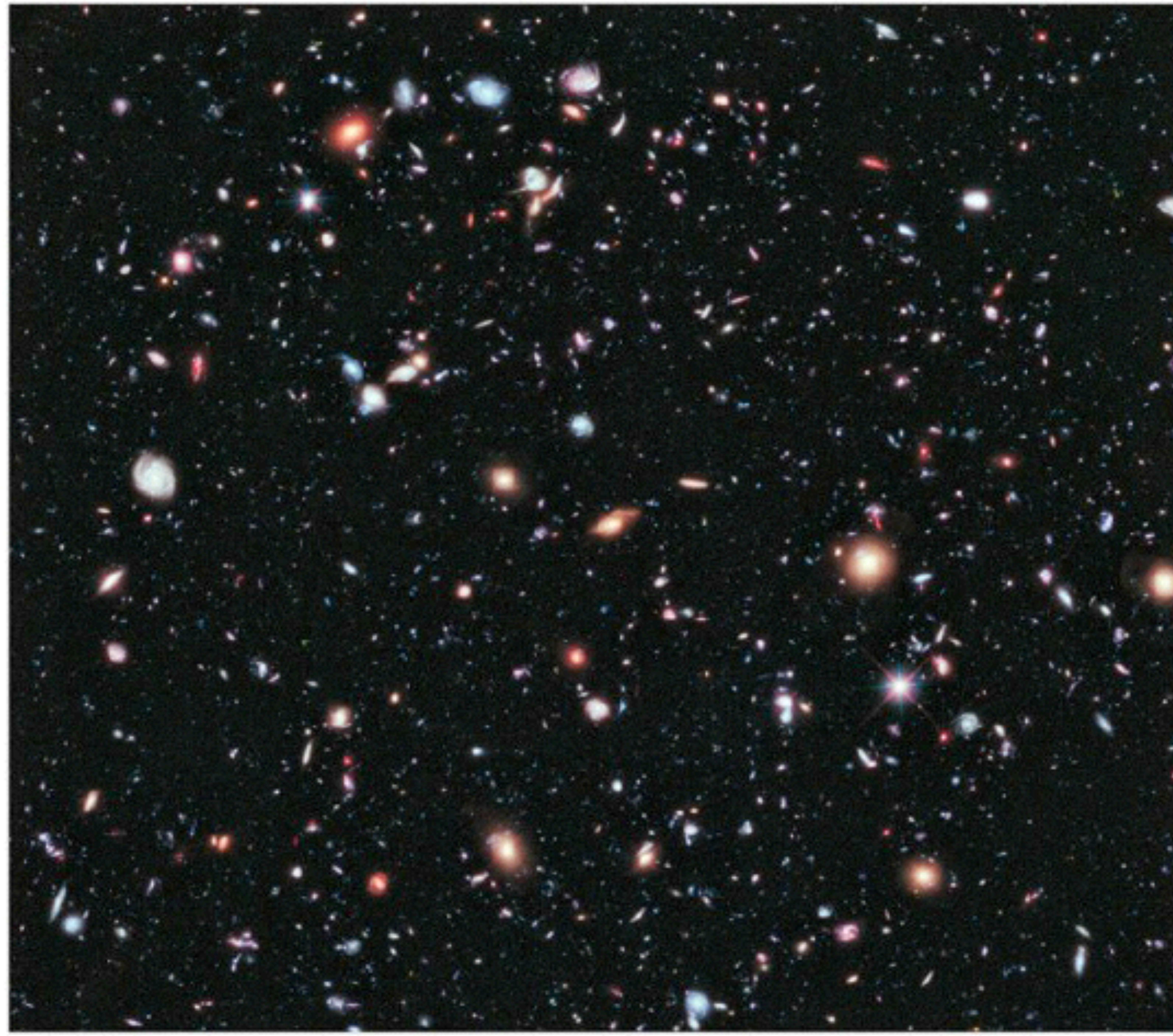

xdf.ucolick.org

available from MAST!

(see Illingworth, Magee, Oesch et al. 2013)

2012
NASA, ESA,
G. ILLINGWORTH, D. MAGEE, AND P. OESCH (UNIVERSITY OF CALIFORNIA, SANTA CRUZ),
R. BOUWENS (LEIDEN UNIVERSITY), AND THE XDF TEAM

SFRD Evolution at z>8

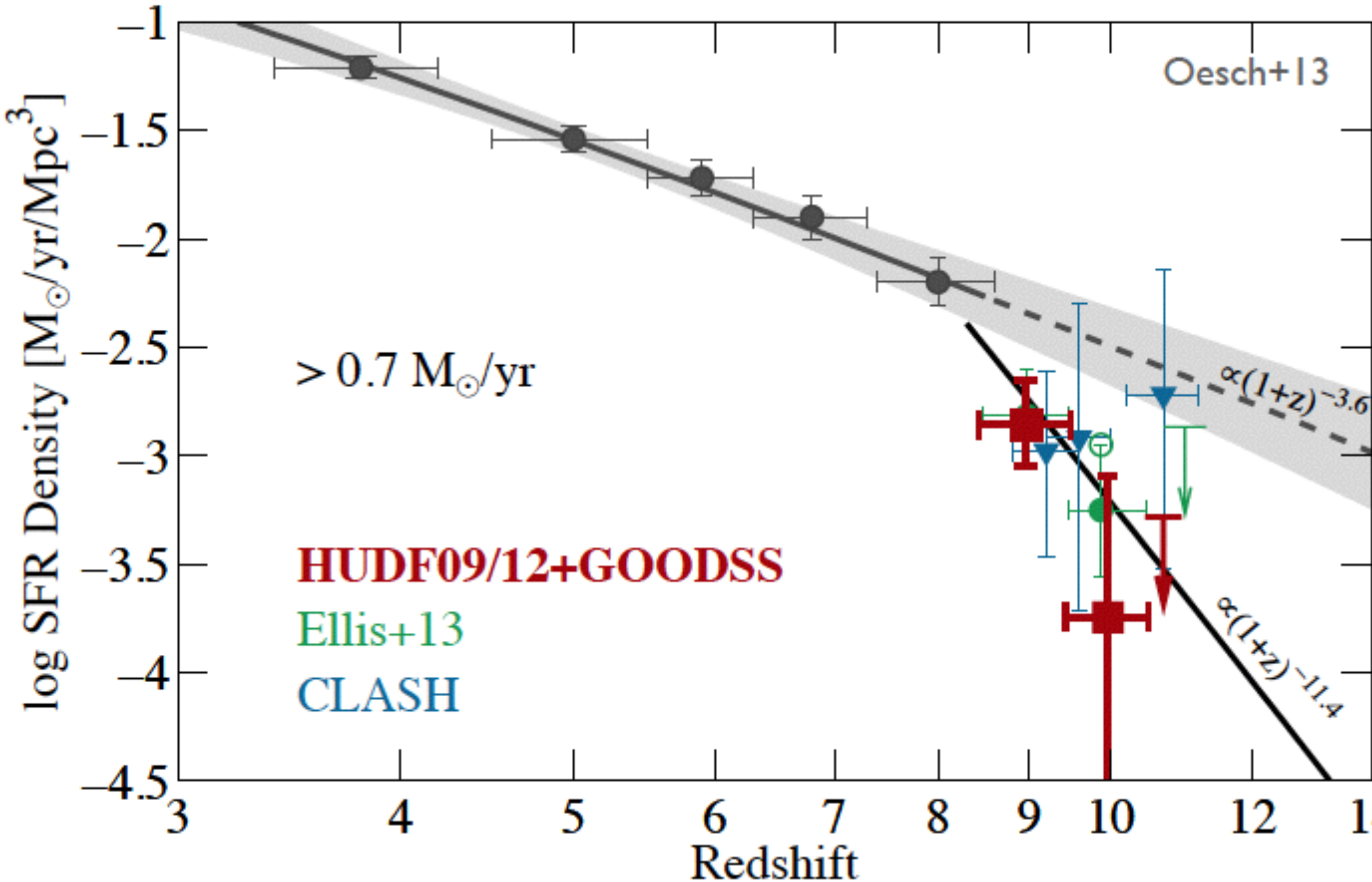

Combining the constraints from CLASH and HUDF+GOODS-S data, we still find extremely rapid evolution in the cosmic SFRD.

Compare with conclusions from: Zheng+12, Coe+13, Bouwens+13, Ellis+13, McLure+13

How many ionizing photons do galaxies produce?

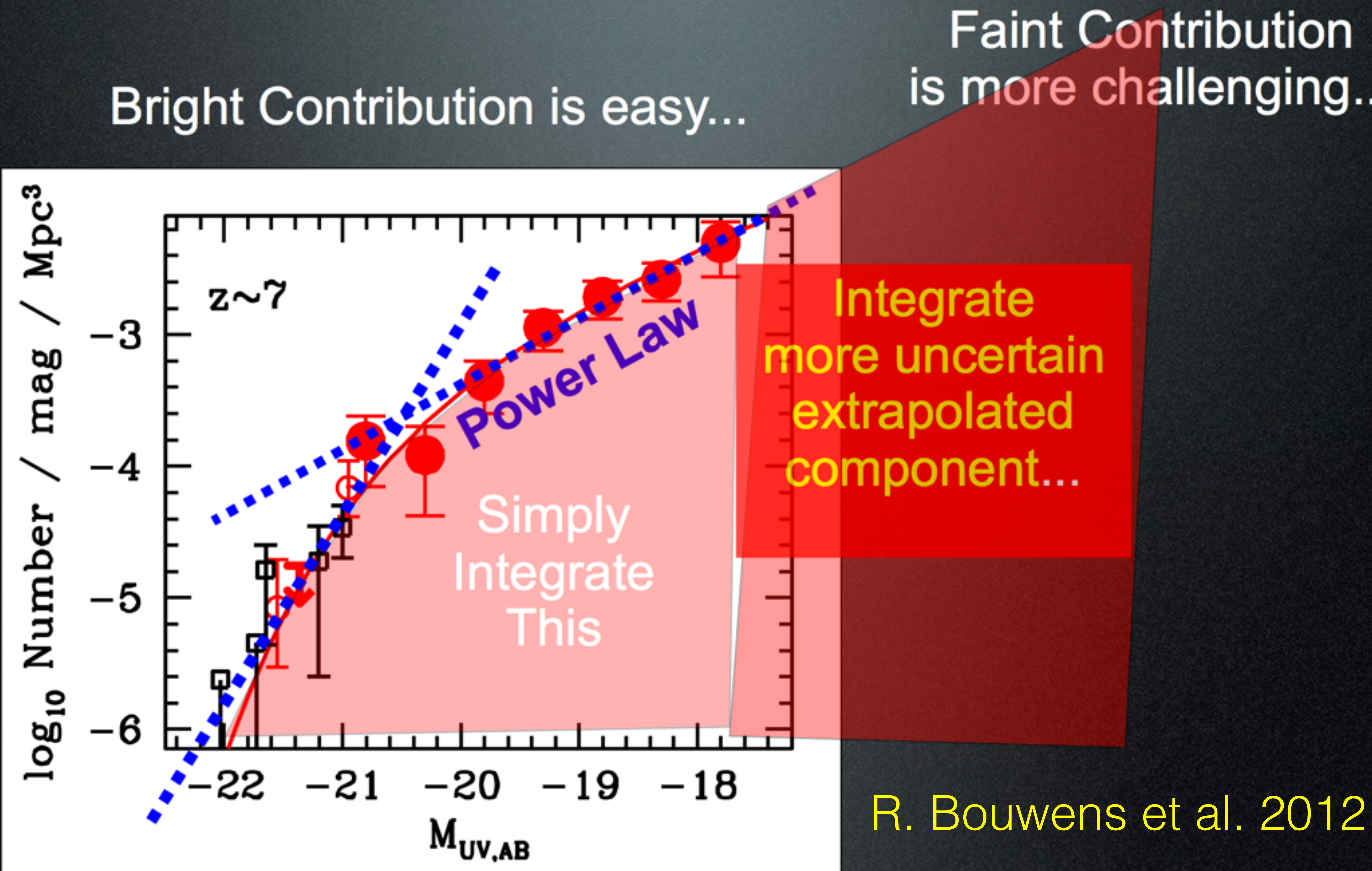

R. Bouwens et al. 2012

The Astrophysical Journal Letters, 752:L5 (6pp), 2012 June 10 2012

LOWER-LUMINOSITY GALAXIES COULD REIONIZE THE UNIVERSE: VERY STEEP FAINT-END SLOPES TO THE UV LUMINOSITY FUNCTIONS AT $z = 5$–8 FROM THE HUDF09 WFC3/IR OBSERVATIONS

R. J. Bouwens, G. D. Illingworth , P. A. Oesch, et al.

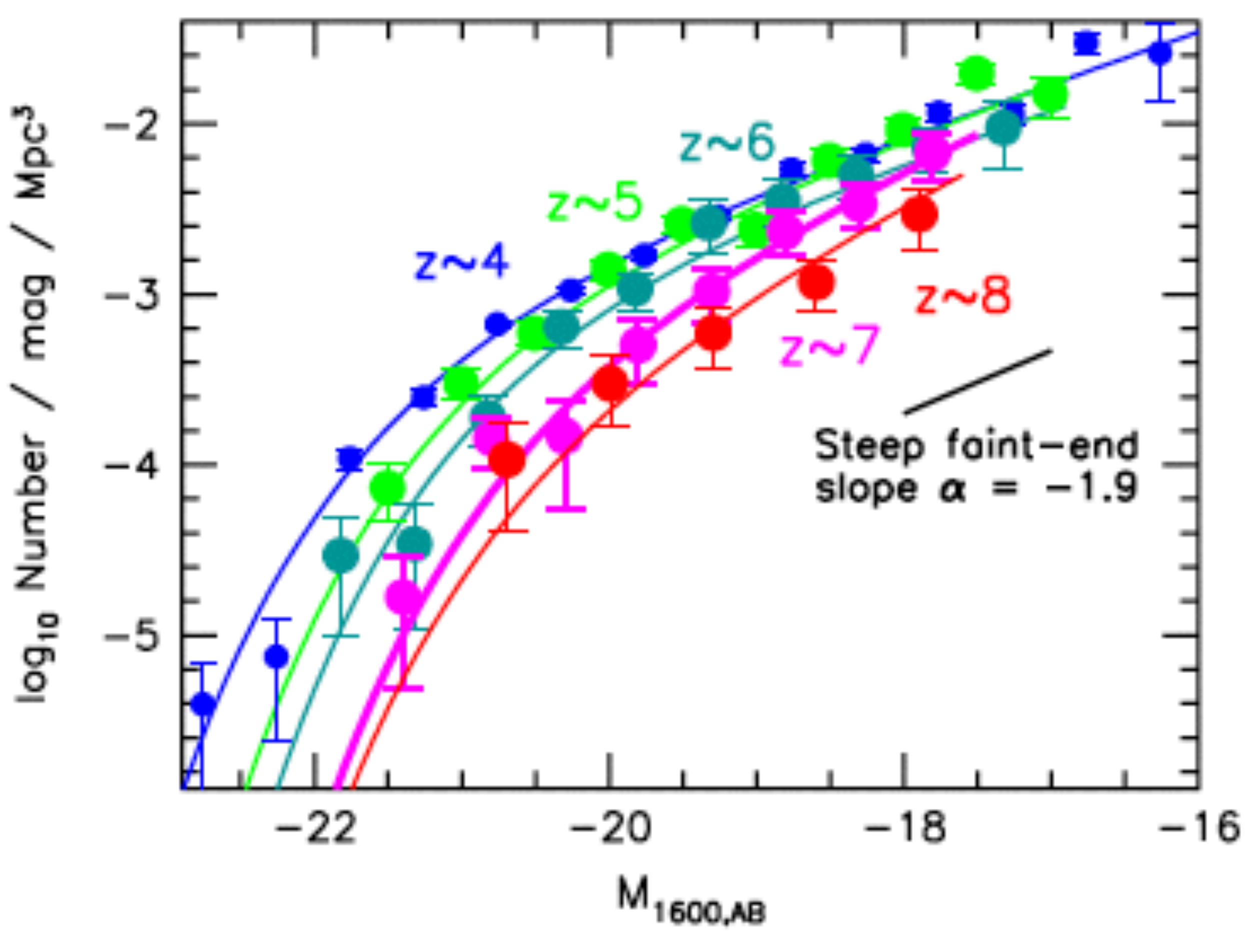

Luminosity Functions at z~4,5,6,7,8

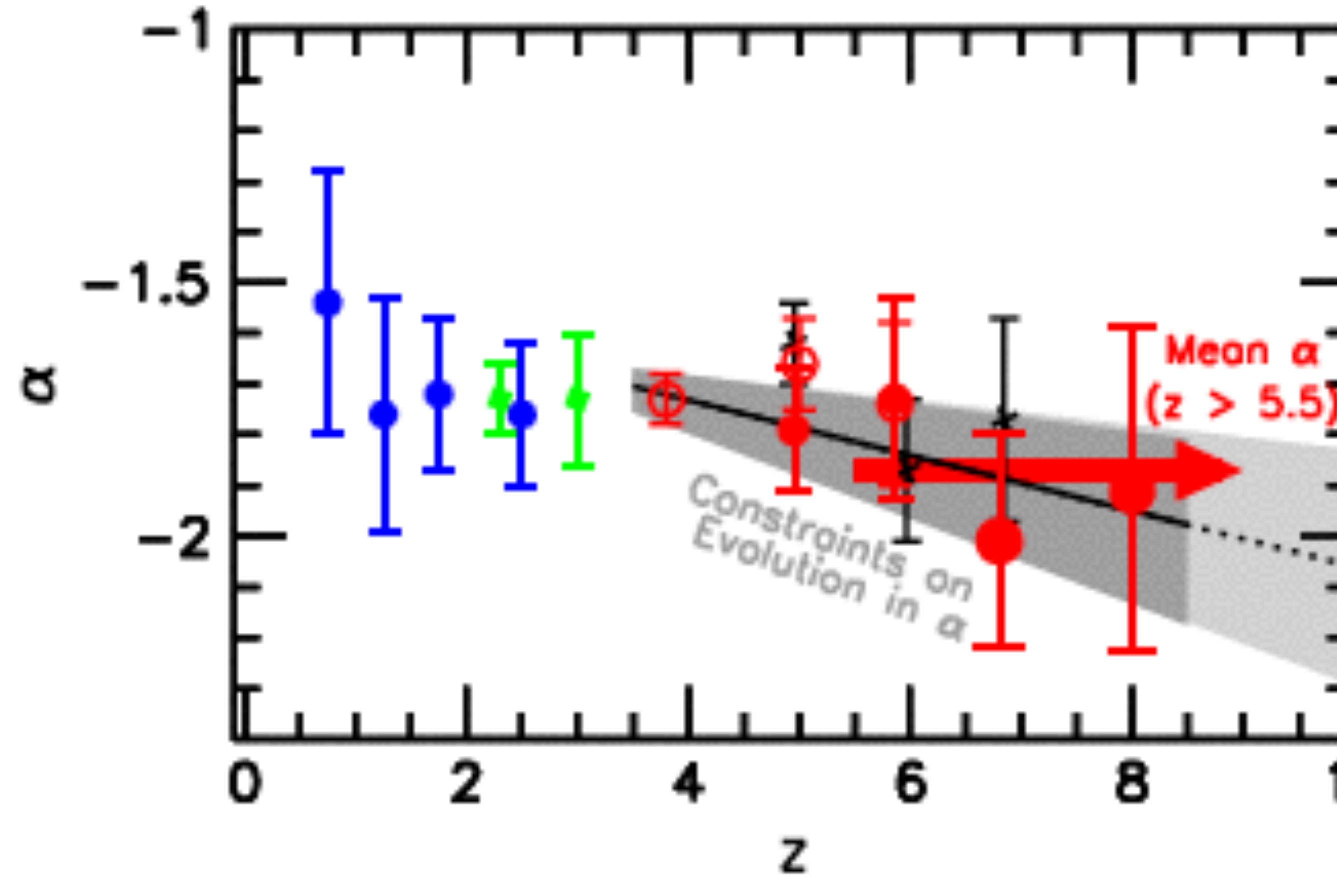

Faint-End Slope α

Schechter LF: number density $\varphi(L) = \varphi^* (L/L^*)^{-\alpha} e^{(-L/L^*)}$

Small-Scale Challenges to ΛCDM

Many more small halos than observed small galaxies

1) Field galaxies
2) Satellite galaxies

Cusp-Core issue at centers of small galaxies

"Too Big to Fail" problem for satellite galaxies

Evidence Supporting ΛCDM

Evidence that the large numbers of small subhalos predicted by ΛCDM actually exist:

1) Gaps in cold stellar streams in the Milky Way
2) Gravitational lensing "flux anomalies"

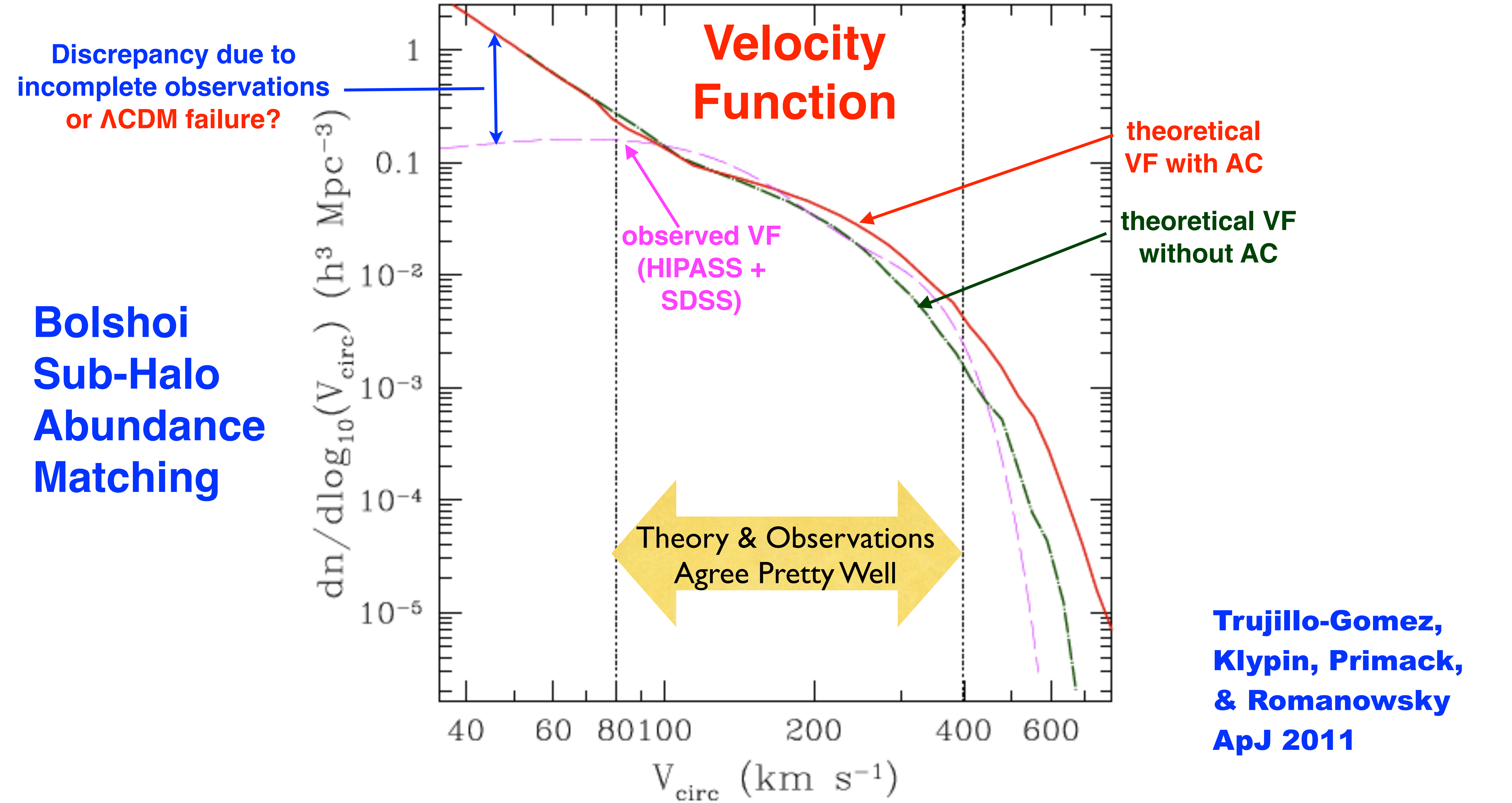

Fig. 11.— Comparison of theoretical (dot-dashed and thick solid curves) and observational (dashed curve) circular velocity functions. The dot-dashed line shows the effect of adding the baryons (stellar and cold gas components) to the central region of each DM halo and measuring the circular velocity at 10 kpc. The thick solid line is the distribution obtained when the adiabatic contraction of the DM halos is considered. Because of uncertainties in the AC models, realistic theoretical predictions should lie between the dot-dashed and solid curves. Both the theory and observations are highly uncertain for rare galaxies with $V_{\rm circ} > 400$ km s^{-1}. Two vertical dotted lines divide the VF into three domains: $V_{\rm circ} > 400$ km s^{-1} with large observational and theoretical uncertainties; < 80 km s^{-1} $< V_{\rm circ} <$ 400 km s^{-1} with a reasonable agreement, and $V_{\rm circ} < 80$ km s^{-1}, where the theory significantly overpredicts the number of dwarfs.

Presented at KITP Conf "First Light and Faintest Dwarfs" Feb 2012 and UCSC Galaxy Workshop Aug 2012

Klypin, Karachentsev, Nasonova 2012

Deeper Local Survey -- better agreement with ΛCDM but still more halos than galaxies below 50 km/s

Local Volume: D <10 Mpc

Total sample: 813 galaxies
Within 10 Mpc: 686
M_B<-13 N=304
M_B<-10 N=611

80-90% are spirals or dIrr (T>0)

Errors of distances are 8-10%

80% with D<10Mpc have HI linewidth

Vrot = 150x10^(-(20.5+M_B)/8.5)km/s

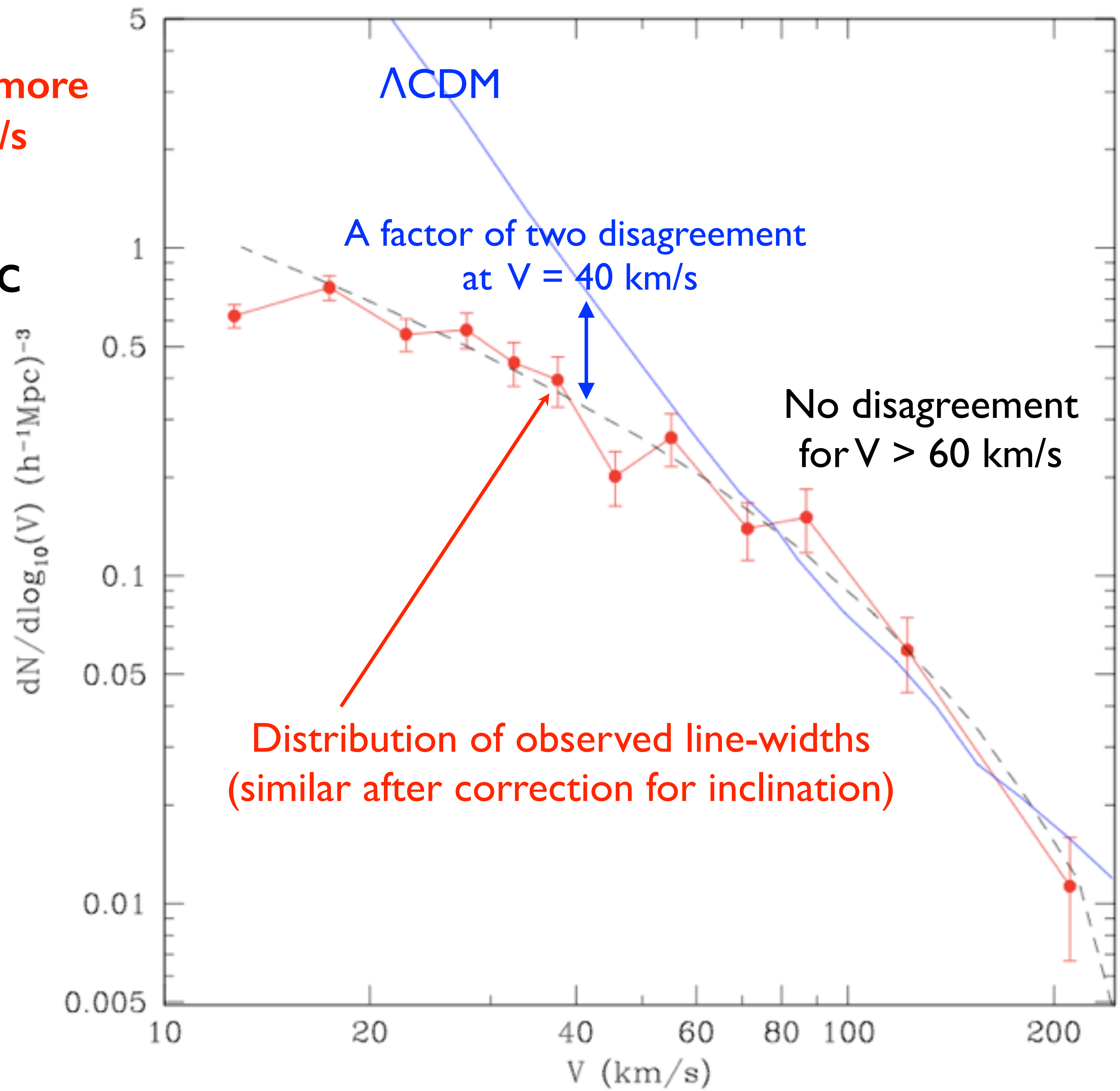

Abundance of field Galaxies

Anatoly Klypin[1*], Igor Karachenrsev[2], Dmitry Makarov[2], and Olga Nasonova[2]
[1]New Mexico State University, Las Cruces, NM 88001, USA
[2]Special Astrophysical Observatory, Nizhny Arkhyz, Russia

We present new measurements of the abundance of galaxies with a given circular velocity in the Local Volume: a region centered on the Milky Way Galaxy and extending to distance ~10 Mpc. The sample of ~ 800 mostly dwarf galaxies provides a unique opportunity to study the abundance and properties of galaxies down to absolute magnitudes MB ≈ −10, and virial masses Mvir = $10^9 M_\odot$. We find that the standard ΛCDM model gives remarkably accurate estimates for the velocity function of galaxies with circular velocities V ≥ 60 km s^{-1} and corresponding virial masses Mvir ≥ 3 × $10^{10} M_\odot$, but it badly fails by over-predicting ~ 5 times the abundance of large dwarfs with velocities V = 30 − 50 km s^{-1}. The Warm Dark Matter (WDM) models cannot explain the data either, regardless of mass of WDM particle. Though reminiscent to the known overabundance of satellites problem, the overabundance of field galaxies is a much more difficult problem. For the standard ΛCDM model to survive, in the 10 Mpc radius of the Milky Way there should be 1000 dark galaxies with virial mass $M_{vir} \approx 10^{10} M_\odot$, extremely low surface brightness and no detectable HI gas. So far none of this type of galaxies have been discovered.

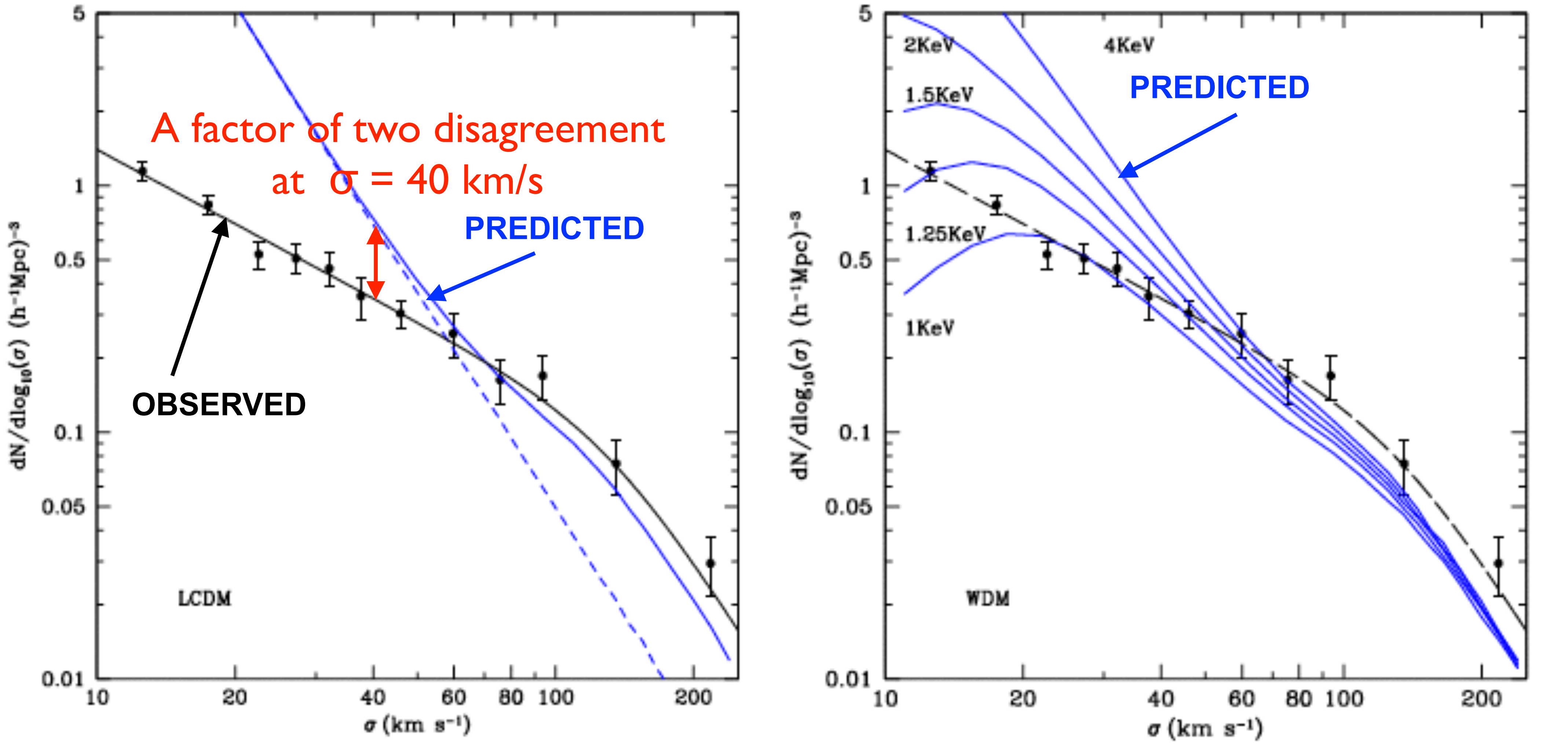

Figure 6. Comparison of the distribution function of line-widths V_{los} for galaxies in the Local Volume with theoretical predictions for the LCDM (left panel) and the Warm Dark Matter models (right panel). *Left:* Filled circles and the full curve present velocity function for the 10 Mpc sample. Theoretical predictions for the ΛCDM model with the Planck cosmological parameters are presented by the upper full curve. The short-dashed curve shows the predictions of the dark matter-only estimates without correction for baryon infall. Enhanced mass of baryons (mostly due to stars) in the central halo regions results in the increase of the circular velocity observed in this plot as the shift from the dashed to the full curve.